WRC RESEARCH REPORT NO. 197

BASINWIDE INSTREAM FLOW ASSESSMENT MODEL TO EVALUATE INSTREAM FLOW NEEDS

By Krishan P. Singh and Sally McConkey Broeren
Illinois State Water Survey
2204 Griffith Drive
Champaign, Illinois 61820

Project Completion Report
Project No. G904-06
Grant Number INT 14 08 0001 G904

November 1985

The research on which this report is based was financed in part by the U.S. Department of the Interior, as authorized by the Water Research and Development Act of 1984 (P.L. 98-242).

University of Illinois
Water Resources Center
Urbana, IL 61801

ABSTRACT

Quantification of sufficient or minimum flows needed to sustain the aquatic habitat is necessary for satisfactory resolution of water use conflicts and planning of water allocation strategies. The Instream Flow Group (IFG) of the U.S. Fish and Wildlife Service has developed a methodology to gage the quantity of suitable habitat in a stream. Application of the methodology requires information on the local variations of depth and velocity in a stream reach. Conventional flow models are inadequate for this application, and evaluation of aquatic habitats requires extensive field work. Results obtained in a study reach cannot be applied to other reaches with dissimilar areas.

To address the problem of defining the local variation of depths and velocities for regional habitat evaluation, a probabilistic flow model is developed. The probabilistic model incorporates hydraulic geometry relationships to evaluate average flow parameter values without the necessity of field observations. Local variations of depth and velocity values are evaluated from probability distribution models developed from field data collected on the Sangamon and South Fork Sangamon River basins. The flow model simulation for calculating stream habitat suitability with the IFG methodology is illustrated.

Singh, Krishan P. and Broeren, Sally McConkey

BASINWIDE INSTREAM FLOW ASSESSMENT MODEL TO EVALUATE INSTREAM FLOW NEEDS Project Completion Report to Department of the Interior, November 1985, Washington, D.C., 97 p.

KEYWORDS--instream flow/ aquatic habitats/ stream fisheries/ channel morphology/ physical models/ simulation/ habitat suitability/ incremental methodology

CONTENTS

Tables

FIGURES

Page

INTRODUCTION

A sufficient level of flow is needed within a stream to maintain stream ecology, fish habitat, and water quality. These instream flow needs must be balanced against off-stream demands such as irrigation, public water supply and industrial use. Optimal utilization of existing water resources requires both reliable quantification of these competing water demands and a rational basis for water allocations.

Instream flow needs may be investigated by relating the amount of suitable habitat to the quantity of flow. The quantity of suitable habitat at various flow levels can be used to assess the impact of flow regulation and water withdrawals on the stream environment. Prediction of habitat response to flow modification is critical to the satisfactory resolution of water-use conflicts as well as to the sequencing of withdrawals to optimize water use.

BACKGROUND INFORMATION AND RELATED RESEARCH

The most significant flow parameters related to aquatic habitat suitability are depth and velocity. Variations of depth and velocity throughout a stream create a continuum of conditions essential to meet the diverse needs of a variety of fish species at different life stages and other riverine life forming the food chain. The Cooperative Instream Flow Group (IFG) of the U. S. Fish and Wildlife Service has developed a methodology (Stalnaker, 1979) to relate these critical stream flow parameters to the quantity of suitable habitat. The basis of the IFG approach is a tabulation of fish species habitat suitability functions for depth and velocity as well as temperature and cover. All suitability functions vary between 0.0 and 1.0, based on the preference of a given species at its different life stages for various depths and velocities. A source file of suitability functions for more than 500 warm and cold water fish species is maintained by the IFG (Loar and Sale, 1981). Typical life stages are adult (A), juvenile (J), fry (F), and spawning (S).

The quantity of suitable habitat is measured by computing the Weighted Usable Area, WUA:

$$WUA = \sum_{i=1}^{N} S(d_i) \times S(V_i) \times A_i \qquad (1)$$

in which $S(d_i)$ and $S(v_i)$ are the suitability indexes for depth, d, and velocity, v, characteristic of a portion of the stream having a flow surface area A_i. $\sum_{i=1}^{N} A_i$ is the total surface area of the study reach. This procedure approximates the total water surface area in a simulated reach to an equivalent area of preferred habitat for a given flow condition. The values of WUA may be compared to assess the relative abundance of habitat expected under various flow scenarios.

The local variations of depth and velocity throughout the stream reach must be known to evaluate the WUA for a given discharge. Currently, the stream hydraulics is determined by measuring the flow velocities and depths in a representative stream reach across about 10 transects for 2 or more discharges. In order to evaluate other discharges a relationship between discharge and local values of velocity and depth must be established. At present the information collected is used to calibrate a hydraulic model based on Manning's equation.

Manning's equation is applicable to uniform flow conditions. Flow is not uniform at low discharges, which are of particular interest in evaluating aquatic habitat conditions at low flows with large variation in flow depth from riffles to pools. Local variations in channel geometry become increasingly significant with diminishing flow quantities, and estimates of depths and velocities are subject to gross inaccuracies at low flows. Extrapolation of the flow data to calculate the WUA for other reaches cannot be readily accomplished because hydraulic conditions may vary considerably. There are no relations to link the variations of depths and velocities measured in one reach to conditions in other reaches of the same stream or in other streams. Thus, a basinwide analysis over a range of flow conditions cannot be accomplished without extensive field work for direct measurement of flow parameters.

The diversity of depths and velocities essential for support of fisheries is created by pools and riffles found in natural streams. During low to medium flows, pools are characterized by relatively large depths and low velocities while riffles are shallow with high velocities. The pool riffle sequence forms in a fairly predictable pattern, repeating on the average every 5 to 7 times the stream width; the width increases with drainage area (Leopold and Wolman, 1957; Harvey, 1975; Nunnally and Keller, 1979). The average pool depth will also increase with increasing drainage area. In an extensive review of river patterns in Russia, Rzhanitsyn (1960) reported that the maximum pool depth to width ratio and riffle depth to width ratio maintain similar relationships when plotted against drainage area for a given discharge frequency such as average annual discharge.

The consistency in the nature of stream channel formation is evidenced in the similarity of relationships between flow parameters (width, depth, and velocity) and discharge for a variety of stream networks. Leopold and Maddock (1953) first stated the concept introducing the hydraulic geometry relations for width (W), depth (D), velocity (V), and flow cross-sectional area (A) as functions of discharge at a particular stream cross section (e.g., station):

$$W = aQ^b$$
$$D = cQ^f \qquad (2)$$
$$V = kQ^m$$

in which $b+f+m=1.0$ and $a \times c \times k = 1.0$, and D is the average depth of flow and equals $Q/(W \times V)$. Similar power functions express the trend of increasing W, D, and V with drainage area for a constant frequency of discharge. Hydraulic geometry relations demonstrate that there is an orderly, consistent progression of change in a stream system.

Station hydraulic geometry relations are calibrated by plotting W, D, and V versus discharge on log-log scale. The data for the station plots are usually obtained from routine current meter discharge measurements made by the USGS personnel at all active gaging stations. A best fit line is drawn for the range of flows between the lowest measured flows to flows at approximately the bankfull level. Parameter values at

low flows tend to depart from a simple linear relationship, and the best fit line may be curvilinear.

Relations linking flow parameters throughout the basin may be constructed as functions of drainage area and and flow duration. Stall and Fok (1968), expanding on the original concepts of hydraulic geometry, defined basin relations for hydraulic parameters in the form:

$$\ln(\text{parameter}) = a + bF + c(\ln A_d) \qquad (3)$$

in which a, b, and c are regression coefficients for a basin, F is the decimal flow duration, and A_d is the drainage area. These general relations were confirmed for Illinois streams and for selected basins in the United States (Stall and Yang, 1970). The simple basinwide relations show good agreement for high discharges, greater than those for the 50% flow duration. Stall and Fok observed that the reliability of the relations diminishes with decreasing discharge (or increasing flow duration).

OBJECTIVES AND SCOPE

The objectives of this research project are:

1) to develop reliable basinwide hydraulic geometry relations for medium to low flows;

2) to conduct a field program of measurements to document the variation of depths and velocities in a natural stream channel for a range of drainage areas;

3) to evaluate statistical parameters describing the variation of depths and velocities and relate those parameters to drainage area and flow duration frequency using the concepts of hydraulic geometry;

4) to compare the results of basin equations with field measurements;

5) to combine the basin hydraulic geometry relations for average depth and average velocity with the statistical variation of these parameters to form a hydraulic model to simulate expected

ranges of depth and velocity in a stream reach as a function of drainage area and flow; and

6) to interface the hydraulic model with the IFG habitat suitability function for basinwide assessment of Weighted Usable Area (WUA).

The Sangamon River in Illinois was selected for this study. The Sangamon River at its outlet to the Illinois River has a drainage area of 5452 square miles. Numerous long- and short-term gaging stations and water quality monitoring stations have been in operation in the basin from which ample discharge measurement data and daily flow records are available. There are five reservoirs in the system, and there are also a variety of unregulated natural channel streams for study.

Hydraulic geometry relations were developed independently for two basins in the Sangamon River system: the South Fork Sangamon and the Sangamon. The basins were delineated on the basis of hydrologic differences. The map in Figure 1 shows the Sangamon River system stream network and the locations of gaging stations. Data from flow measurements at these stations were used in developing the basin equations for stream hydraulic geometry. The principles of hydraulic geometry are applicable to natural streams. Only data collected near gaging stations situated in a reach of natural channel were used in the analysis.

Nine stream reaches representing a range of drainage areas were selected for field measurement of depths and velocities: four along the South Fork Sangamon and five along the main stem of the Sangamon. Two adjacent pool and riffle sequences were identified to define each reach. Velocities and depths were measured at two different discharges for each reach. The reaches studied are also shown in Figure 1.

ACKNOWLEDGMENTS

The help of the staff of the U.S. Geological Survey, Urbana office, in providing flow measurement information for the years of record at various stations in the Sangamon Basin is deeply appreciated.

Robin King conducted and supervised field measurements in riffle-pool sequences in various river reaches. Joseph Odencrantz,

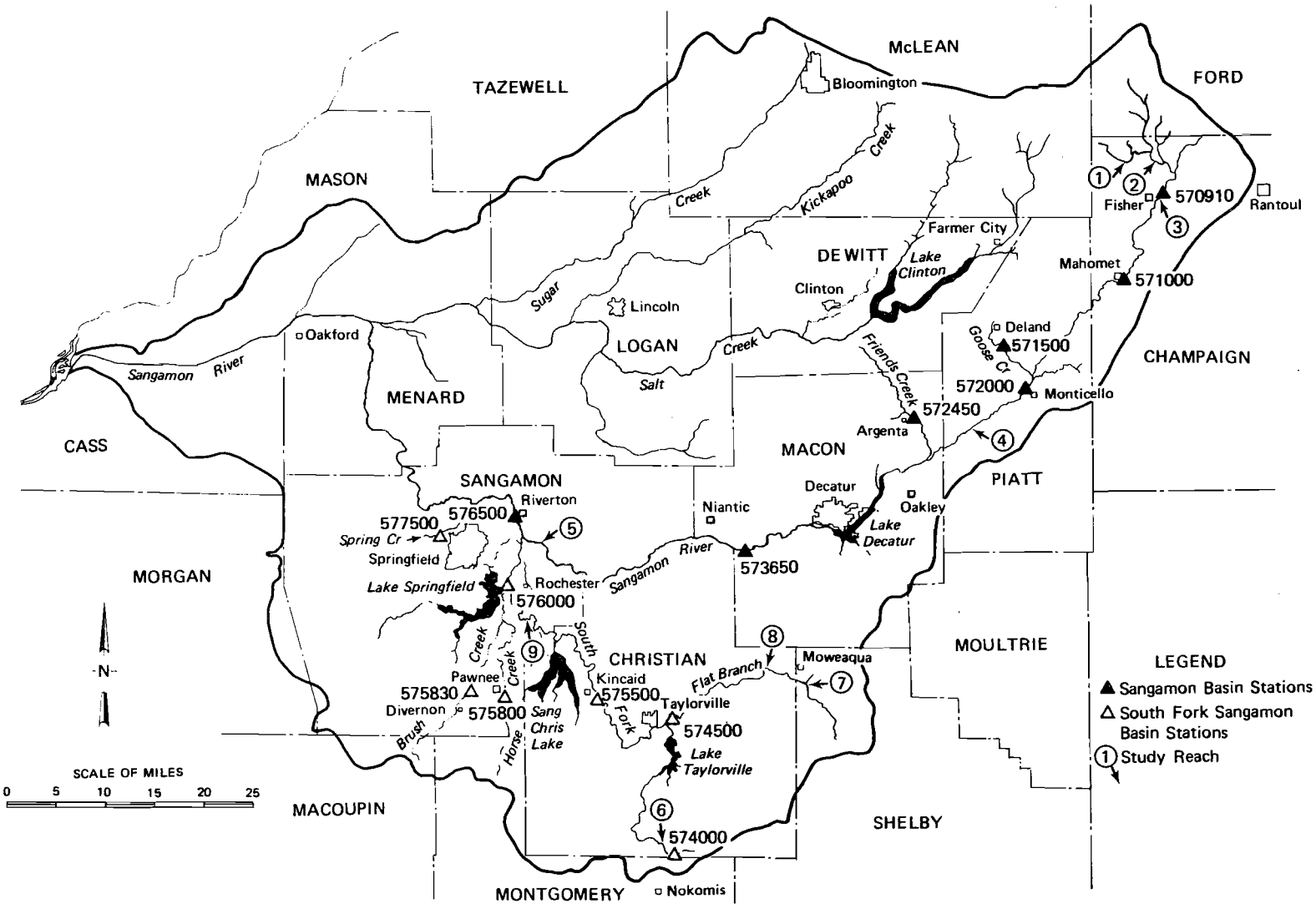

Figure 1. Sangamon River stream network, USGS gaging stations, and study reaches

graduate research assistant, helped in field work, computerization of data, and development of some programs. Paul Mueller, John Baliga, and Michael Pubentz, students at the University of Illinois, helped in data storage and processing. Kathleen Brown typed the camera-ready copy.

HYDRAULIC DIVISIONS OF THE SANGAMON RIVER BASIN ABOVE OAKFORD

The Sangamon River above Oakford may be divided into three hydrologically homogeneous basins: those of the Sangamon, the South Fork Sangamon, and Salt Creek. Singh (1981) demonstrated the homogeneity of each of these basins in a study of stream flow variability and flow duration. The relationship between the 7-day 10-year low flow and drainage area also supports this division.

Daily flow data from 22 gaging stations on the Sangamon, South Fork Sangamon, and Salt Creek were analyzed to evaluate relations between discharge and drainage area. Discharge may be expressed as a function of drainage area for a given flow duration. The relationship may be generalized for a basin in an expression of the form:

$$\log Q_j = a_j + b_j \ (\log A_d) \qquad (4)$$

where A_d = drainage area

Q_j = discharge at flow duration j

a_j and b_j = regression coefficients for flow duration j

The regression coefficients a_j and b_j vary with flow duration. Higher correlations are achieved if a_j is evaluated independently for each of the three basins. The b_j or the slope of the log Q versus log A_d line is practically constant for a given flow duration for the three basins. The regression coefficients for the 10% through 90% flow durations are listed in Table 1 for each basin. Equation 4 is modified to

$$\log Q_{i,j} = a_{i,j} + b_j \ (\log A_d) \qquad (5)$$

The subscript i (i=1, 2, or 3) denotes the Sangamon, South Fork Sangamon, or Salt Creek basin. The regression analysis was performed using two dummy variables, D_1 and D_2, given by

$$a_{2,j} = a_{1,j} + D_1$$
$$a_{3,j} = a_{1,j} + D_2 \qquad (6)$$

The reliability of these relations is indicated by the high correlation coefficients, r, and low standard errors of estimate, S_e, which are also included in Table 1. The basin equations developed for discharge

TABLE 1

Basin Regression Coefficients for Discharge
$\log(VAR) = a_{i,j} + b_j (\log A_d)$ (i=1,2,3)

VAR(j)	Sangamon	South Fork Sangamon	Salt Creek		Regression statistics		Sample size
	Regression coefficients						
	$a_{1,j}$	$a_{2,j}$	$a_{3,j}$	b_j	r	S_e	n
Q(99)	-5.1183	-5.5025	-4.4167	1.9488	0.924	0.3172	12
Q(95)	-3.6001	-4.0998	-3.1499	1.5833	0.967	0.1864	13
Q(90)	-2.8257	-3.1131	-2.4983	1.3909	0.975	0.1351	13
Q(80)	-2.2448	-2.3825	-2.0045	1.2864	0.984	0.0974	13
Q(70)	-1.7144	-1.8431	-1.5770	1.2070	0.991	0.0736	14
Q(60)	-1.1887	-1.3260	-1.1065	1.1220	0.995	0.0540	14
Q(50)	-0.7843	-0.9254	-0.7571	1.0640	0.996	0.0434	14
Q(40)	-0.5583	-0.6833	-0.5453	1.0507	0.997	0.0357	14
Q(30)	-0.3554	-0.4473	-0.3559	1.0433	0.998	0.0296	14
Q(20)	-0.0880	-0.1742	-0.1181	1.0222	0.998	0.0304	14
Q(10)	0.1903	0.1581	0.1424	1.0175	0.996	0.0409	14
Q(5)	0.4516	0.4686	0.3926	0.9991	0.996	0.0429	14
Q(1)	1.0833	1.1219	1.0392	0.8964	0.996	0.0373	14

corresponding to various flow durations for the Sangamon and South Fork Sangamon were used in this study.

Flow measurement data from which hydraulic geometry relations are developed are collected at long-term gaging stations, temporary gaging stations, water quality sites, and partial-record low-flow stations maintained by the U.S. Geological Survey. A sufficient record of daily flow data to construct flow duration curves is not collected at all of these stations. Therefore, the basin flow-duration equations were used in lieu of flow duration curves developed from daily flow data. The basin discharge equations provide a consistent method of computing discharges for a given flow duration at all stations within a hydrologically homogeneous region.

STATION HYDRAULIC GEOMETRY EQUATIONS

The fundamental building blocks of the regional hydraulic geometry relations are the station equations. These equations relate flow parameters width (W), depth (D), cross-sectional area (A), and velocity (V) to discharge measured at cross sections near the station. When plotted on a log-log scale, W, D, A, and V increase in a consistent manner with increasing discharge at a section. Typically, the station hydraulic rating curves are fit by eye to the data.

The station relationship for the log-transformed variables may be evaluated by regression analysis, expressing them as polynomial function relationships between log (D, V, W, or A) and log Q. Alternative formulations with different order polynomials may then be compared on the basis of regression parameters qualifying the goodness of fit. Polynomial regression analysis has the advantage of providing a compact mathematical expression instead of a graphical relation, and repeatability given the same data and criteria. The value and reliability of the regression equations are dependent on the data used to compute them. The available data from the stream gaging stations were carefully screened before inclusion in the development of the station relations and ultimately the basin hydraulic geometry relations.

DATA

The U.S. Geological Survey conducts an extensive program of stream flow measurements. As part of that continuing program, between 10 to 20 detailed current meter flow measurements are made every year at each active gaging station. Through this effort there is available a mass of data on stream flow and channel geometry. For each measurement, velocities and depths are sampled at a stream cross section, the top width (W) is measured, and gage height is recorded. The flow cross-sectional area (A), the average velocity (V), and discharge (Q) are computed. The average depth (D) defined as the hydraulic depth may be computed from $D = A/W$ (Chow, 1959). Low to medium flows are typically measured by wading along a stream cross section. High flows with depths exceeding approximately 3 feet are usually measured from a bridge near

the gage installation, from a cable car if available, or from a boat. The data are not published but are available at USGS district offices.

Data collected near nineteen stream gaging or water quality stations on the Sangamon main stem and South Fork Sangamon Rivers were obtained from the USGS district office in Urbana, Illinois. Data from five stations and some data points from other stations were not included in developing the final equations, as discussed later. Hydraulic geometry relations were developed from data obtained near fourteen stations; the stations, drainage areas, and years of record used are listed in Table 2.

Data used in developing parameter rating curves must be obtained at cross sections representative of the natural channel (Leopold and Maddock, 1953). Stream reaches which are dredged or leveed, or where flows are regulated or influenced by a dam or backwater, are typically not representative of the stream system hydraulics. The relationship between depth or velocity with discharge at a section, constricted by bridge piers or abutments, will differ from that found at a natural section.

Detailed gaging station descriptions and histories were gathered from the USGS for each of the stations initially reviewed. Information provided in the descriptions led to the elimination of five stations from the study: Gage 05583000 at Oakford is located in a dredged and leveed reach; Gage 05573540 at Highway 48 near Decatur was not used as all flows may be affected by gate operation of the Lake Decatur Dam; Gage 05572500 at Oakley was affected by backwater from the Lake Decatur Dam; all low and medium flows measured at the temporary gage near Petersburg are made directly upstream of a dam; and for Gage 05572100 on Wildcat Creek, flows are measured at a culvert. The gaging station descriptions also document activities which may have modified the hydraulic conditions or stream morphology at the gage such as dam or bridge construction in the reach during the period of record, relocation of the gaging installation, or flow diversion at high stages. For each station only flow measurement data representative of a homogeneous hydraulic regime were included.

TABLE 2

Gaging Stations

USGS No.	Stream name	Station	Drainage area (mi^2)	Period of record	Number of data points
		Sangamon River			
05571500	Goose Creek	DeLand	47.3	6/51 to 4/59	55
05572450	Friends Creek	Argenta	111.0	9/66 to 10/82	134
05570910	Sangamon	Fisher	240.0	8/78 to 9/82	31
05571000	Sangamon	Mahomet	362.0	3/48 to 9/78	246
05572000	Sangamon	Monticello	550.0	3/41 to 11/68	177
05573650	Sangamon	Niantic	1054.0	12/77 to 8/83	23
05576500	Sangamon	Riverton	2618.0	11/34 to 12/56	69
		South Fork Sangamon River			
05574000	So. Fork Sang.	Nokomis	10.8	1/51 to 10/75	155
05575830	Brush Creek	Divernon	32.4	9/73 to 10/82	74
05575800	Horse Creek	Pawnee	52.2	4/66 to 11/82	113
05577500	Spring Creek	Springfield	107.0	6/58 to 10/82	158
05574500	Flat Branch	Taylorville	279.0	7/49 to 9/82	203
05575500	So. Fork Sang.	Kincaid	562.0	10/33 to 8/60	88
05576000	So. Fork Sang.	Rochester	867.0	4/66 to 10/82	80

The hydraulic consistency and accuracy of the flow data were checked by examining the stage discharge relationship for the period of record and also by verifying that the physical law, $Q = V \times A$, was satisfied by the recorded information. Gage height versus discharge was plotted on log-log scale from the available data. In a few cases multiple rating curves were evident. Only data forming a single curve were retained. This elimination process reduced data scatter in the flow parameter versus discharge plots to some extent. Measurements were omitted if $V \times A$ was not within ±5% of the reported discharge. Usually 1 to 5% of the measurements were omitted from the final data set because of these considerations.

The original field notes for each measurement were reviewed to identify it as a wading measurement (information collected by field personnel traversing the stream on foot or by boat) or bridge measurement (measurement made by lowering equipment into the stream from a bridge). There are no cable car installations in the Sangamon Basin. The approximate location of the measured section relative to the gage was noted if reported.

STATION HYDRAULIC GEOMETRY

Station hydraulic geometry plots were developed from the final data sets. There are four log-log plots for each station: W, D, A, and V versus Q. The plots for each station appear in Figures 2 through 15. Data collected at a wading section are plotted with a 0 symbol, and data obtained at a bridge section are plotted with a + symbol. The vertical dashed line labeled "cut off" in each graph is plotted at a discharge equal to 1.5 times the 10% flow duration discharge. The relationships developed in this project were limited to flows at or below this limit. Flows less than this limit may be expected to be contained within the channel banks. One exception is at the gage located near Fisher, where flows exceeding approximately 200 cfs are diverted through a culvert; here 200 cfs was used as the "cut off."

Several general observations are clearly illustrated in the plots. There is a discontinuity between the wading data and the bridge data in nearly every station graph. This discontinuity does not correspond to

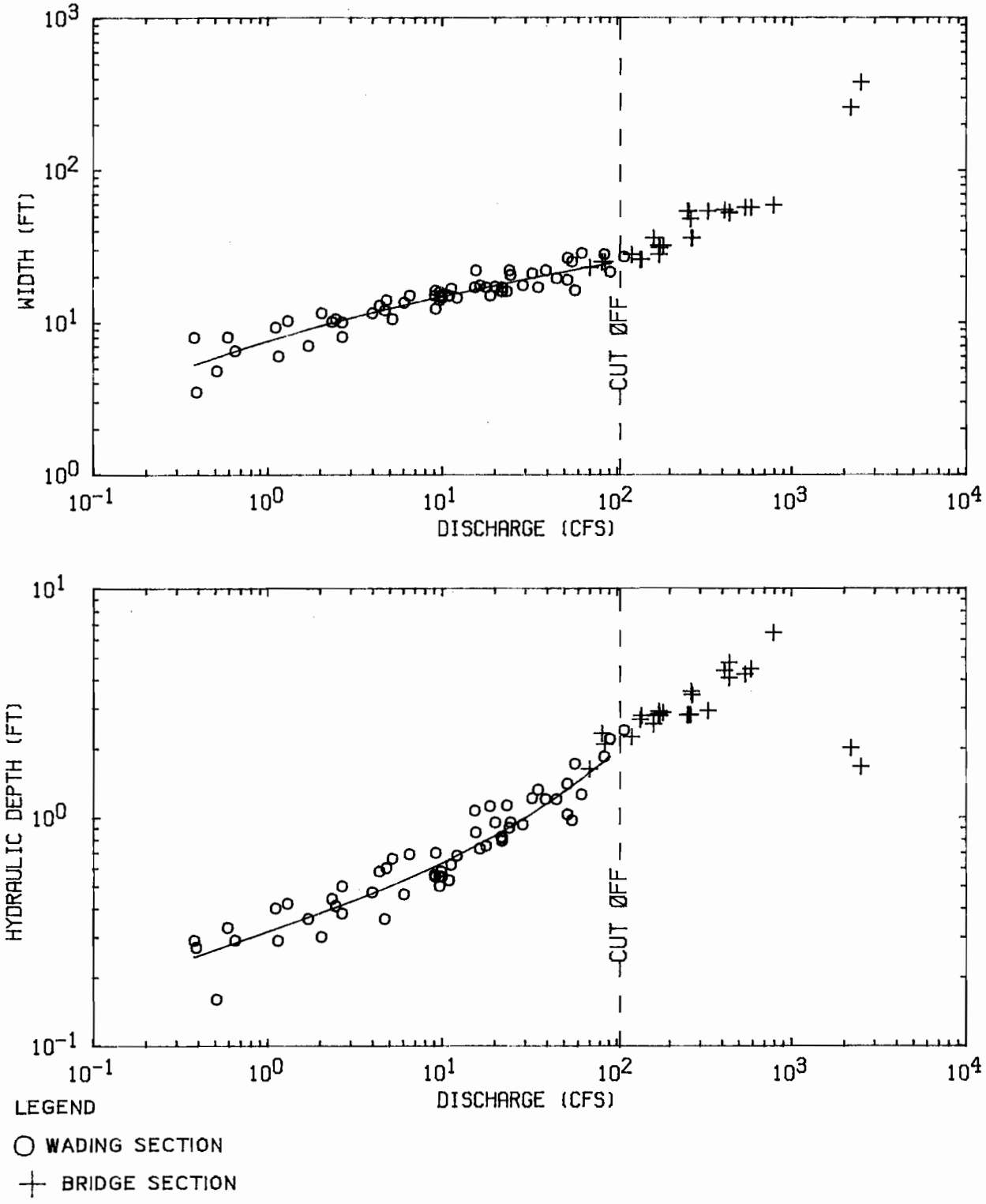

Figure 2a. Station hydraulic geometry, Goose Creek near DeLand

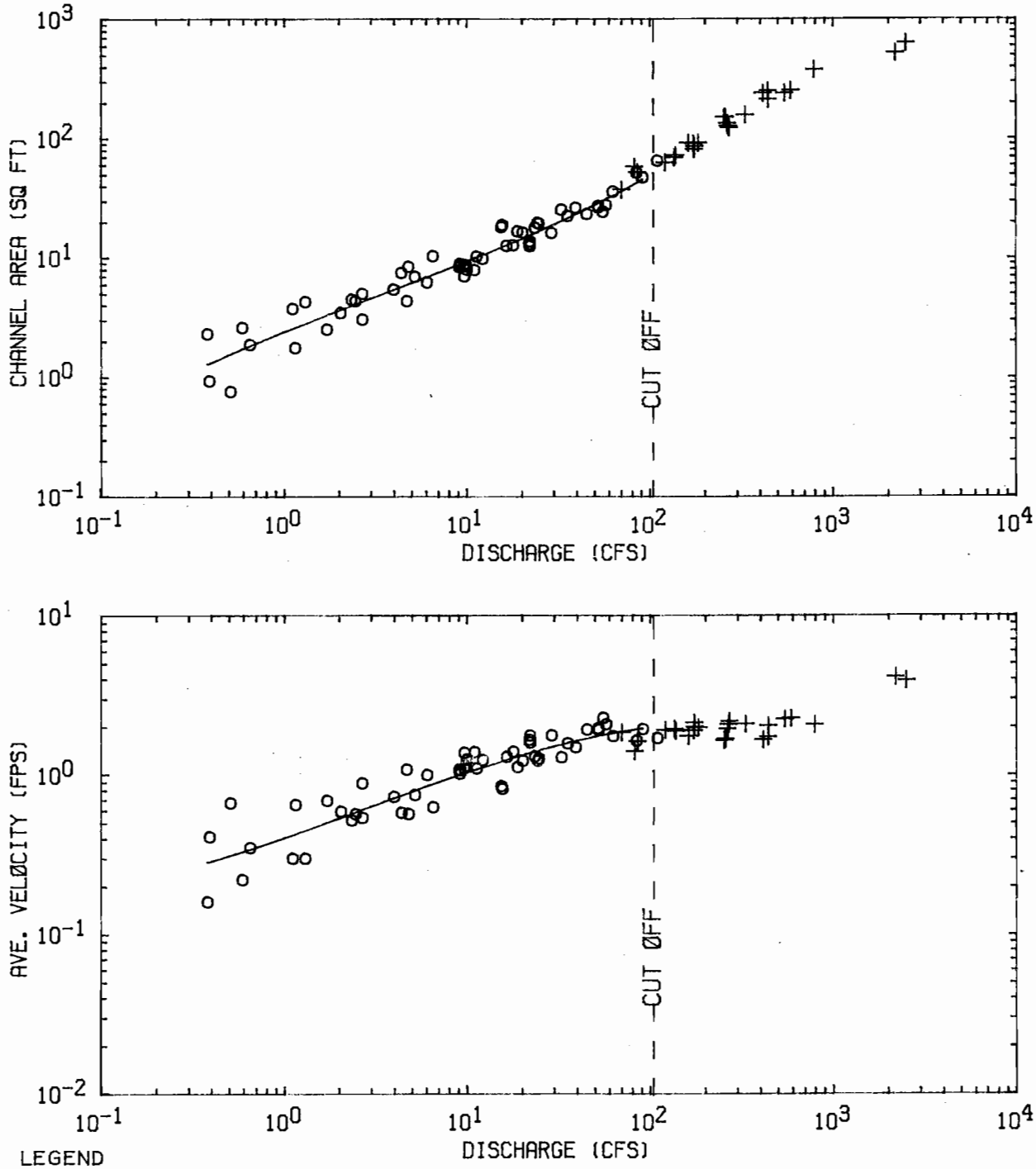

Figure 2b. Station hydraulic geometry, Goose Creek near DeLand

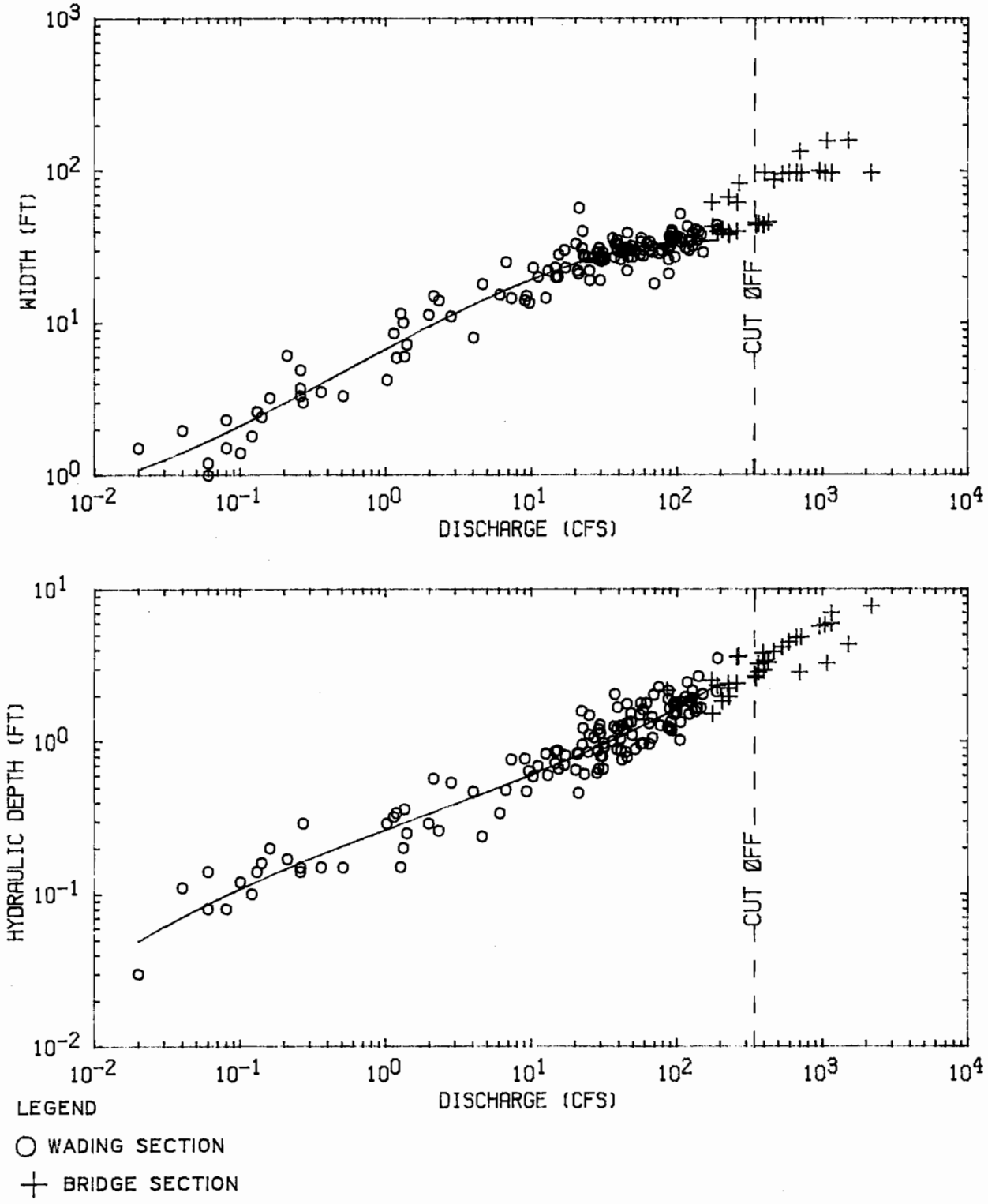

Figure 3a. Station hydraulic geometry, Friends Creek at Argenta

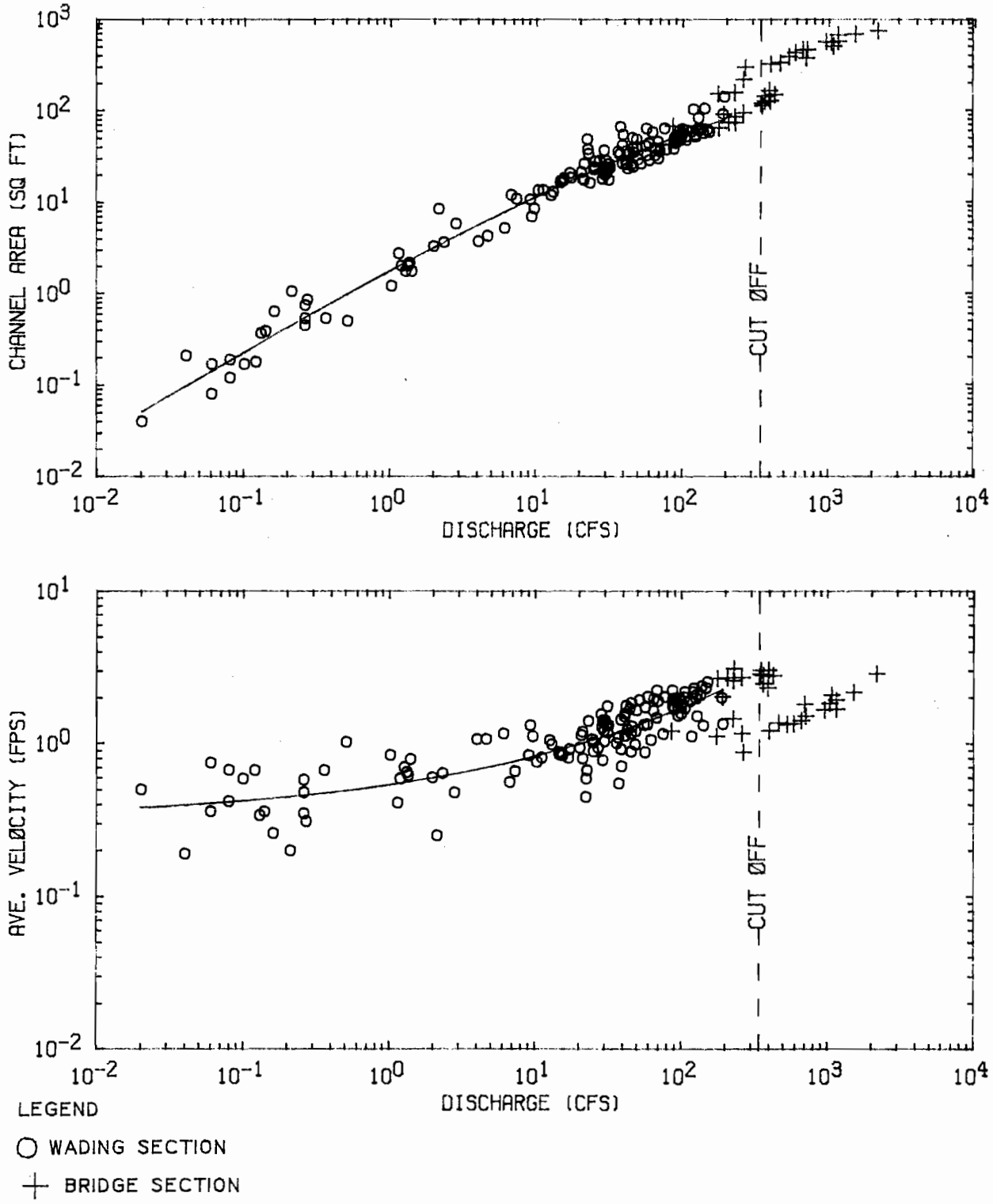

Figure 3b. Station hydraulic geometry, Friends Creek at Argenta

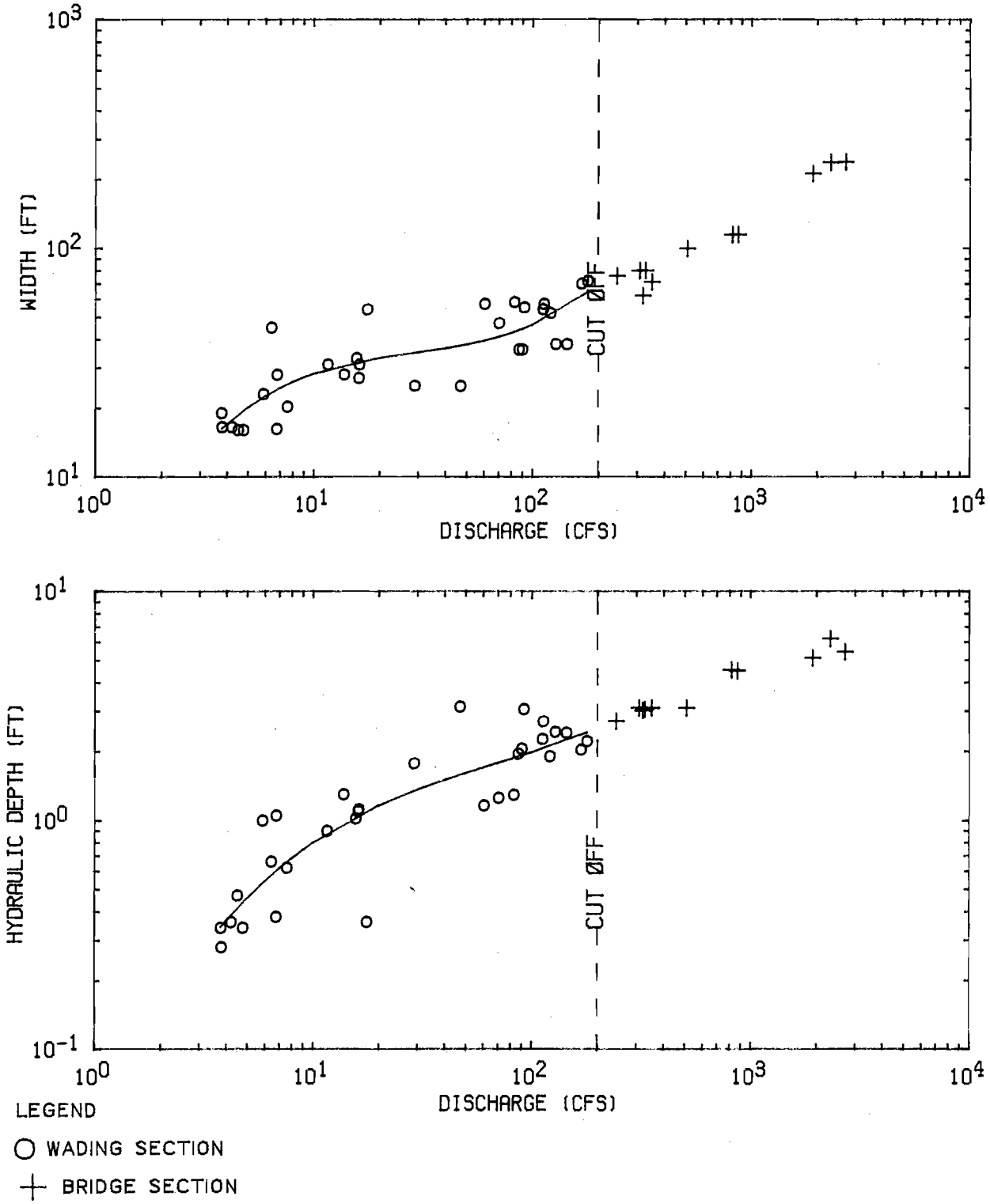

Figure 4a. Station hydraulic geometry, Sangamon River at Fisher

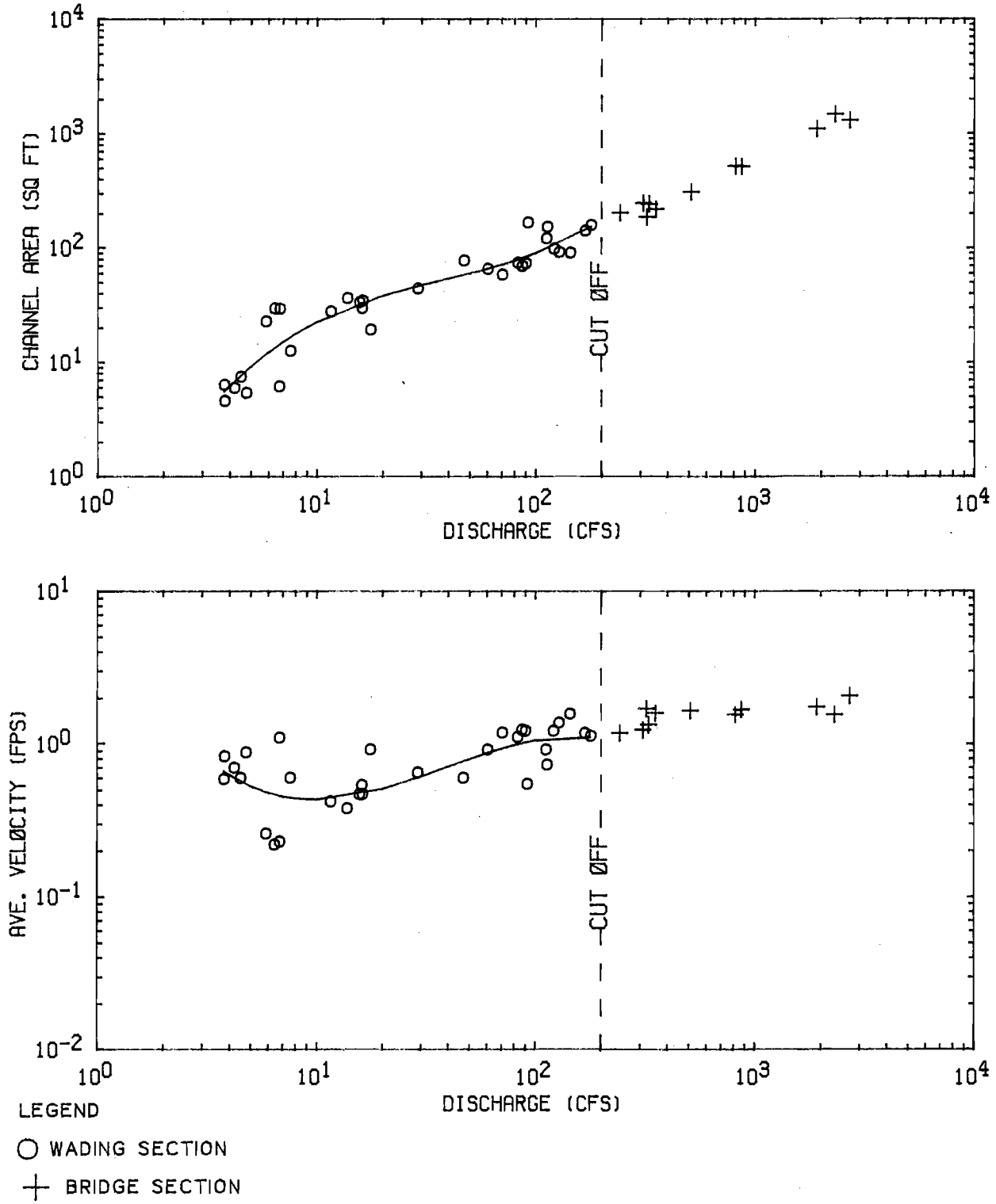

Figure 4b. Station hydraulic geometry, Sangamon River at Fisher

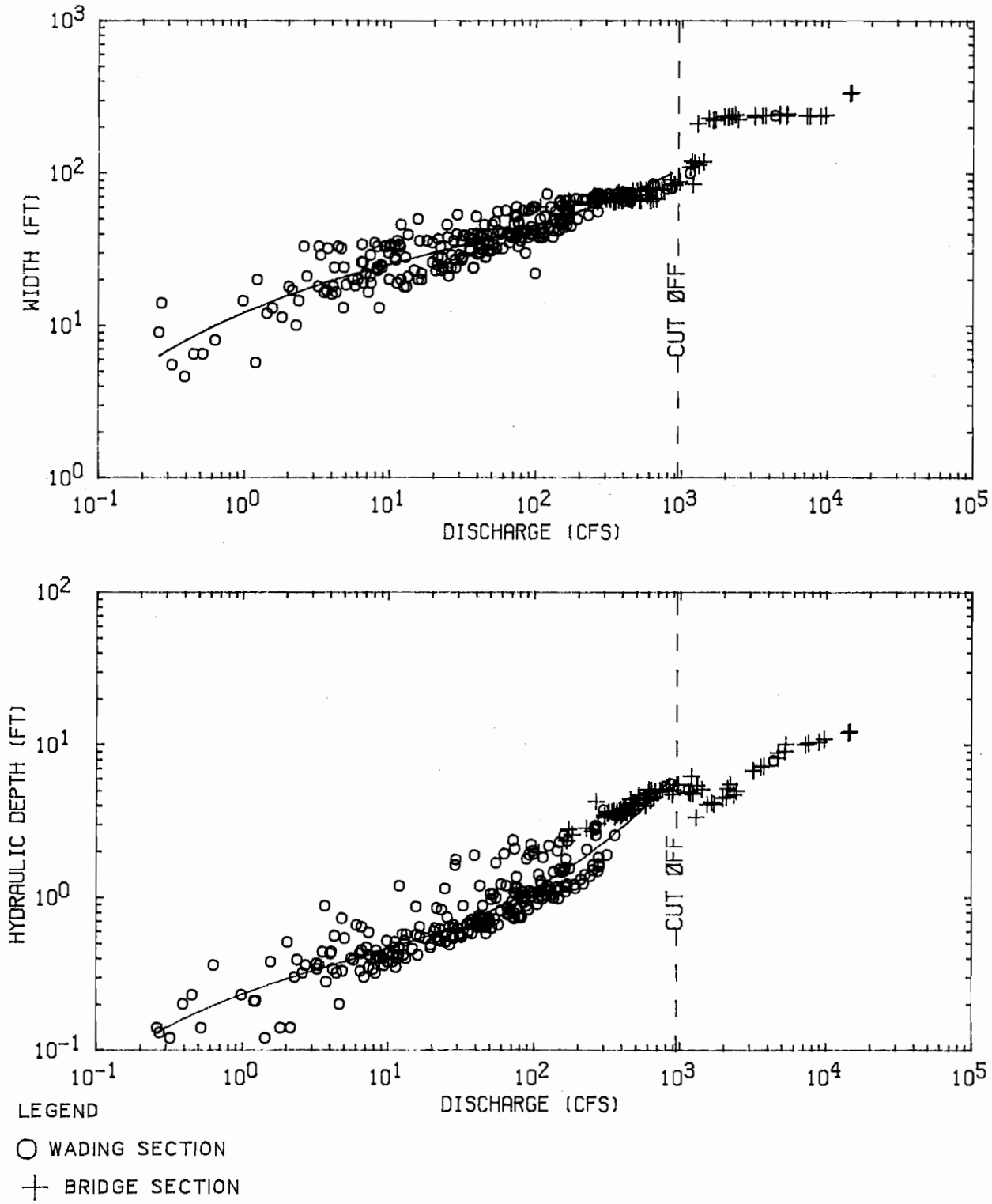

Figure 5a. Station hydraulic geometry, Sangamon River at Mahomet

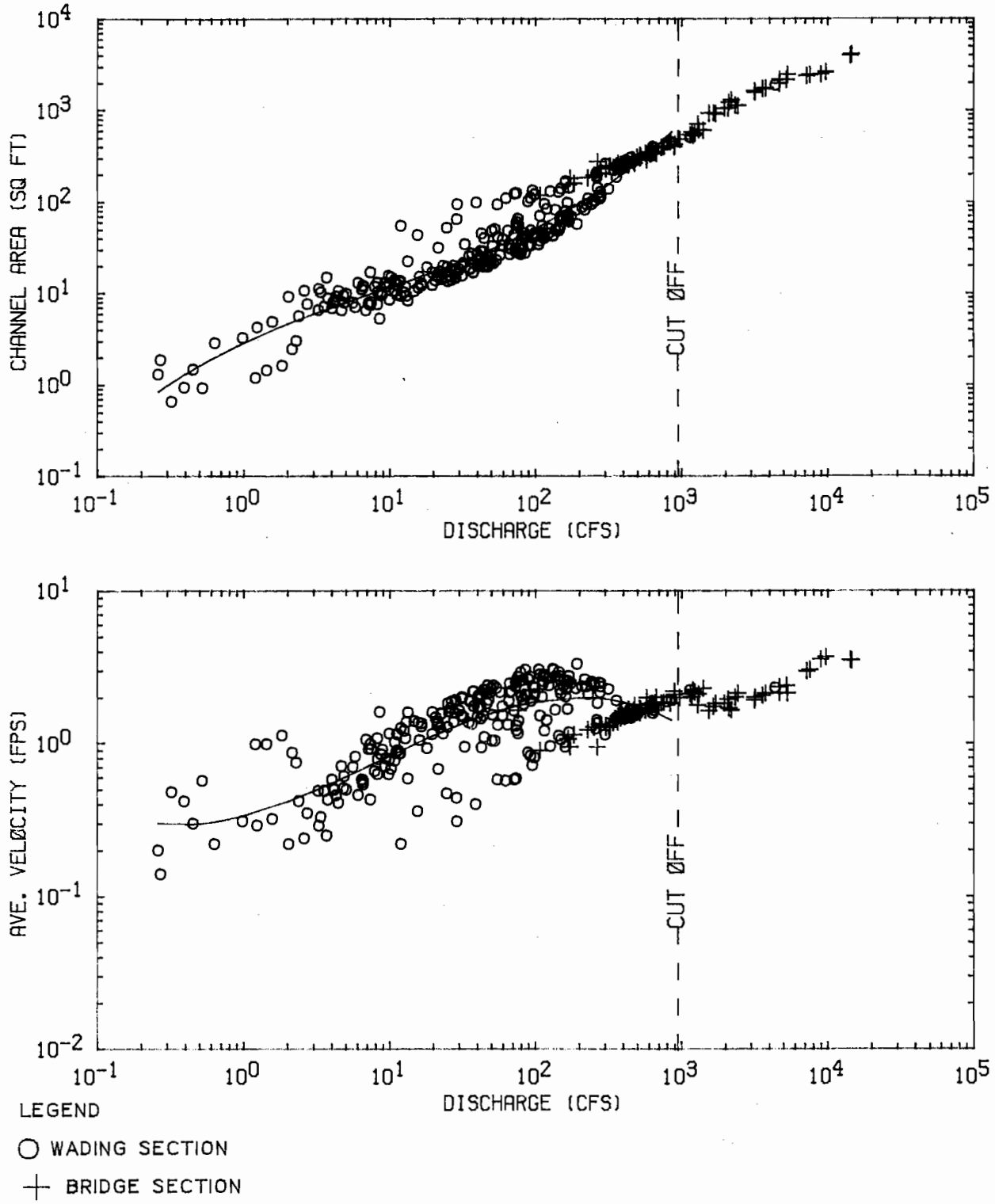

Figure 5b. Station hydraulic geometry, Sangamon River at Mahomet

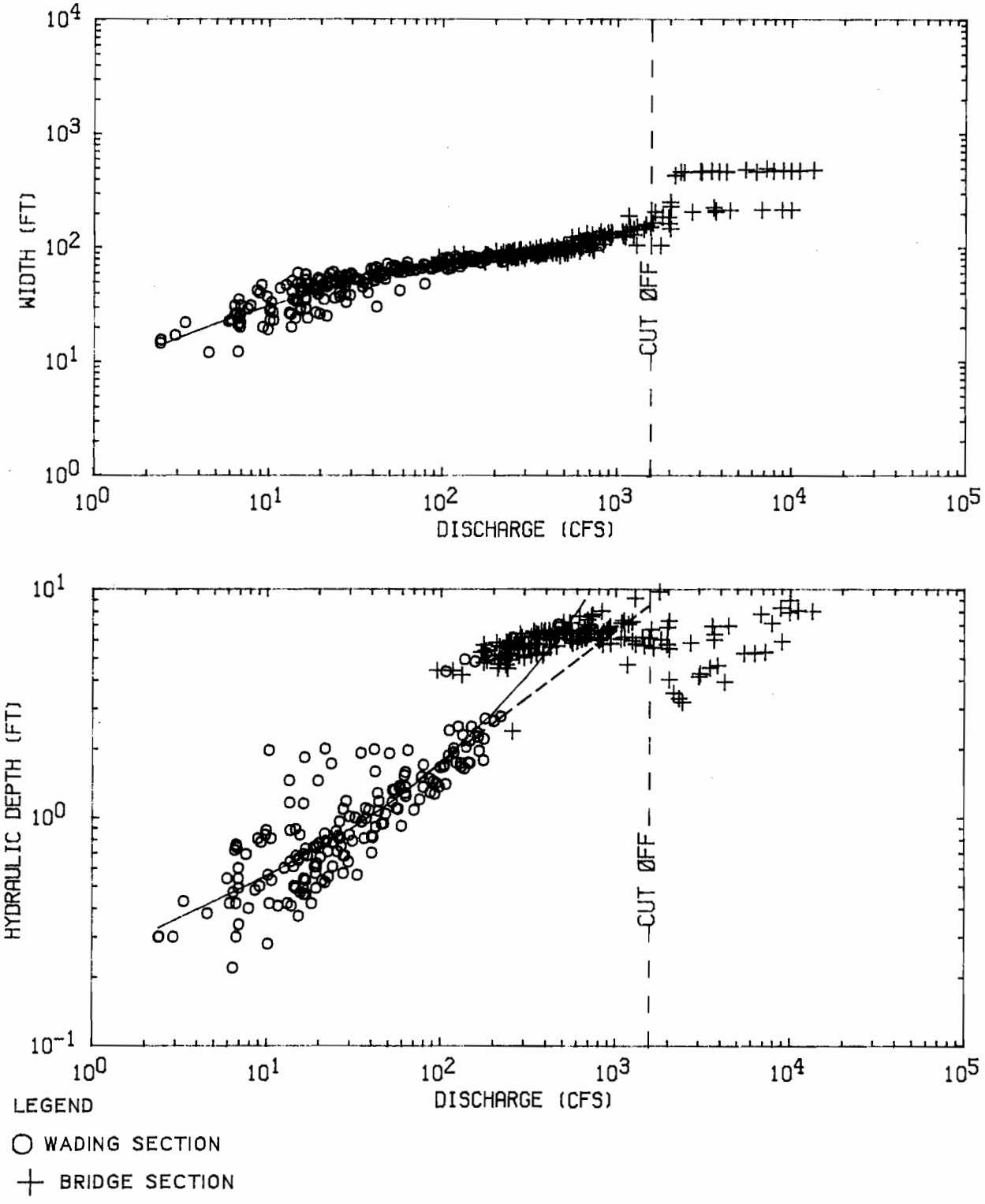

Figure 6a. Station hydraulic geometry, Sangamon River at Monticello

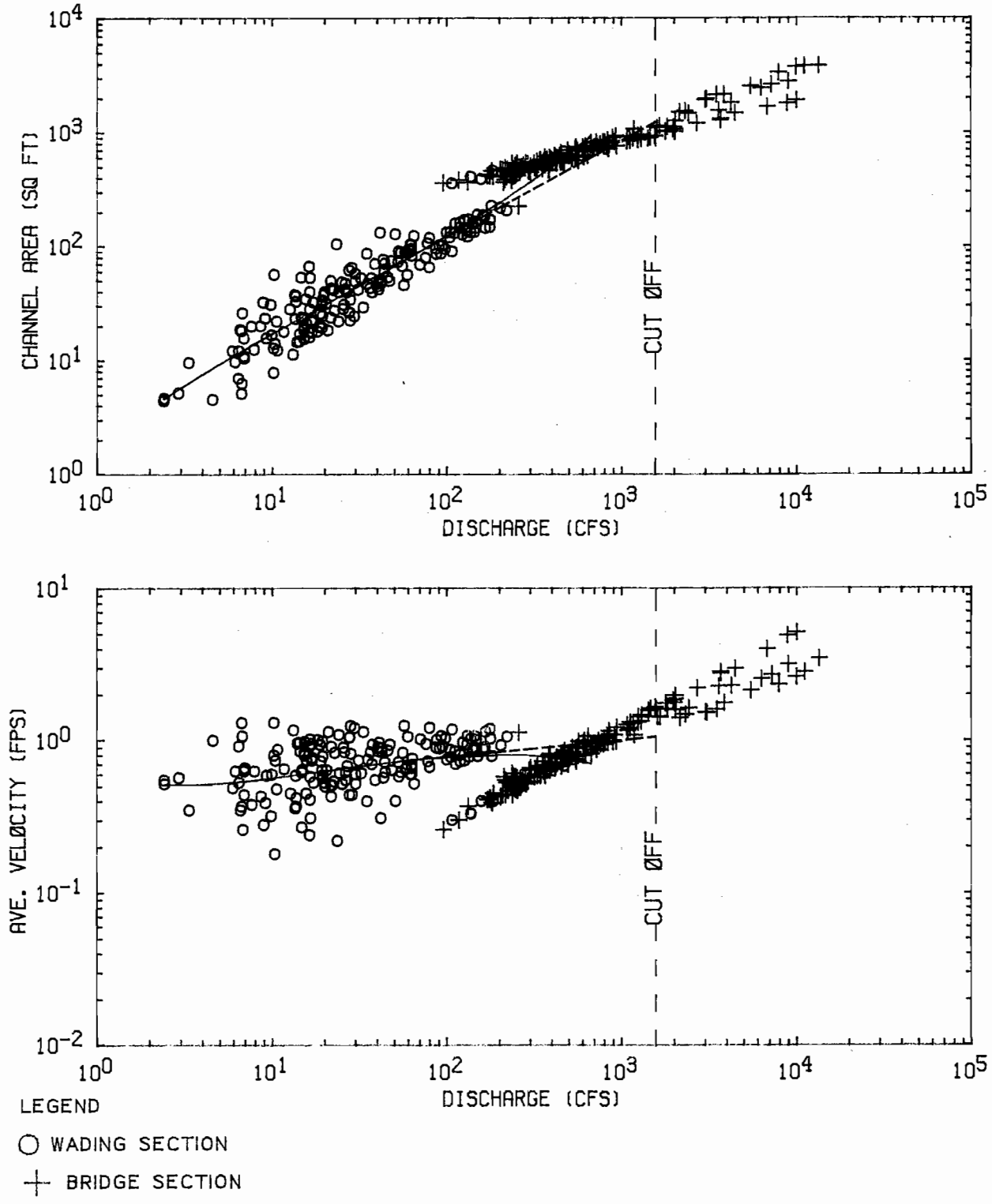

Figure 6b. Station hydraulic geometry, Sangamon River at Monticello

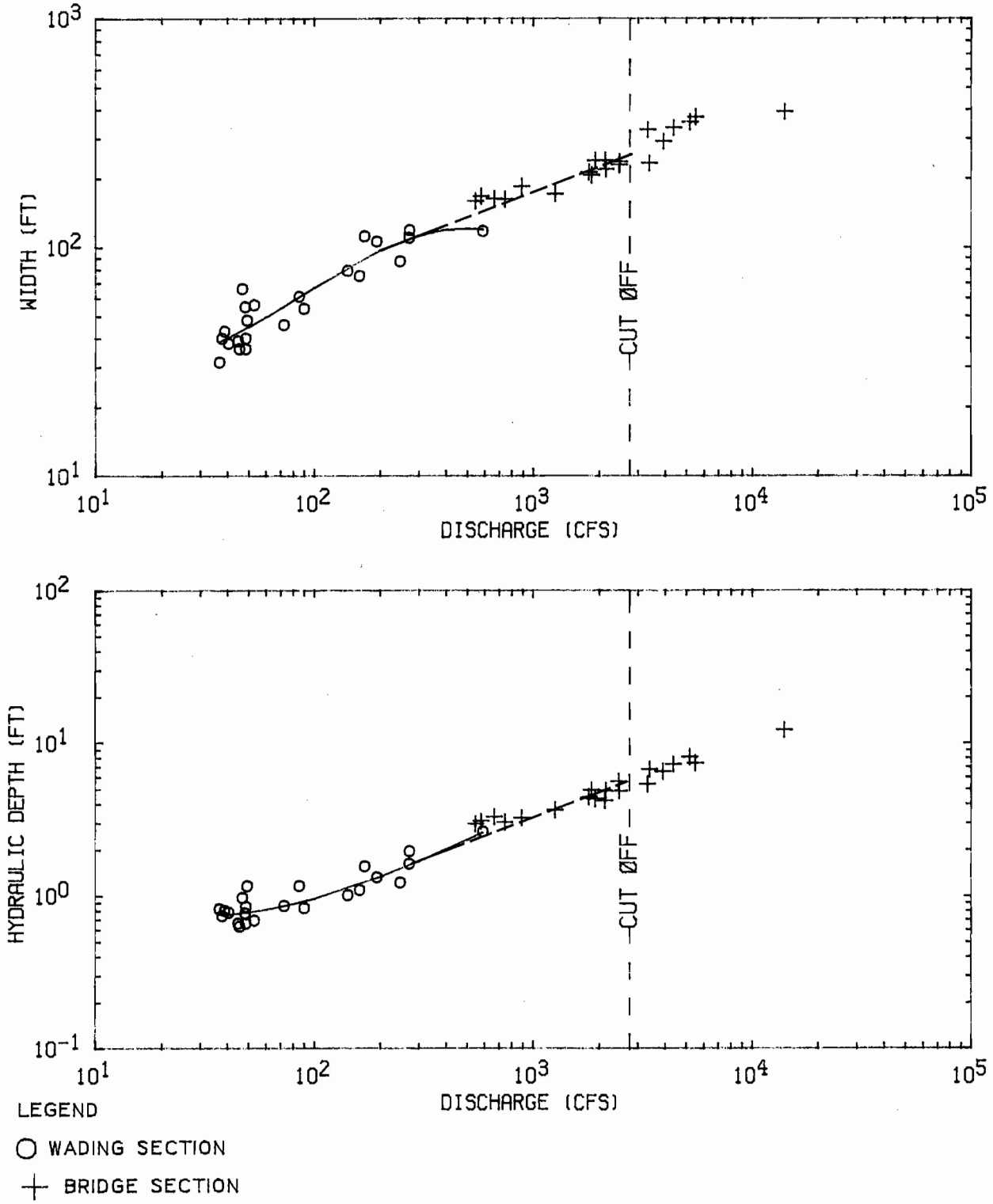

Figure 7a. Station hydraulic geometry, Sangamon River near Niantic

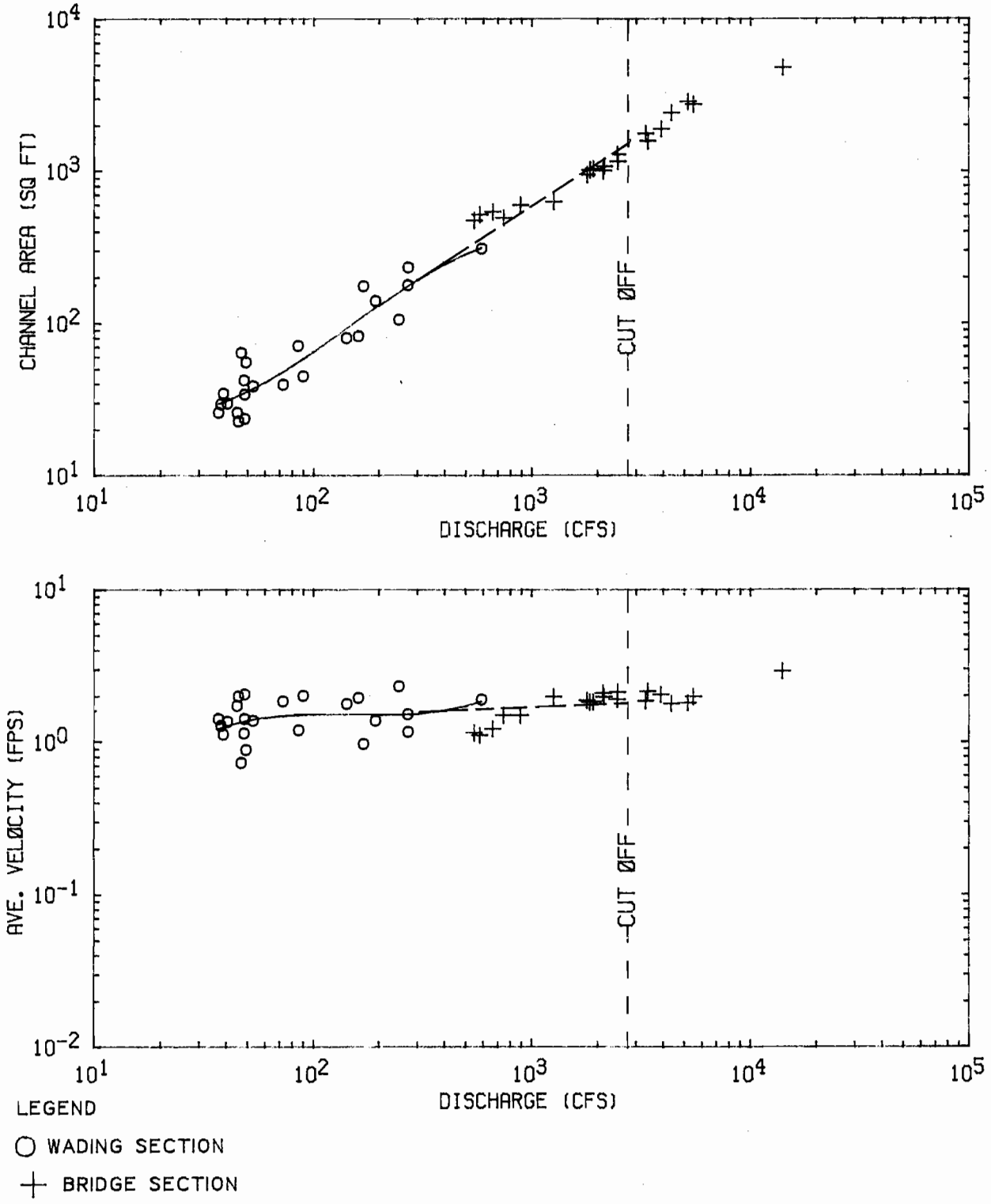

Figure 7b. Station hydraulic geometry, Sangamon River near Niantic

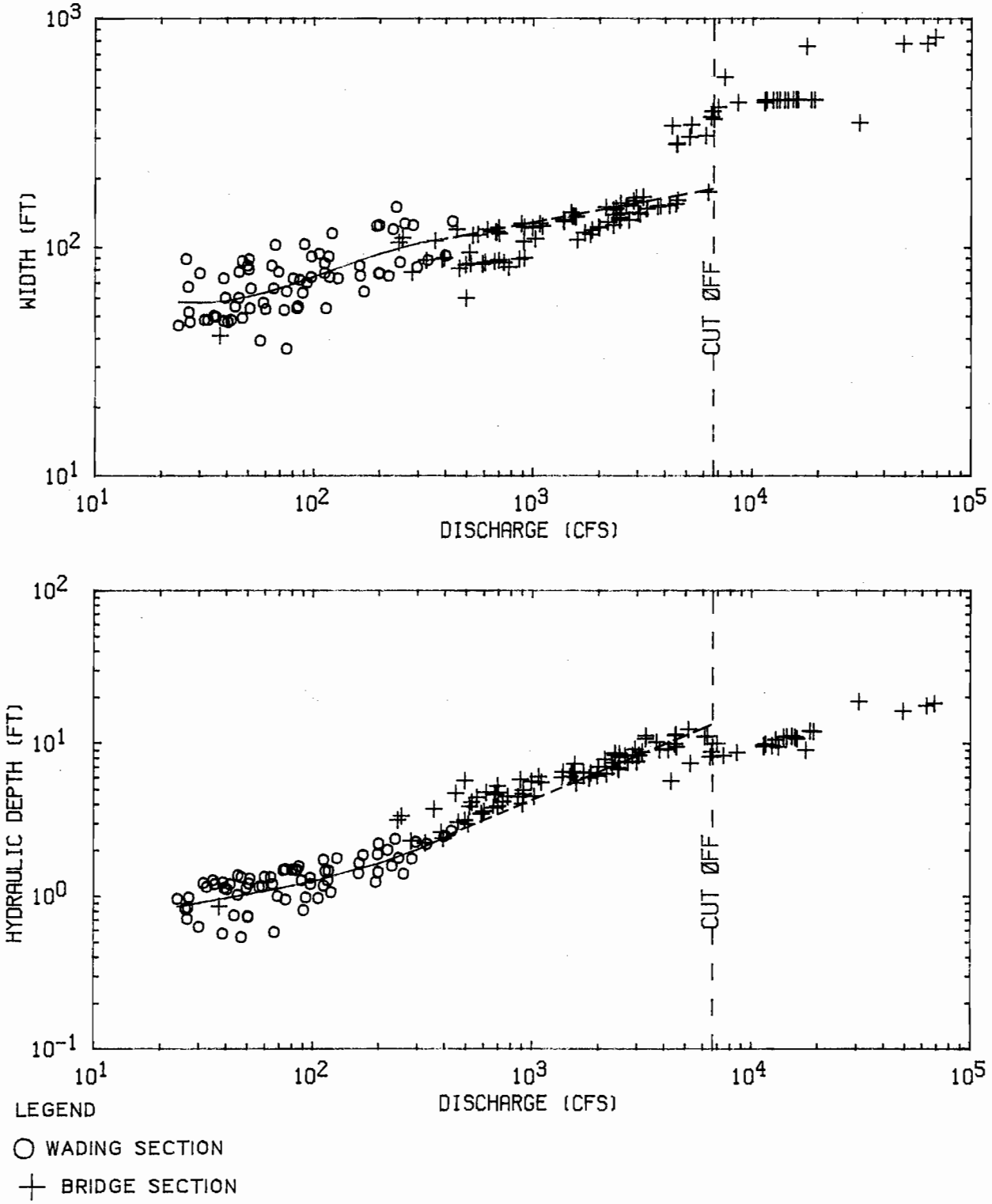

Figure 8a. Station hydraulic geometry, Sangamon River at Riverton

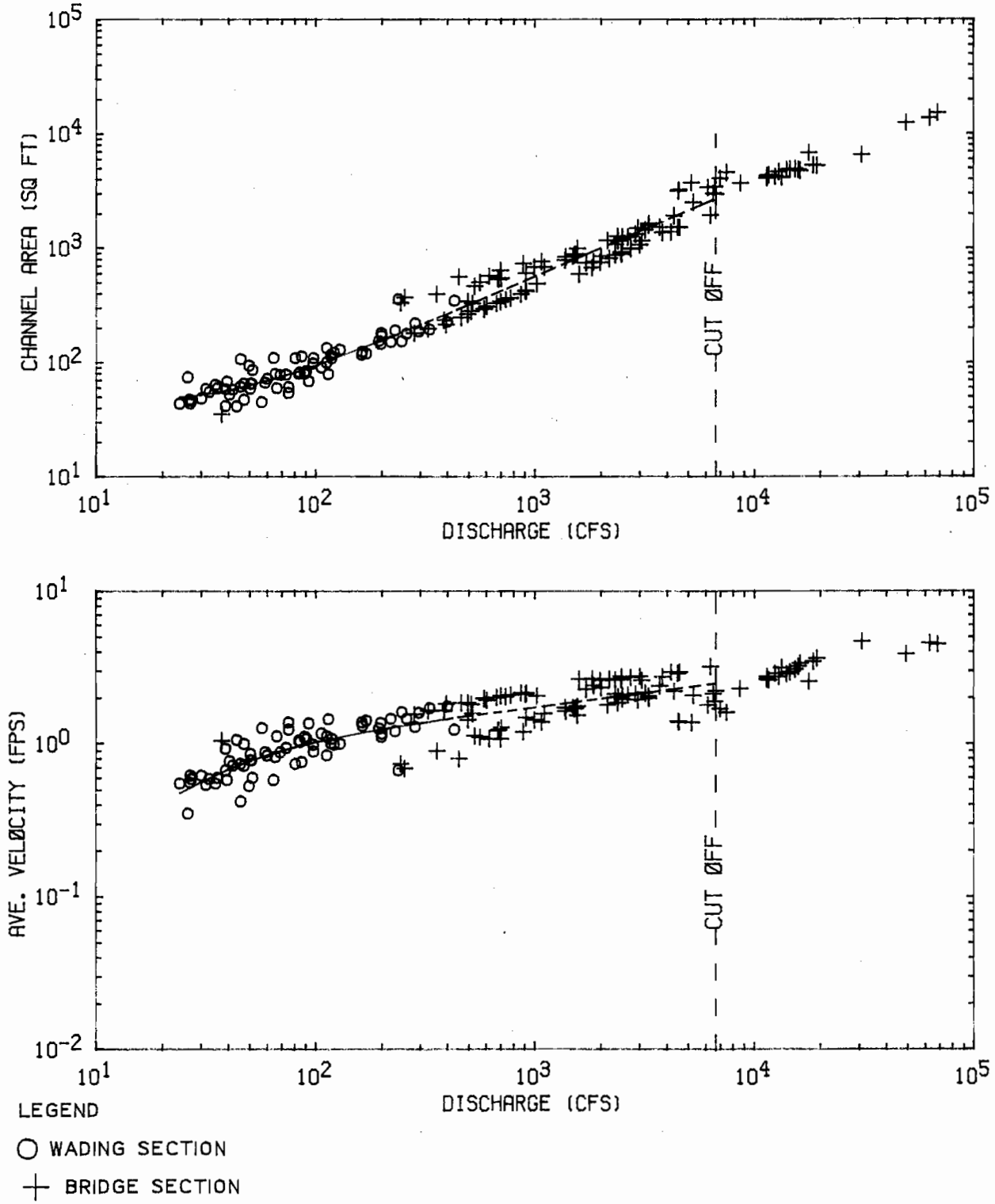

Figure 8b. Station hydraulic geometry, Sangamon River at Riverton

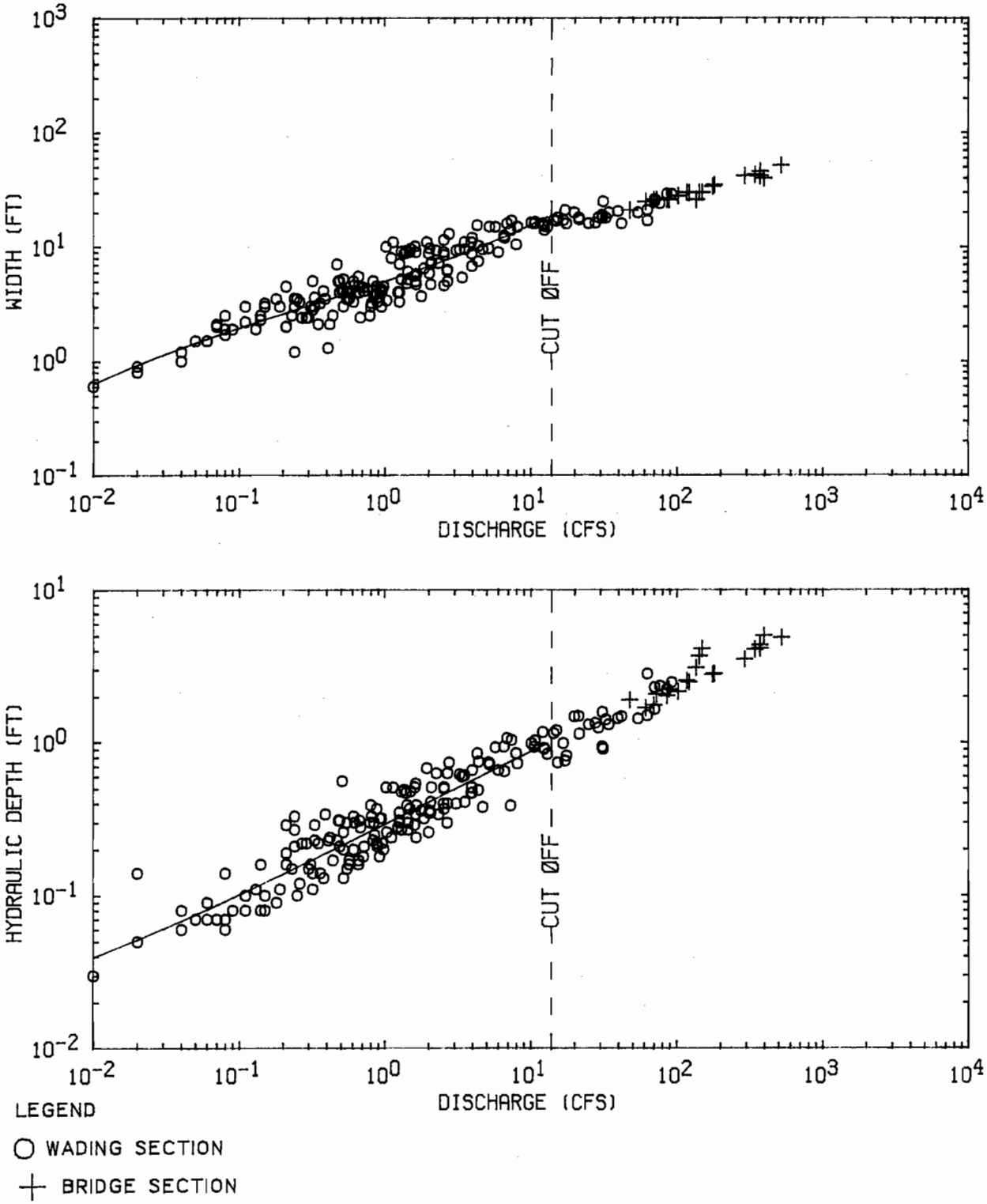

Figure 9a. Station hydraulic geometry, South Fork Sangamon near Nokomis

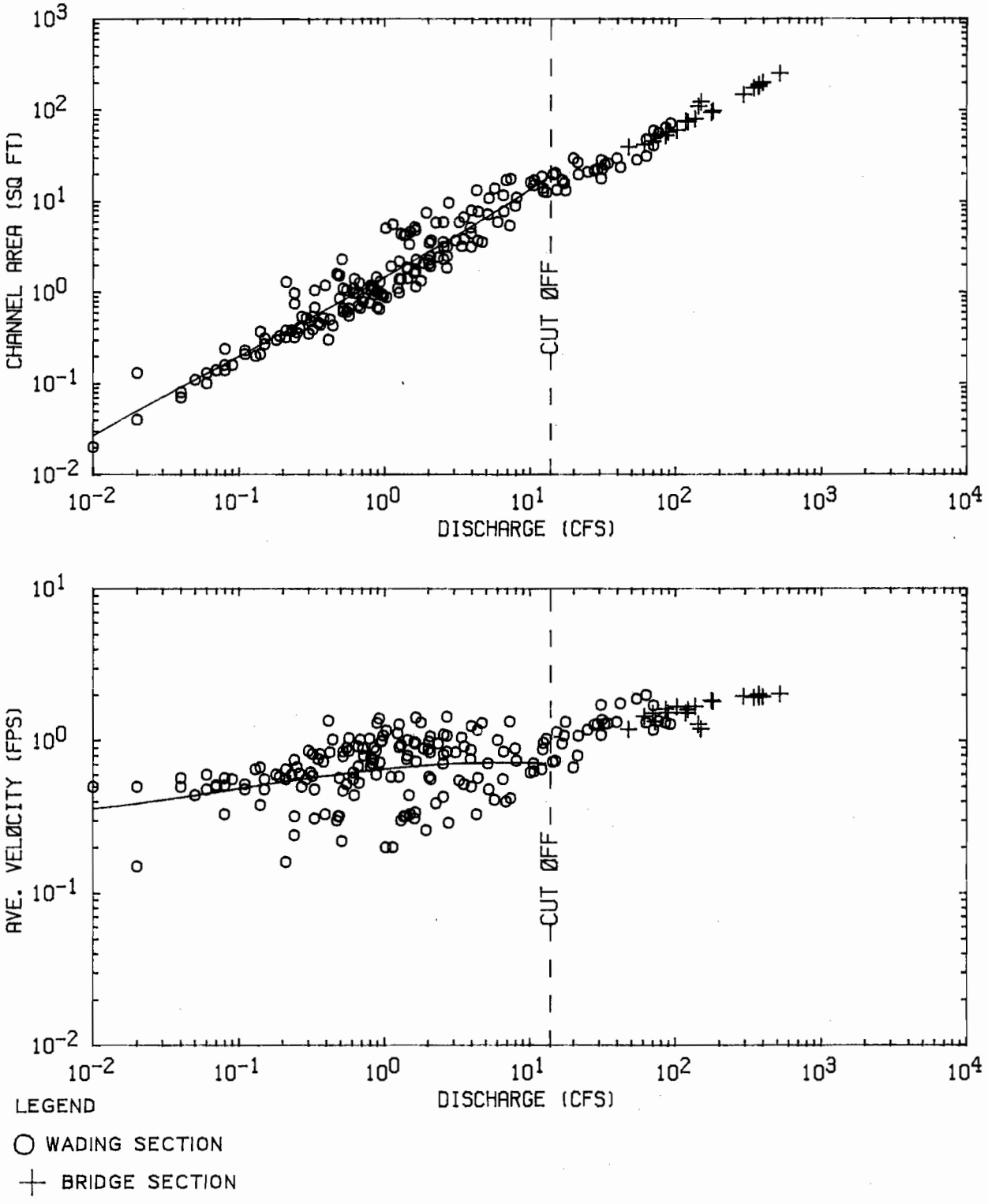

Figure 9b. Station hydraulic geometry, South Fork Sangamon near Nokomis

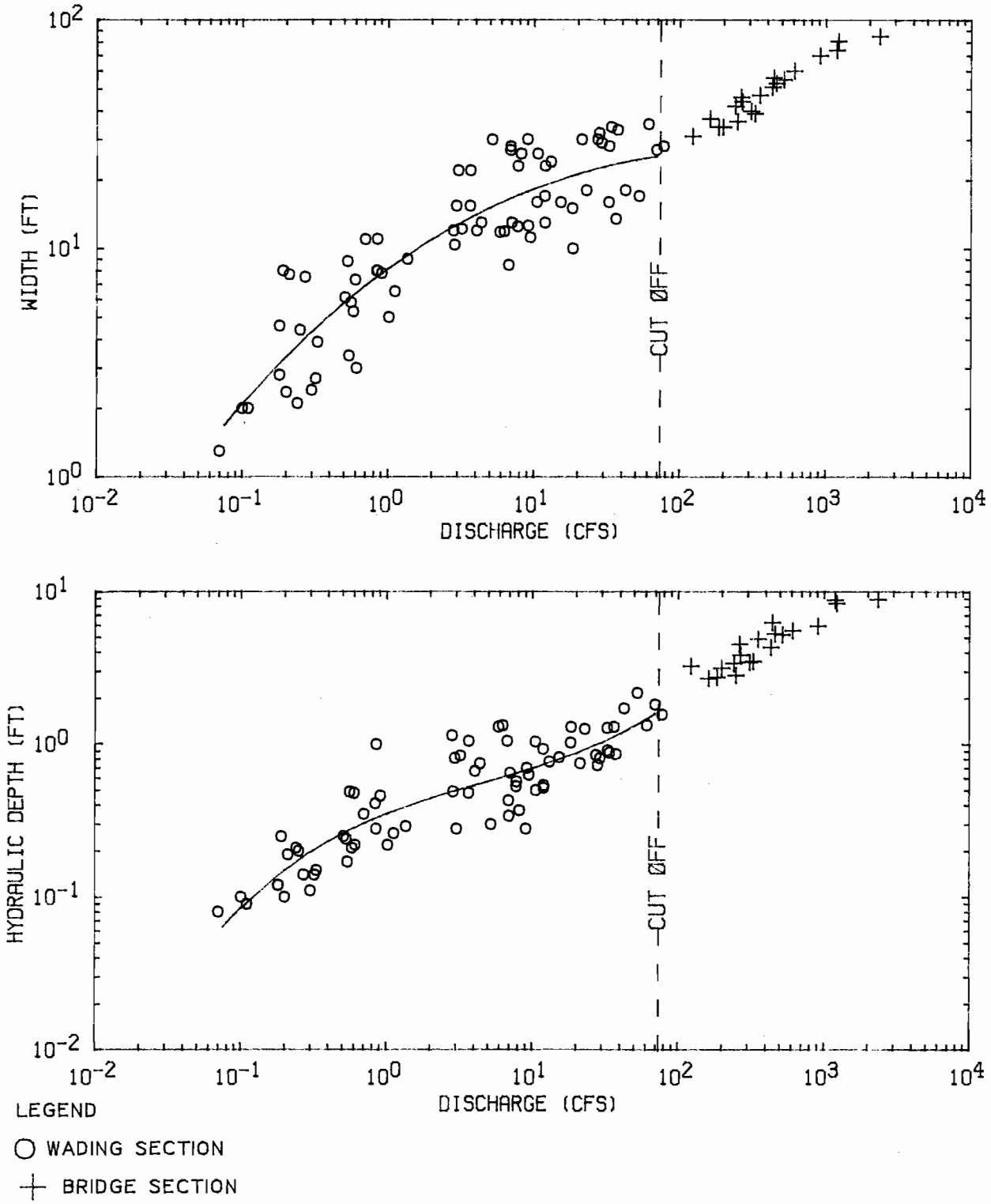

Figure 10a. Station hydraulic geometry, Brush Creek near Divernon

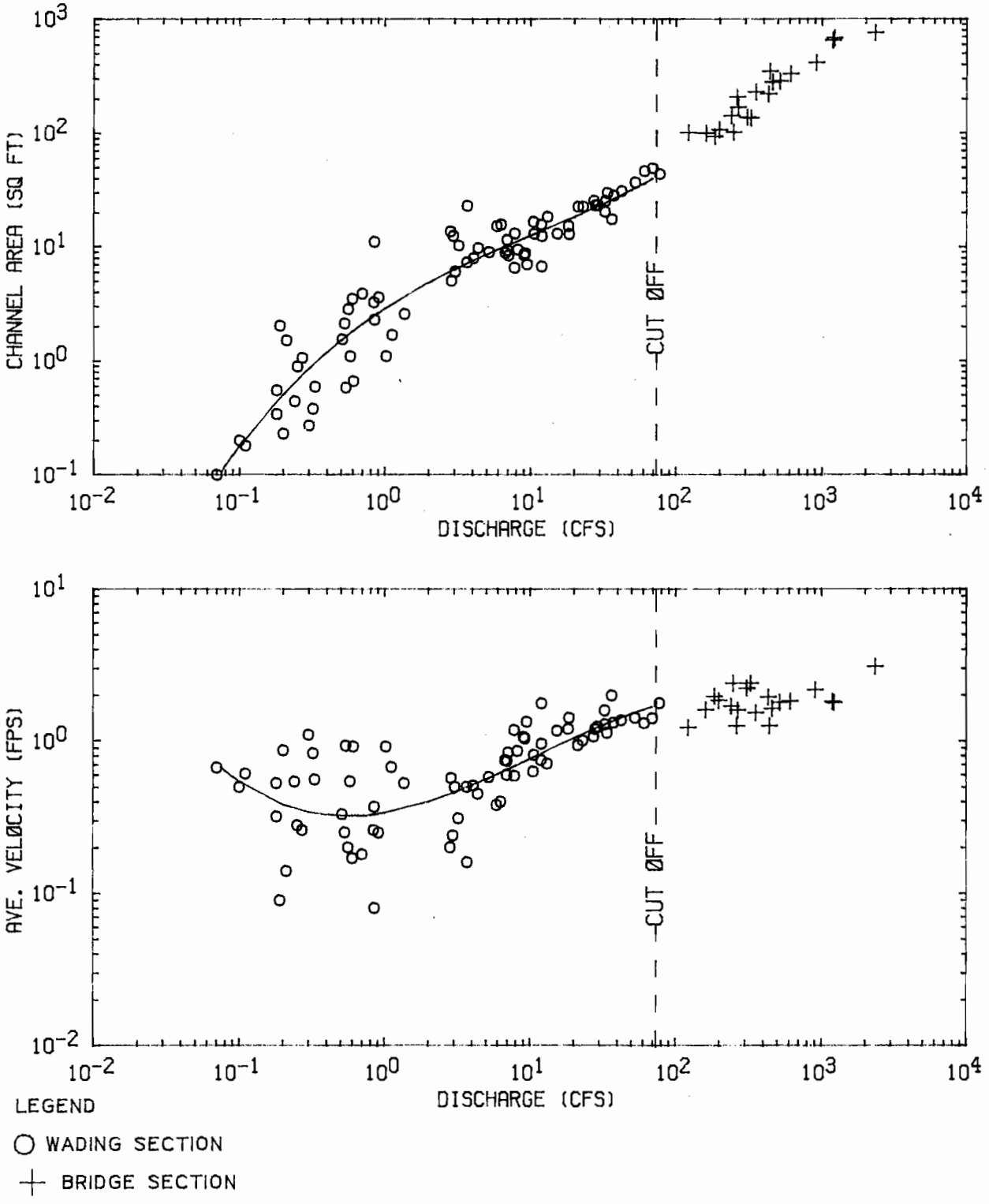

Figure 10b. Station hydraulic geometry, Brush Creek near Divernon

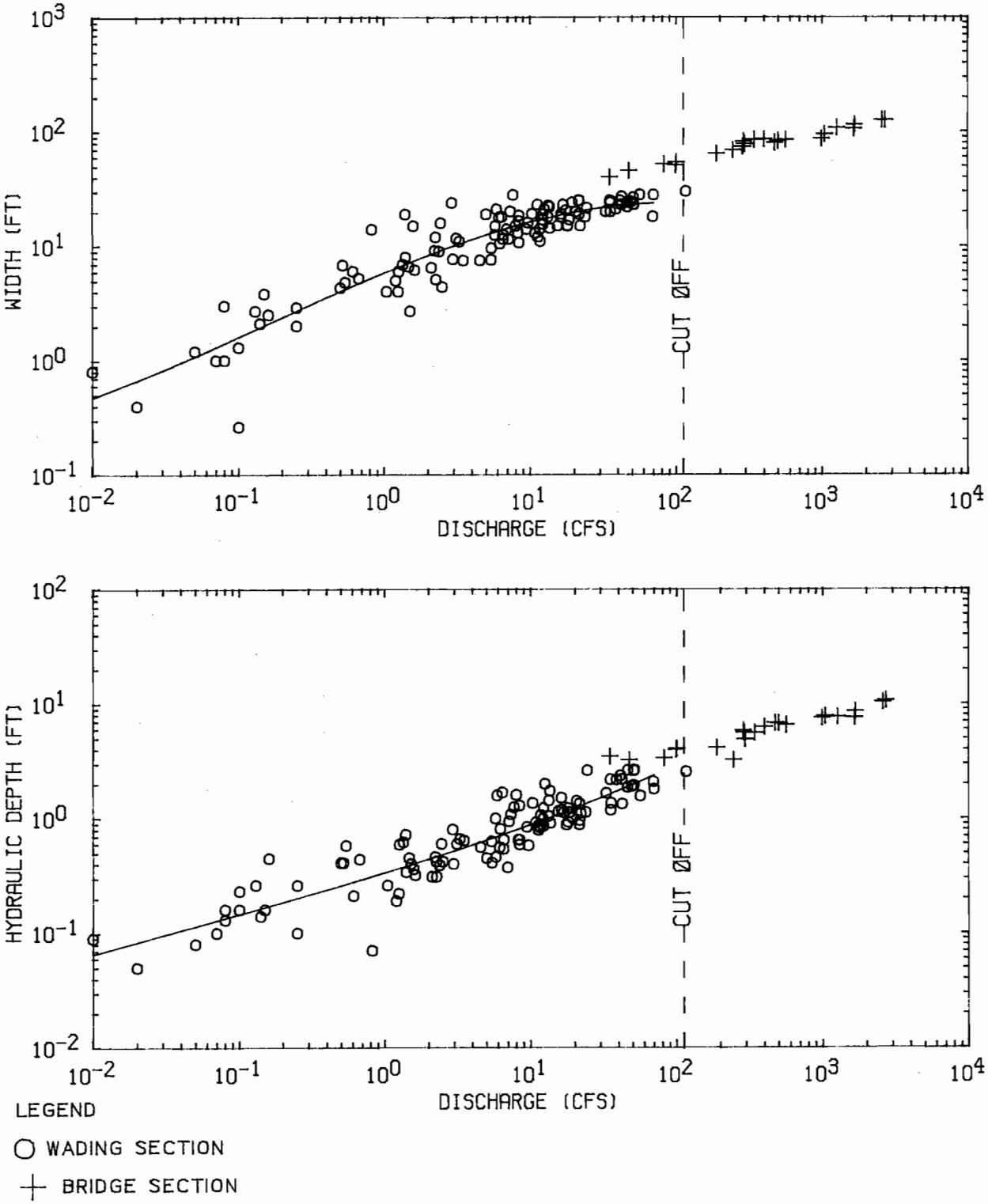

Figure 11a. Station hydraulic geometry, Horse Creek at Pawnee

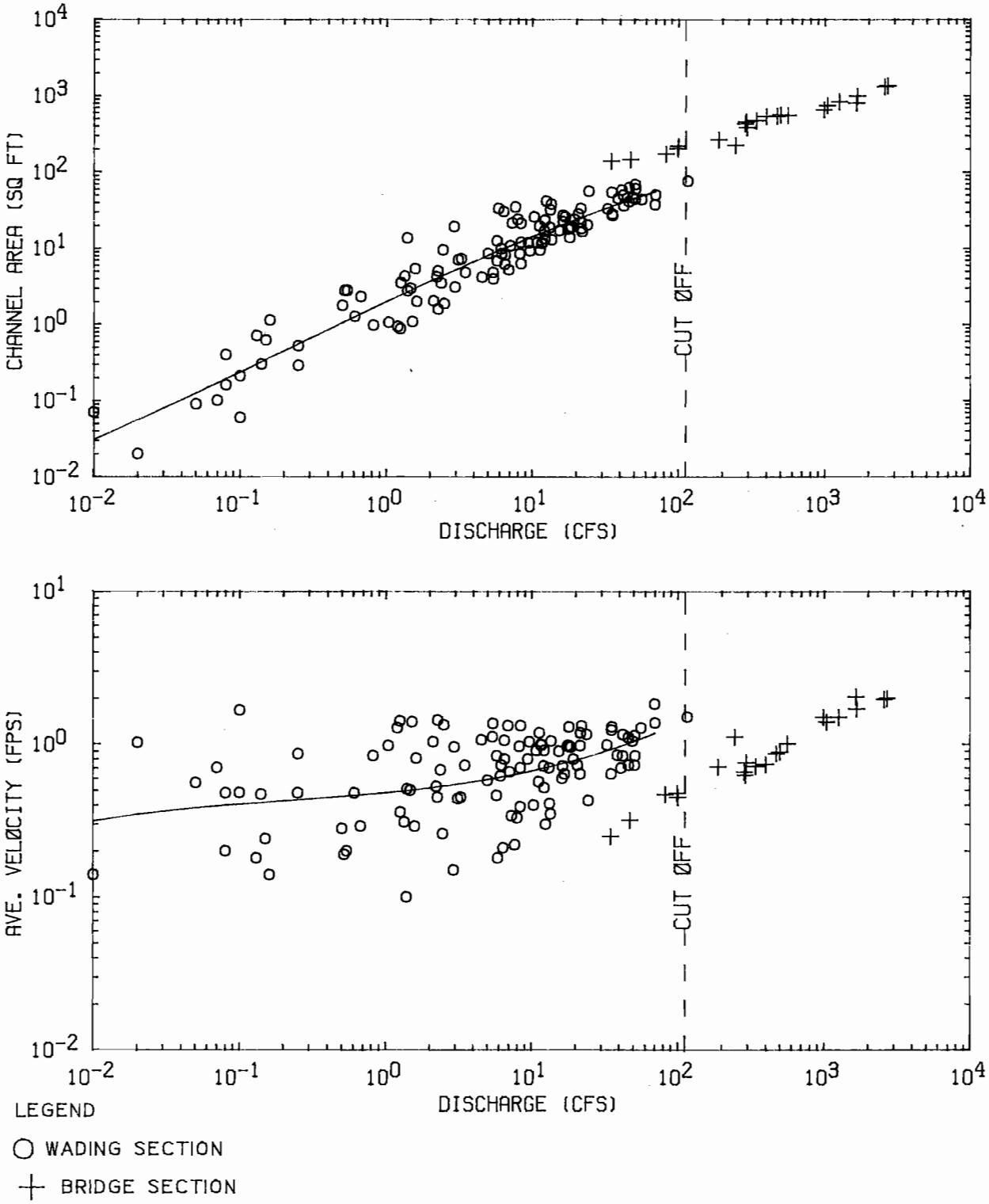

Figure 11b. Station hydraulic geometry, Horse Creek at Pawnee

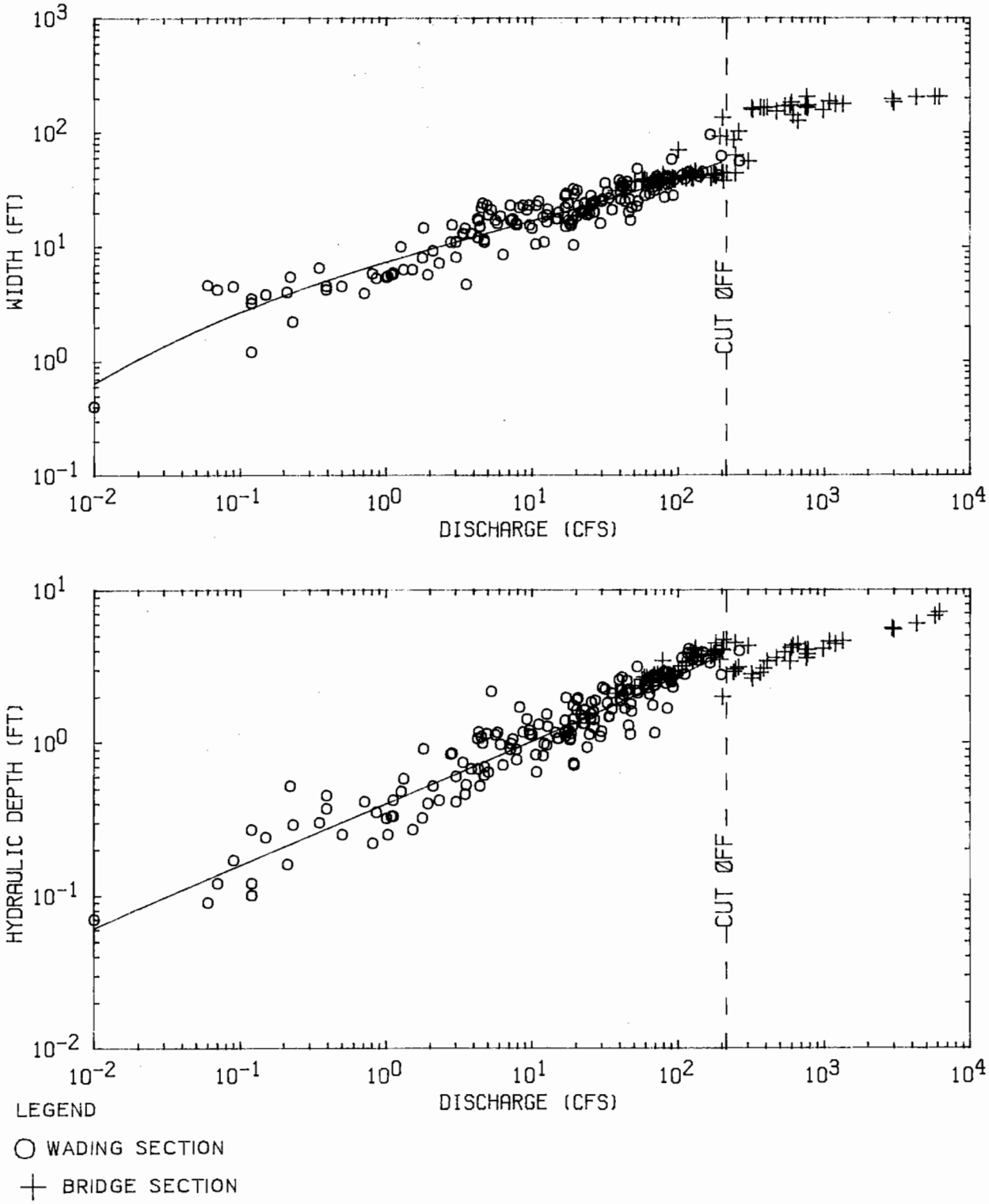

Figure 12a. Station hydraulic geometry, Spring Creek at Springfield

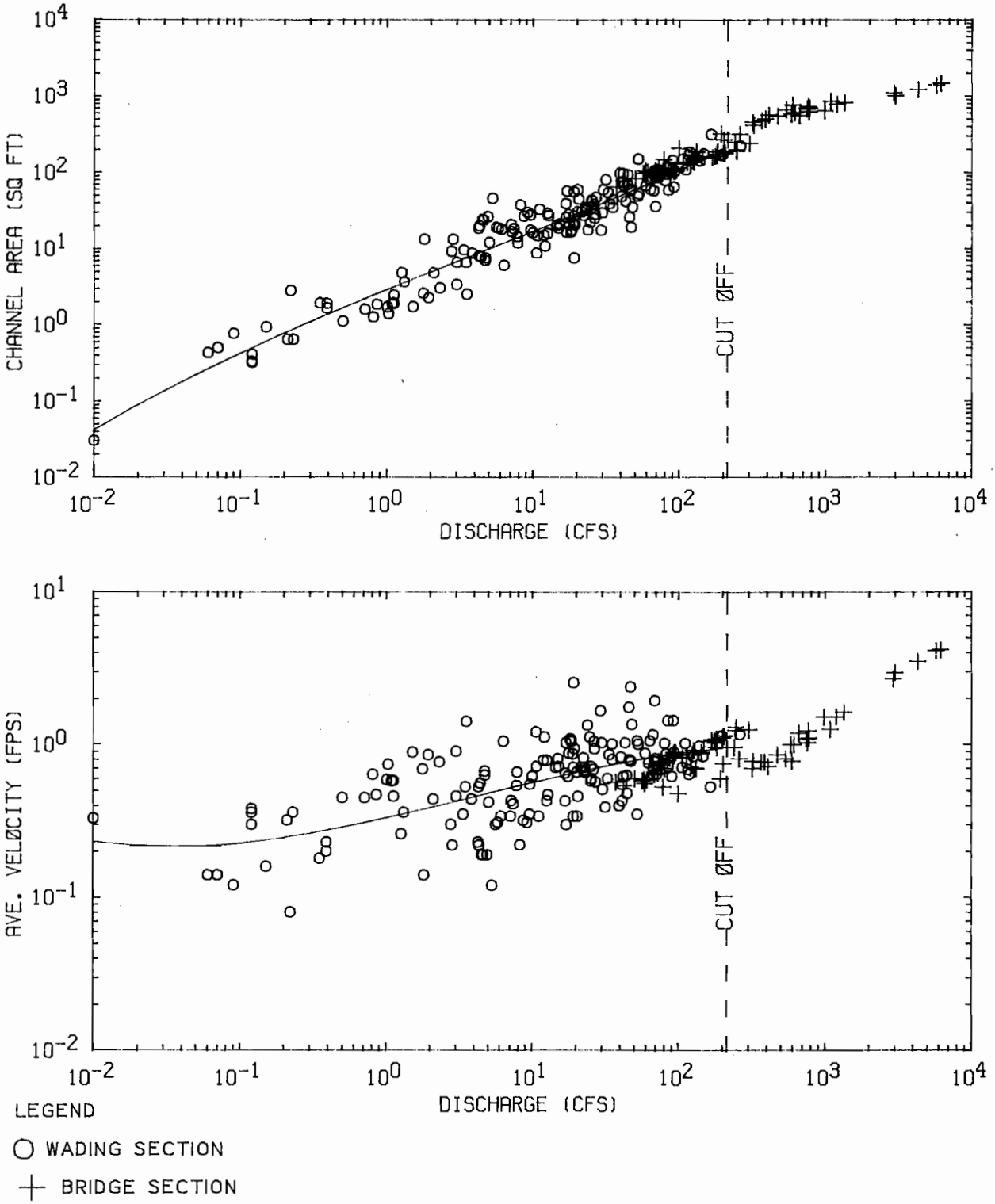

Figure 12b. Station hydraulic geometry, Spring Creek at Springfield

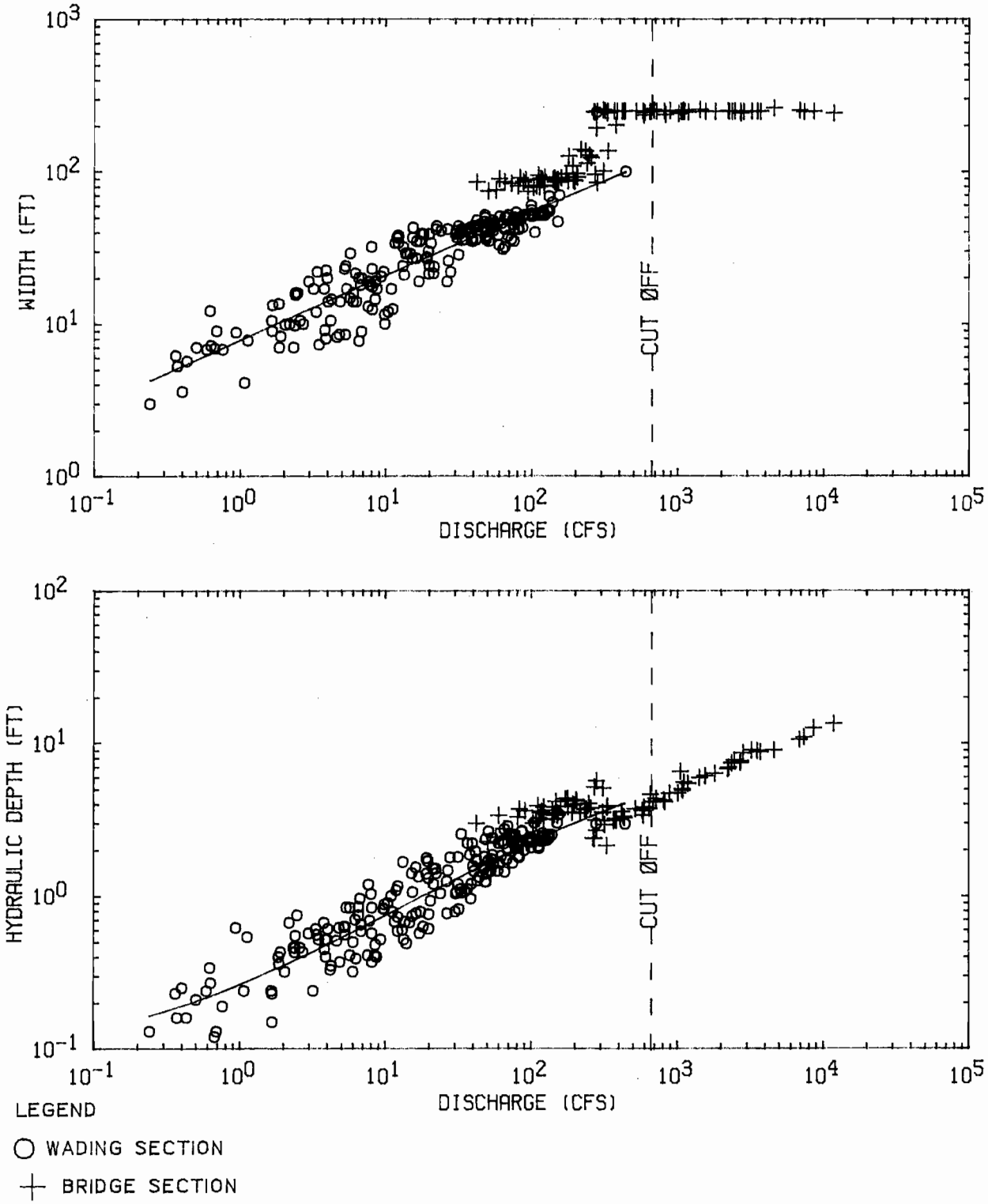

Figure 13a. Station hydraulic geometry, Flat Branch near Taylorville

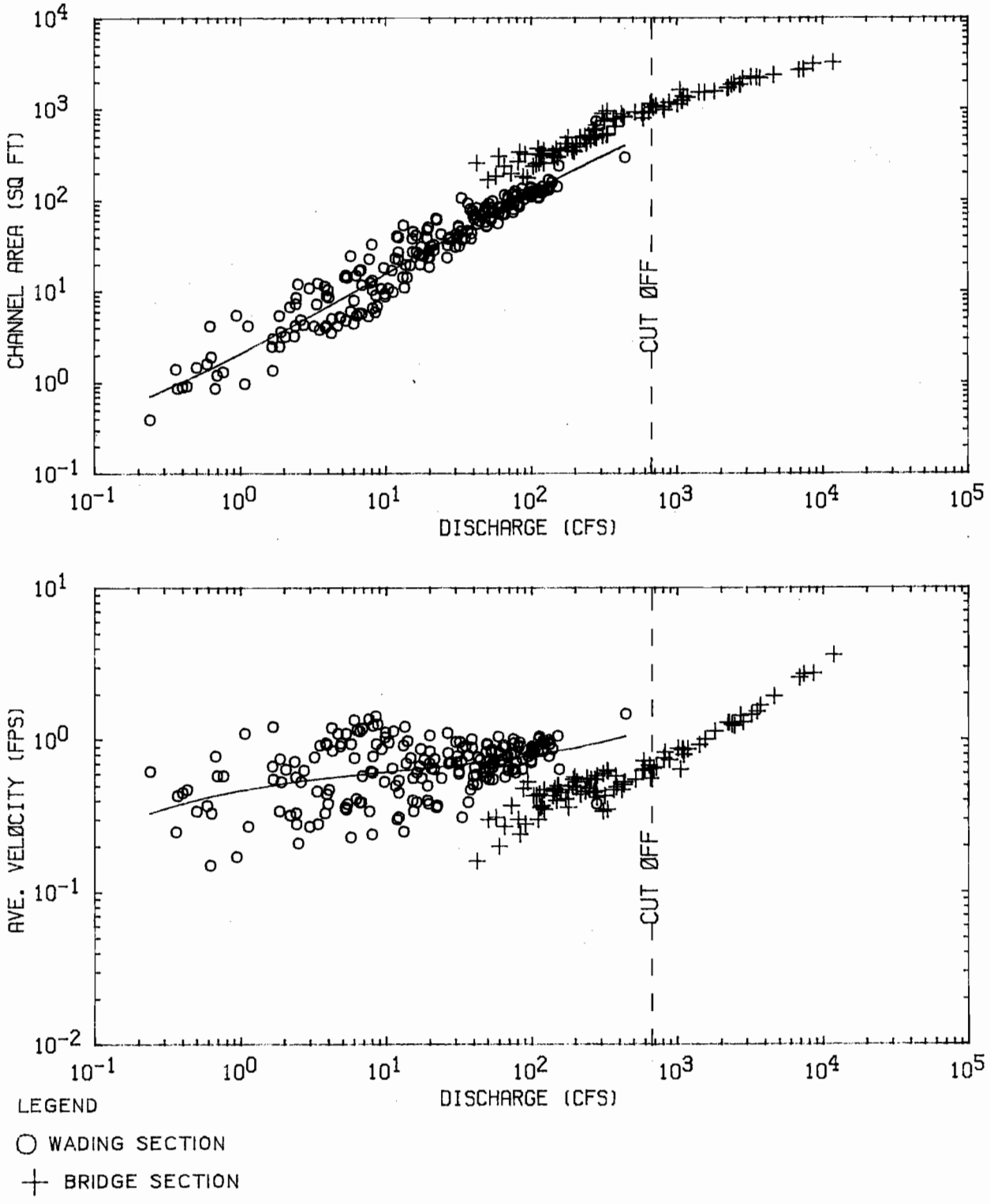

Figure 13b. Station hydraulic geometry, Flat Branch near Taylorville

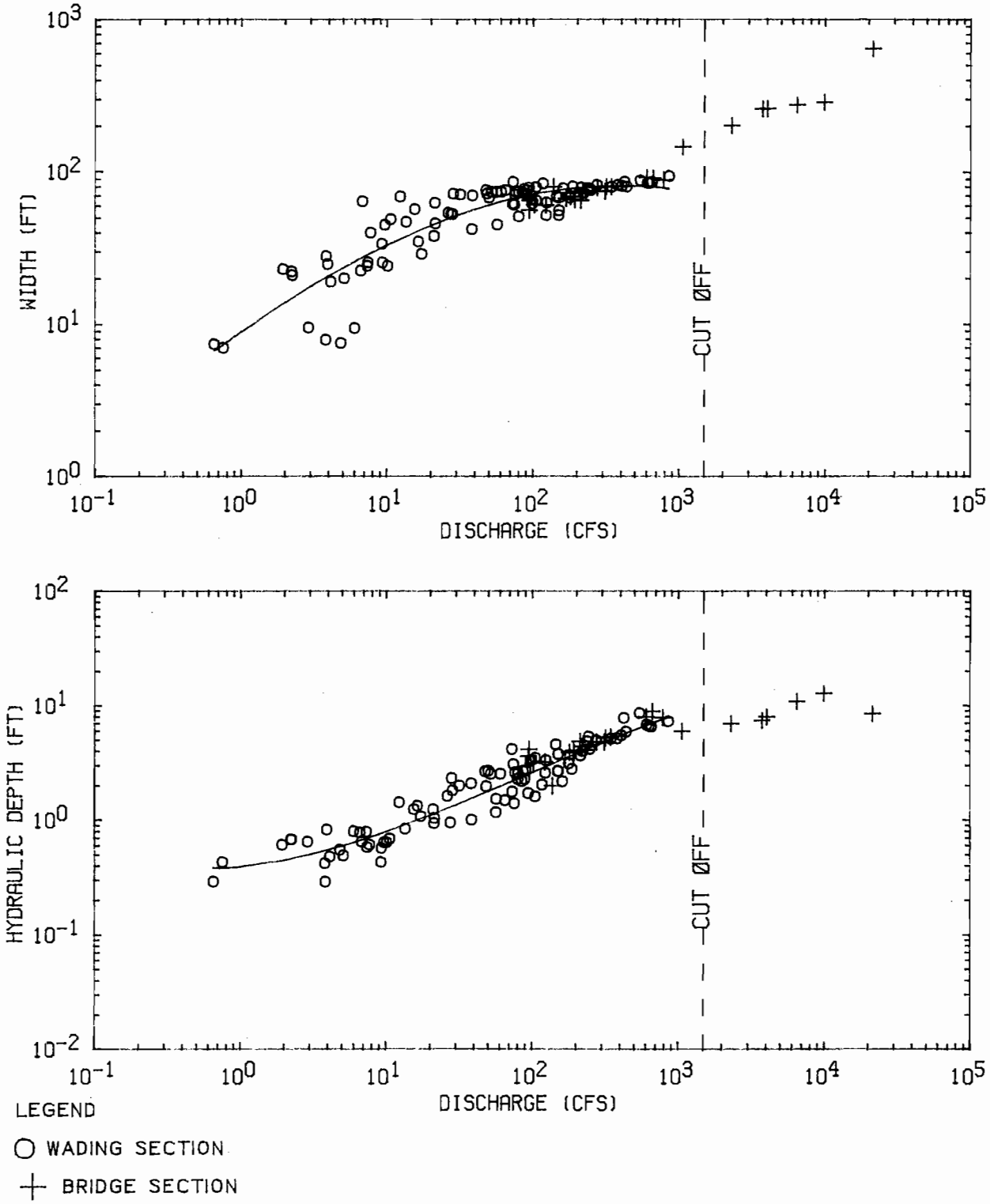

Figure 14a. Station hydraulic geometry, South Fork Sangamon at Kincaid

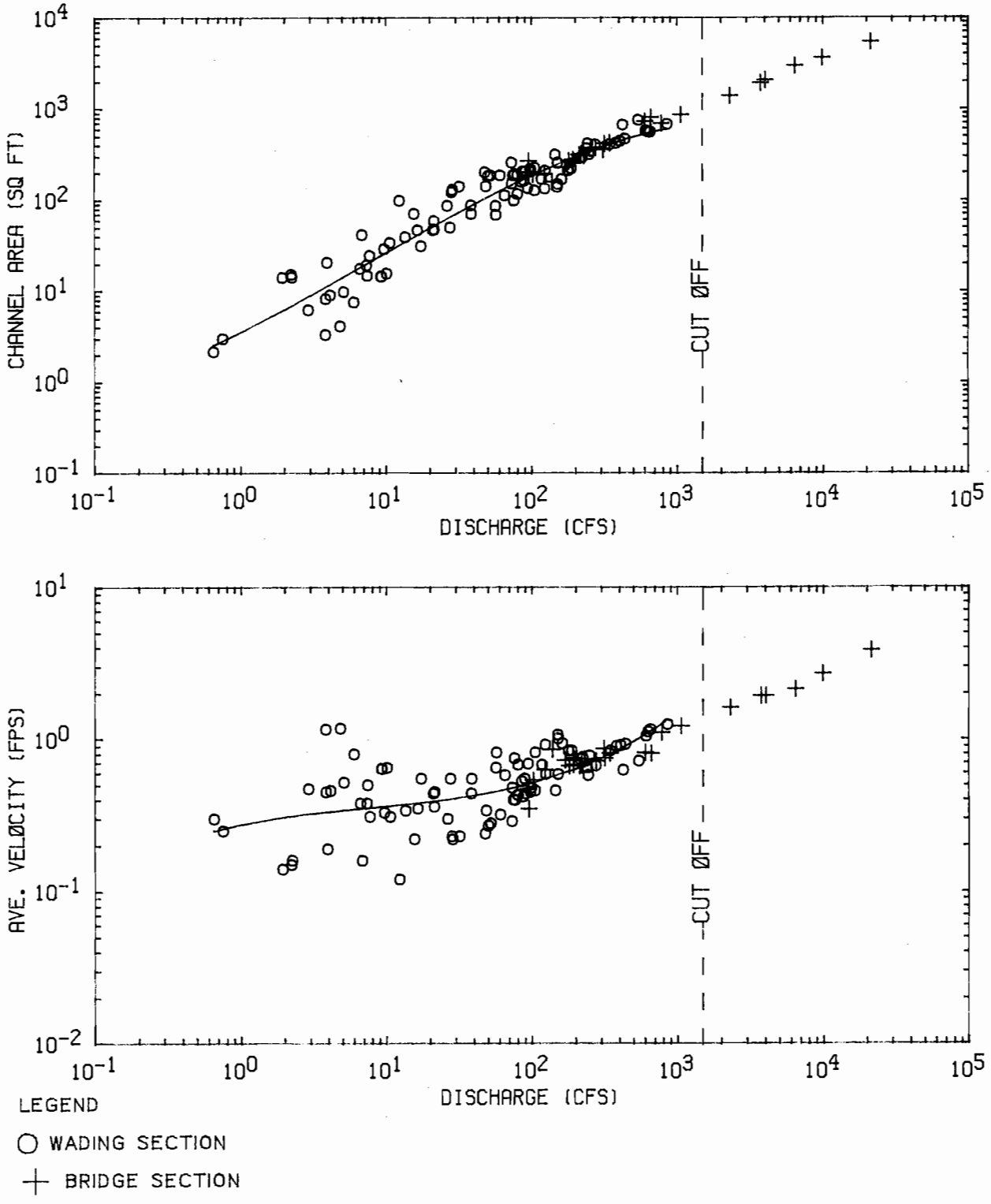

Figure 14b. Station hydraulic geometry, South Fork Sangamon at Kincaid

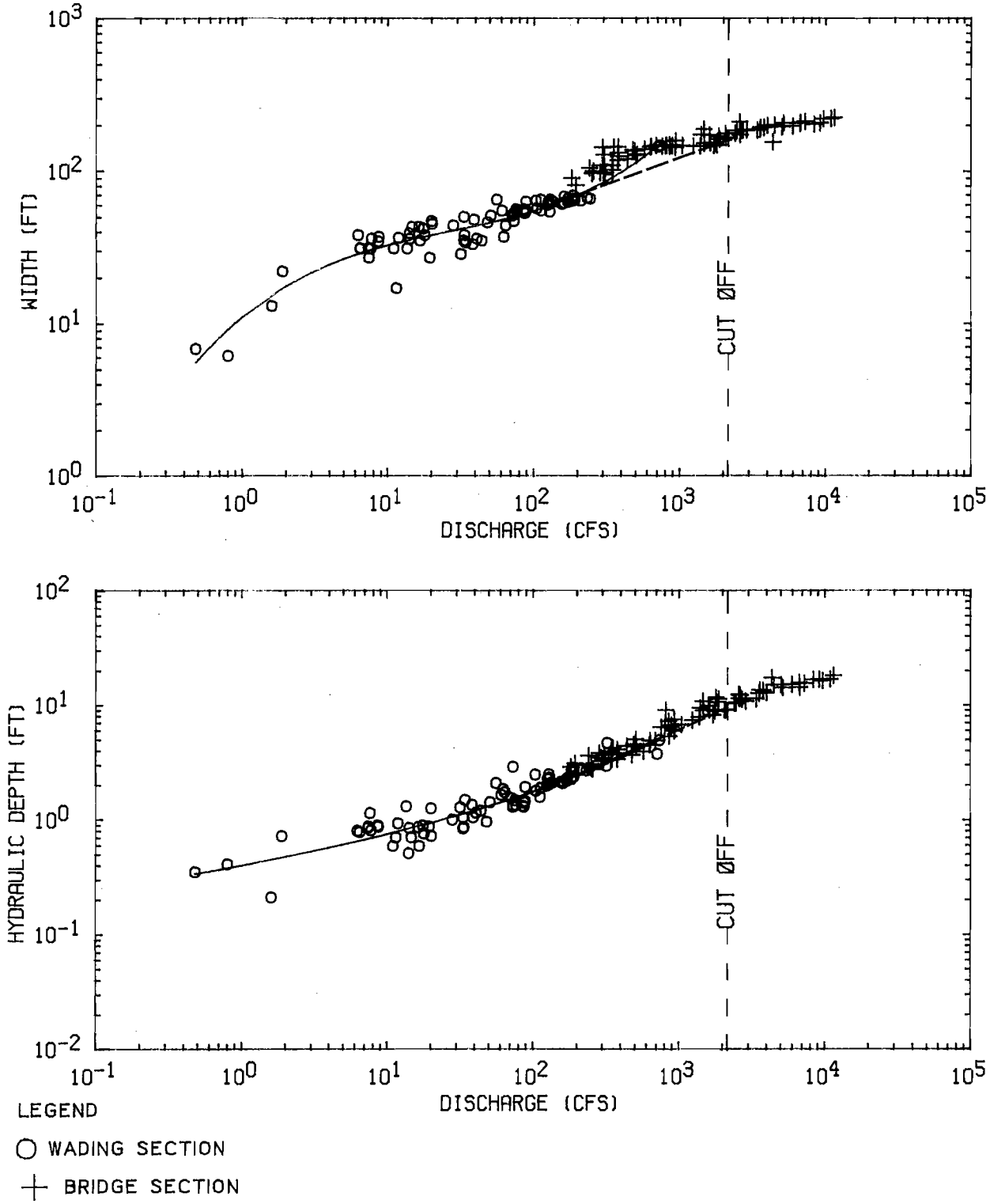

Figure 15a. Station hydraulic geometry, South Fork Sangamon near Rochester

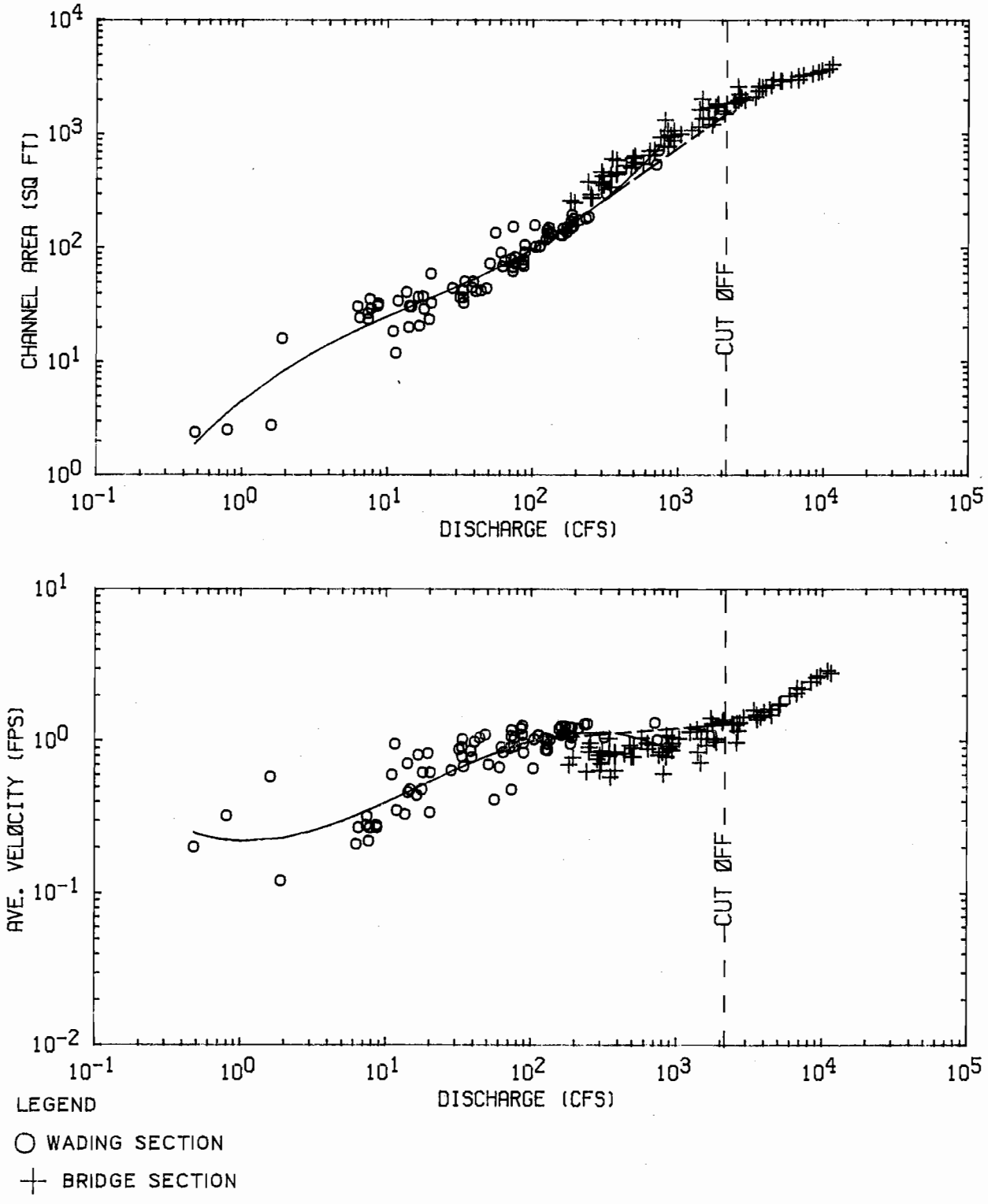

Figure 15b. Station hydraulic geometry, South Fork Sangamon near Rochester

the bankfull event. The slope of the data from wading sections is different from the bridge data, suggesting that the relationship between flow parameters and discharge is different at wading sections and bridge sections. Also, there is consistently less scatter in the data collected at bridge sections than at wading sections.

The difference in channel geometry for a wading section and a bridge section is illustrated in Figure 16. Three channel cross sections are plotted from discharge measurement data: one section at a bridge near the Rochester gage and two natural sections downstream of the gage. The measured discharges are within 2%, but the flow parameters are quite different, as can be seen from Table 3.

For some stations, bridge sections tend to have greater flow widths and lesser velocities than wading sections, while depths seem to be similar. This is best exemplified in the station plots for Rochester and Pawnee. The notably greater depths measured at bridges for the Mahomet and Monticello stations suggest that the bridge sections are subject to more scour than the wading sections. The relative differences between trends exhibited by wading and bridge data are site-specific.

Differences in the slope of the V, W, D, and A versus Q curves fitted to the bridge data and wading data yield different coefficients for the hydraulic geometry equations. The wading sections are clearly more representative of the majority of the stream length. Therefore, only data collected at wading sections were used in the regression analysis to evaluate the station equations. Station hydraulic geometry plots show the correspondence of flow parameters to discharge at a single cross section. The scatter in the data at lower discharges in Figures 2-15 is attributed to the fact that wading measurements are not made at the same place each time (Dunne and Leopold, 1978). This was further confirmed by review of the hydrographer's notes for the gaging stations. The band width of the data is an indication of the variation of depths and velocities which may be observed in a natural channel. It was observed that measurements made at lesser depths have higher velocities and those at greater depths have lower velocities. Thus, the extremes of the data bands reflect the velocities and depths approaching pool and riffle conditions. Further conclusions cannot be drawn from the gaging

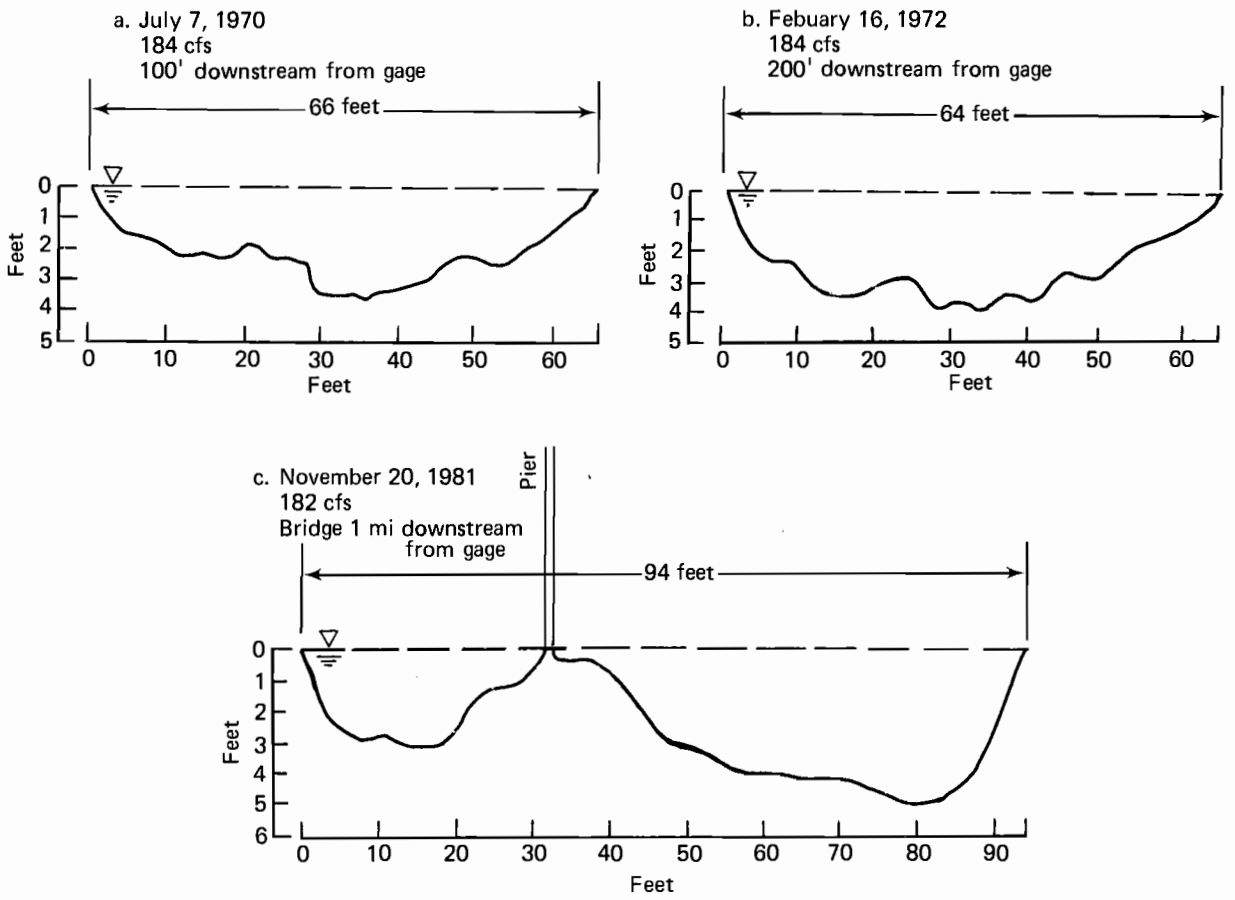

Figure 16. Channel cross sections near the USGS Rochester gage

TABLE 3

Comparison of Hydraulic Data Collected near the USGS Rochester Gage, South Fork Sangamon

Location of section	Date	Q (cfs)	W (ft)	D (ft)	A (ft^2)	V (fps)
wading 100 ft downstream of gage (Figure 16a)	07-07-70	184	66.0	2.26	149.0	1.23
wading 200 ft downstream of gage (Figure 16b)	02-16-72	184	64.0	2.66	170.0	1.09
bridge, 1 mile downstream of gage (Figure 16c)	11-20-81	182	90.0	2.88	259.0	0.70

station data because the hydrographer's field notes do not specify the location of the measurement relative to the riffle pool sequence. There was no seasonal variation apparent in the data trends. Based on the reported locations of the measurements recorded in the field notes, the data for a few sample stations were sorted and plotted. The plots of data collected at roughly the same location did appear to have less scatter in most of the cases studied. However, a sufficient number of measurements were not available at any one location to reliably develop the hydraulic geometry equations for that location. The locations are only roughly estimated by field personnel and may vary considerably for different personnel over the years.

REGRESSION ANALYSIS

The formulation originally proposed by Leopold and Maddock (1953) is a linear function of the log transformed variables:

$$\log \text{Var} = b + a \times \log Q \qquad (7)$$

where Var = W, D, V, or A. The logarithmic data plots do not clearly follow a straight line, as illustrated in Figures 2-15. Computerized regression analyses were performed to determine the best polynomial relation for each flow parameter as a function of Q. The general form of the relation tested is:

$$\log \text{Var} = a_0 + a_1 \log Q + a_2(\log Q)^2 + a_3(\log Q)^3 + \ldots + a_6(\log Q)^6 \qquad (8)$$

Overall, the third-order polynomial approximation of the station flow parameters had the highest correlation and lowest standard error, S_e, for the wading data. A fourth-order polynomial had a slightly higher correlation in some cases. However, the difference between the third-order and fourth-order polynomial correlation and S_e was typically negligible. There were no instances of the first, second, or any other degree polynomial having the best fit. The correlation and standard error of the third-order polynomial approximation was not significantly better than the linear approximation in many cases. However, a comparison of the linear and curvilinear functions plotted with the data indicated that the curvilinear function had a better fit at the lower discharges. Because the lower range of discharges was targeted for this

study, the third-order polynomial relation was selected for the station hydraulic geometry relations. The station hydraulic geometry equations developed are consistent with the physical laws $Q = V \times A$ and $A = W \times D$.

The coefficients for the station hydraulic geometry equations are listed in Tables 4 and 5 (Sangamon and South Fork Sangamon) along with the range of discharges to which they apply, the multiple correlation coefficient, R, and standard error, S_e. The equations are plotted in Figures 2-15 with a solid line from the lowest discharge measured at a wading section to the highest discharge.

The correlation of width, depth, and area with discharge is significant as evidenced by the correlation coefficients shown in Tables 4 and 5. The correlation between velocity and discharge is less than for the other parameters. The values of measured velocity are highly variable; there is considerably more scatter in all station plots of velocity than in plots of the other parameters. This implies that another factor, possibly the position of the measured section relative to the riffle pool sequence, significantly influences the velocities measured at that section for a given discharge.

APPROXIMATIONS FOR HIGH FLOWS NOT MEASURED AT WADING SECTIONS

Only data collected at wading sections were used in defining the hydraulic geometry relations. Wading measurements are usually not made at depths exceeding 3 feet. As drainage area increases, the flow duration at which the wading depth is exceeded also increases. For example, wading measurements at DeLand, A_d = 47.3 sq mi, continue beyond the 10% flow duration discharge; however, wading measurements at Rochester, A_d = 867 sq mi, stop at approximately the 50% flow duration discharge. Four of the stations did not have wading data for high discharges. Relationships developed for the wading data could not be extrapolated through the needed range of discharges for Rochester on the South Fork and for Monticello, Niantic, and Riverton on the Sangamon River.

The hydraulic relations for the range of discharges not measured at a wading section were approximated for these stations. A straight line

TABLE 4

Sangamon Basin Station Hydraulic Geometry Equations

$$\log(VAR) = a_0 + a_1(\log Q) + a_2(\log Q)^2 + a_3(\log Q)^3$$

Station	VAR	a_0	a_1	a_2	a_3	R	S_e	Range of discharges Q_{min}	Q_{max}
DELAND	W	0.878	0.345	-0.062	0.0097	0.928	0.0698	0.38	91.4
	D	-0.493	0.263	0.004	0.0308	0.946	0.0770		
	A	0.385	0.616	-0.066	0.0432	0.967	0.1048		
	V	-0.386	0.396	0.053	-0.0390	0.913	0.1058		
ARGENTA	W	0.827	0.508	-0.022	-0.0276	0.970	0.0982	0.02	192.0
	D	-0.571	0.356	-0.014	0.0172	0.956	0.1173		
	A	0.262	0.862	-0.042	-0.0075	0.986	0.1312		
	V	-0.262	0.137	0.042	0.0077	0.847	0.1310		
FISHER	W	0.367	2.155	-1.388	0.3175	0.844	0.1105	3.78	179.0
	D	-1.360	2.058	-0.968	0.1772	0.885	0.1503		
	A	-1.001	4.226	-2.364	0.4963	0.946	0.1572		
	V	0.986	-3.189	2.336	-0.4900	0.729	0.1565		
MAHOMET	W	1.085	0.408	-0.120	0.0298	0.891	0.1042	0.26	855.0
	D	-0.623	0.354	-0.109	0.0514	0.912	0.1308		
	A	0.465	0.756	-0.226	0.0806	0.940	0.1792		
	V	-0.465	0.246	0.224	-0.0803	0.787	0.1789		
MONTICELLO	W	0.874	0.756	-0.153	0.0103	0.888	0.0907	2.41	100.0
	D	-0.626	0.415	-0.090	0.0499	0.865	0.1430		
	A	0.255	1.161	-0.238	0.0592	0.933	0.1612		
	V	-0.250	-0.173	0.246	-0.0608	0.347	0.1616		
	W	1.260	0.300					100.0	1575.0
	D	-0.901	0.570						
	A	0.359	0.870						
	V	-0.359	0.130						
NIANTIC	W	3.288	-3.481	2.089	-0.3574	0.930	0.0698	36.8	300.0
	D	1.272	-2.107	0.949	-0.1080	0.908	0.0682		
	A	4.618	-5.674	3.080	-0.4720	0.936	0.1203		
	V	-4.690	6.773	-3.123	0.4782	0.370	0.1204		
	W	1.123	0.370					300.0	2768.0
	D	-1.093	0.540						
	A	0.030	0.910						
	V	-0.030	0.090						

Concluded on next page

TABLE 4

(concluded)

Station	VAR	a_0	a_1	a_2	a_3	R	S_e	Q_{min}	Q_{max}
RIVERTON	W	3.786	-3.400	1.794	-0.2864	0.660	0.1034	24.0	430.0
	D	-0.958	1.284	-0.647	0.1355	0.749	0.1017		
	A	2.822	-2.109	1.145	-0.1507	0.914	0.0902		
	V	-2.869	3.186	-1.187	0.1581	0.819	0.0906		
	W	1.517	0.200					430.0	6690.0
	D	-1.220	0.620						
	A	0.297	0.820						
	V	-0.297	0.180						

TABLE 5

South Fork Sangamon Basin Station Hydraulic Geometry Equations

$$\log(VAR) = a_0 + a_1(\log Q) + a_2(\log Q)^2 + a_3(\log Q)^3$$

Station	VAR	a_0	a_1	a_2	a_3	R	S_e	Range of discharges Q_{min}	Q_{max}
NOKOMIS	W	0.698	0.424	0.043	0.0276	0.910	0.1290	0.01	13.0
	D	-0.525	0.474	0.006	-0.0068	0.913	0.1320		
	A	0.172	0.901	0.049	0.0166	0.949	0.1910		
	V	-0.174	0.100	-0.048	-0.0164	0.332	0.1910		
DIVERNON	W	0.911	0.464	-0.121	0.0077	0.887	0.1659	0.08	69.3
	D	-0.448	0.377	-0.161	0.0808	0.879	0.1722		
	A	0.464	0.839	-0.285	0.0908	0.944	0.2221		
	V	-0.463	0.162	0.280	-0.0885	0.710	0.2219		
PAWNEE	W	0.768	0.529	-0.060	-0.0257	0.921	0.1610	0.05	69.9
	D	-0.463	0.383	0.029	0.0071	0.906	0.1630		
	A	0.306	0.910	-0.033	-0.0174	0.947	0.2440		
	V	-0.307	0.090	0.033	0.0173	0.463	0.2440		
SPRINGFIELD	W	0.866	0.384	-0.040	0.0166	0.929	0.1283	0.07	197.0
	D	-0.393	0.402	0.003	0.0024	0.940	0.1243		
	A	0.471	0.785	-0.034	0.0174	0.953	0.2100		
	V	-0.471	0.215	0.033	-0.0172	0.627	0.2092		
TAYLORVILLE	W	0.893	0.429	0.000	-0.0016	0.919	0.1230	0.24	440.0
	D	-0.570	0.391	0.083	-0.0232	0.924	0.1290		
	A	0.323	0.820	0.083	-0.0248	0.961	0.1730		
	V	-0.324	0.180	-0.082	0.0245	0.419	0.1730		
KINCAID	W	0.949	0.664	-0.080	-0.0127	0.887	0.1300	0.65	853.0
	D	-0.395	0.127	0.212	-0.0354	0.946	0.1200		
	A	0.554	0.791	0.132	-0.0480	0.955	0.1820		
	V	-0.553	0.204	-0.129	0.0475	0.640	0.1820		
ROCHESTER	W	1.039	0.793	-0.415	0.0965	0.946	0.0707	0.48	200.0
	D	-0.387	0.243	0.018	0.0105	0.922	0.0986		
	A	0.651	1.037	-0.397	0.1071	0.960	0.1267		
	V	-0.652	-0.033	0.394	-0.1064	0.851	0.1262		
	W	1.014	0.360					200.0	2175.0
	D	-0.915	0.570						
	A	0.099	0.930						
	V	-0.099	0.070						

was fit on the logarithmic plots through the needed range of flows. The line was constructed to follow the trend indicated by the wading data and guided by the values measured at bridge sections. The coefficients and range of discharges to which these relations apply are listed with the regression coefficients for lower discharges in Tables 4 and 5. The functions are plotted with a dashed line in the station hydraulic geometry plots in Figures 2 through 15.

The data plots in Figures 2-15 illustrate typical hydraulic geometry relations for a station using available USGS measurements. The solid lines in the plots are the graphical representation of third-order polynomials fit to the data. The dashed lines in some of the figures show approximate linear relations developed in the absence of flow measurements made at representative natural channel cross sections. These relations are used to develop regional hydraulic geometry equations for the two basins.

BASIN HYDRAULIC GEOMETRY RELATIONS

Basin hydraulic geometry relations define the average values of width W, depth D, velocity V, and flow section area A for a given streamflow or for a given flow duration and drainage area. These parameters increase in a consistent manner with drainage area when compared at the same flow duration. Thus, each parameter varies with drainage area and flow duration. Equations expressing the relationship are calibrated for a given stream network using parameter values calculated from station equations representing a range of drainage areas.

Basin equations were developed for each study basin using multiple regression analysis. The parameter values used in the analysis were calculated from the equations developed for the seven stations in each basin at nine different discharges. Discharges for flow durations 10, 20, 30, 40, 50, 60, 70, 80, and 90% were computed using the flow duration relationship and the coefficients in Table 1. The W, D, A and V at the computed discharges were then determined for each station. A typical station data set is shown in Table 6. Similar data sets were compiled for each of the fourteen stations.

Several relationships linking a flow parameter to drainage area and flow duration were investigated. The relations studied are:

$$\log (VAR) = a + bF + c(\log A_d) \quad (9)$$

$$\log (VAR) = a + b_1F + b_2F^2 + c(\log A_d) \quad (10)$$

$$\log (VAR) = a + bF + c_1(\log A_d) + c_2(\log A_d)^2 \quad (11)$$

$$\log (VAR) = a + b_1F + b_2 F^2 + c_1(\log A_d) + c_2(\log A_d)^2 \quad (12)$$

$$\log (VAR) = A_f + B_f (\log A_d) \quad (13)$$

where VAR = W, D, A, or V; F is the decimal flow duration; A_d is the drainage area in sq mi; a, b, and c are regression coefficients; and A_f and B_f are regression coefficients for a specific flow duration f. The flow parameters assume the role of dependent variables and $(\log A_d)$, F, $(\log A_d)^2$ and F^2 are the independent variables.

The degree of association between the dependent variable and multiple independent variables may be expressed by the coefficient of determination, R^2 (Chow, 1964). If the sample size is small, the

TABLE 6

Typical Data Set of W, D, A, and V Computed
from Station Hydraulic Geometry Equations

USGS Gaging Station 05571500, Goose Creek near DeLand
A_d = 47.3 mi^2

% Flow duration F	Q (cfs)	W (ft)	D (ft)	A (ft^2)	V (fps)
90	0.32	4.94	0.24	1.16	0.27
80	0.81	7.06	0.31	2.15	0.38
70	2.03	9.56	0.39	3.74	0.55
60	4.90	12.35	0.50	6.26	0.80
50	9.95	14.85	0.64	9.56	1.06
40	15.90	16.64	0.77	12.84	1.26
30	24.66	18.43	0.93	17.18	1.46
20	42.08	20.78	1.20	25.15	1.70
10	78.43	23.78	1.71	41.07	1.95

*$Q(j) = a_{i,j} + b_j (\log A_d)$; see Table 1

coefficient is adjusted for the degrees of freedom. The unbiased coefficient, commonly referred to as the adjusted R^2, is expressed as

$$R^2 = 1 - \hat{S}^2/\hat{s}^2 \tag{14}$$

in which s is the unbiased standard deviation of the marginal distribution of the dependent variable, x.

$$\hat{s} = [\Sigma (x-\bar{x})^2/(N-1)]^{0.5} \tag{15}$$

N = sample size

$\hat{S}$ is the unbiased standard deviation of residuals in which $\Sigma\Delta^2$ is the sum of squared residuals and m is the number of variables.

$$\hat{S} = [\Sigma\Delta^2/(N-m)]^{0.5} \tag{16}$$

The first four formulations, equations 9-12, were compared on the basis of the adjusted R^2, the standard error, S_e, and the confidence interval of the regression equation coefficients. The 95% confidence intervals are evaluated using Student's t test. The higher-order formulations including the terms $(\log A_d)^2$ and F^2 did not have significantly higher correlations or lower standard error compared to the first-order relationship, given by equation 9.

The additional terms in equations 10 through 12 reduced the degrees of freedom in the analysis. Subsequently, due to the limited size of the data set, the significance of the coefficients as measured by the value of Student's t was reduced. The lower value of Student's t is further reflected in an increase in the range of coefficient values estimated to be within the 95% confidence limits. This implies a greater range of values which may be assumed by the coefficients when developed from different data samples and therefore reduces the reliability of the equations. The coefficients evaluated for the first-order relationship, $\log (Var) = a + bF + c(\log A_d)$, have less variability and thus this expression is most reliably calibrated with the available data. The regression coefficients evaluated for each basin are shown in Table 7 for this equation. The adjusted R^2 and standard error of the estimate are

TABLE 7

Basin Hydraulic Geometry Equations

$\log(VAR) = a + bF + c(\log A_d)$

F = decimal flow duration

A_d = drainage area (sq mi)

VAR	a (95% conf. limits) (Student's t)	b (95% conf. limits) (Student's t)	c (95% conf. limits) (Student's t)	Adj R^2	S_e
SANGAMON					
W	0.55 (0.43 to 0.67) 9.4	-0.77 (-0.86 to -0.69) -17.4	0.58 (0.54 to 0.63) 28.0	.95	.088
D	-0.32 (-0.44 to -0.20) -5.4	-1.17 (-1.26 to -1.08) -25.8	0.41 (0.36 to 0.45) 19.1	.94	.089
V	-0.0054 (-0.18 to 0.17) -0.06	-0.53 (-0.66 to -0.40) -8.2	0.13 (0.07 to 0.19) 4.2	.58	.128
A	0.23 (0.06 to 0.40) 2.7	-1.94 (-2.07 to -1.81) -29.5	0.99 (0.93 to 1.05) 32.1	.97	.129
SOUTH FORK SANGAMON					
W	0.68 (0.59 to 0.78) 14.8	-0.93 (-1.03 to -0.83) -18.7	0.55 (0.51 to 0.59) 27.4	.94	.091
D	-0.31 (-0.38 to -0.24) -8.9	-1.22 (-1.30 to -1.15) -32.6	0.45 (0.42 to 0.48) 30.3	.97	.068
V	-0.025 (-0.12 to 0.07) -0.54	-0.59 (-0.69 to -0.49) -11.8	0.067 (0.03 to 0.11) 3.3	.71	.090
A	0.37 (0.25 to 0.49) 6.25	-2.15 (-2.28 to -2.03) -33.8	1.00 (0.95 to 1.05) 39.4	.98	.116

listed as well as Student's t for each coefficient and the 95% confidence interval for the coefficient values. The simple correlation coefficients for each variable with F and A_d alone are noted in Table 8.

Width and area have a stronger correlation with drainage area, A_d, than with the decimal flow duration, F, as demonstrated by the values of the simple correlation coefficients in Table 8 and as reflected in the higher values for Student's t for the respective regression coefficients in Table 7. Depth has a higher correlation with flow duration than drainage area. The correlation between velocity and the decimal flow duration is significant, but the correlation between velocity and drainage area is statistically less significant. Generally, the hydraulic radius increases and the bed slope decreases with increase in drainage area. The velocity, being a function of both hydraulic radius and bed slope, is not affected considerably by change in drainage area for similar flow conditions. The irregularity of natural channel measurements at different cross sections introduces more variability in flow velocities. It is not surprising, therefore, that the V versus A_d relation is not as significant as V versus F.

The relationships between flow parameters and drainage area defined by the coefficients listed in Table 7 are graphically illustrated for flow durations 10, 30, 50, 70 and 90% in Figures 17 and 18, for the Sangamon and South Fork Sangamon Basins, respectively. The underlying assumption in using equation 9 is that the value of a flow parameter increases with increase in drainage area at the same rate (given by c in equation 9) over the entire range of flow durations, or that this rate of increase is independent of flow duration. Only the intercept of each line shown in the plots in Figures 17 and 18 changes with flow duration. This intercept corresponds to $a + bF$ for $A_d = 1$.

The validity of the constant-c assumption was tested by examining the variation of the coefficients A_f and B_f with respect to F (in decimals) for each parameter. The regression coefficients were computed for flow durations 10%, 20%, ...,90%. Examining equations 9 and 13, it can be observed that A_f replaces $a + bF$ and is thus expected to vary linearly with flow duration if B_f is practically the same as c.

TABLE 8

Simple Correlation Coefficients for W, D, V, and A with A_d and F

Basin	Var	log A_d r	F r
Sangamon	W	.82	-.49
	D	.56	-.77
	V	.33	-.68
	A	.71	-.65
South Fork Sangamon	W	.77	-.44
	D	.59	-.66
	V	.08	-.81
	A	.70	-.56

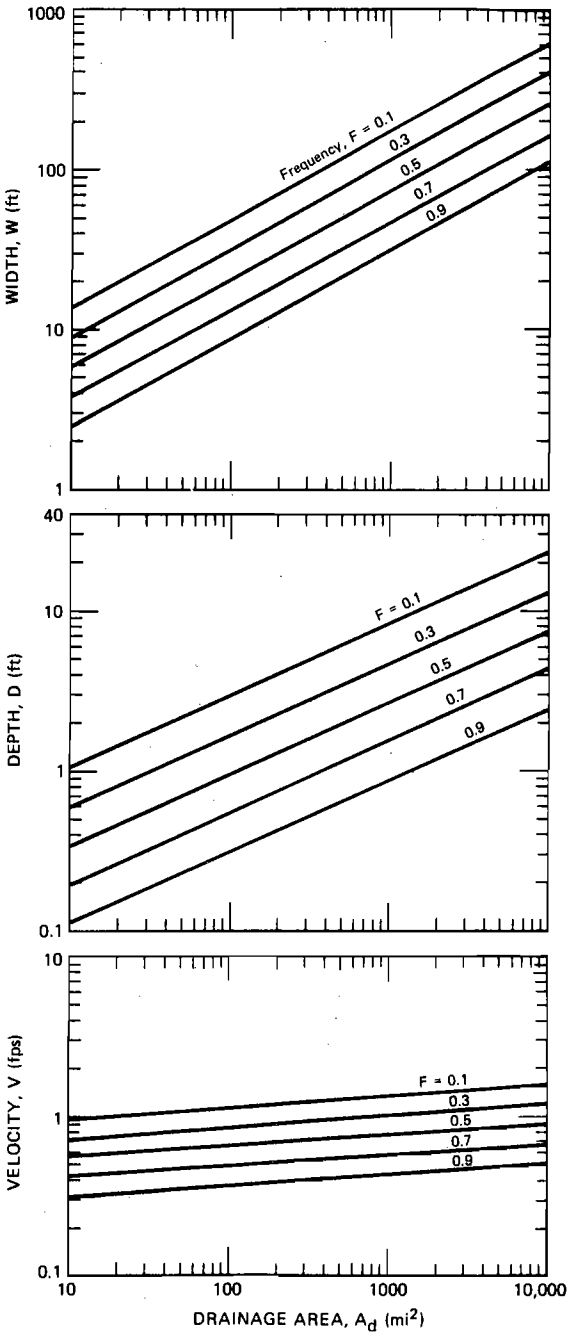

Figure 17. Sangamon basin hydraulic geometry relations

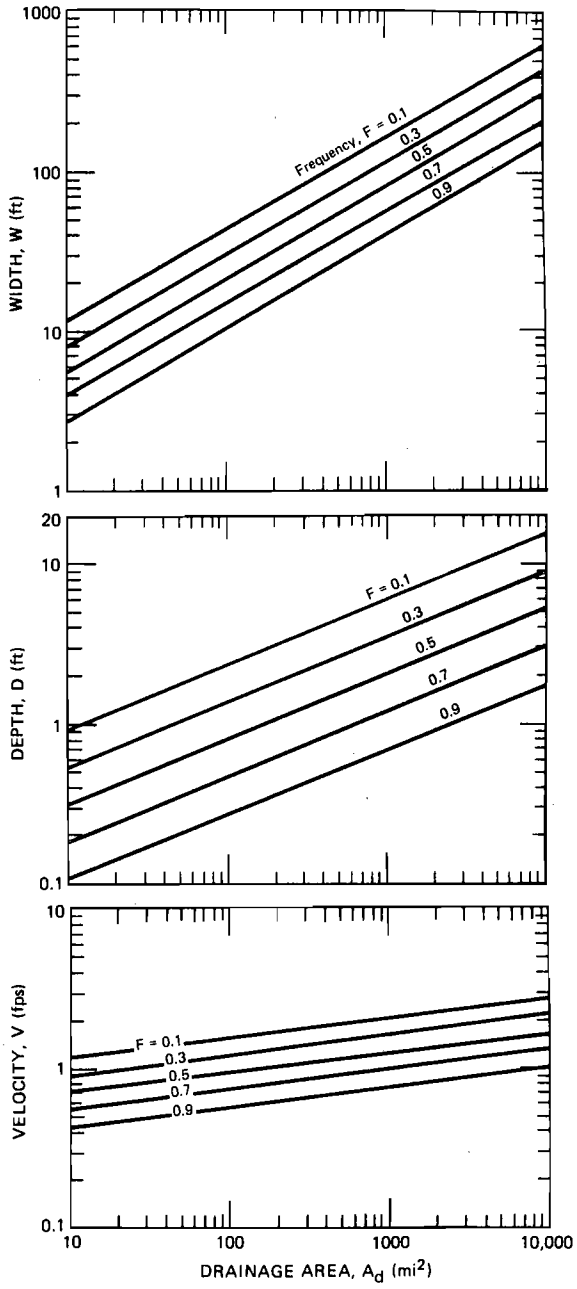

Figure 18. South Fork Sangamon basin hydraulic geometry relations

Plots of A_f versus F for each flow parameter (in each basin) exhibit a nearly linear relationship for flow durations from 10% up to 70%. In nearly all cases there was a significant departure from the linear trend for flow durations exceeding 70%. The value of B_f varies with flow duration for a given parameter, indicating that c is an average value. The value of B_f is the rate of increase of a parameter (W, D, or V) with increase in drainage area; as B_f varies with the flow duration so must the relationship between W, D, or V and drainage area vary. However, the variation of B_f is not large, particularly in the range of flow durations between 20% and 60%. A graphical depiction of the variation of the coefficients for depth is shown in Figures 19 and 20 for the Sangamon and South Fork Sangamon, respectively. For comparison, the corresponding coefficients evaluated from equations conforming to equation 9 are also plotted.

The variations in the values of A_f and B_f tend to offset each other. The difference between the results of the two equations (9 and 13) is rather small. This can be seen in a tabulation of computed parameter values from both relationships for drainage areas 50, 200, and 500 sq mi in Table 9. Depths predicted by equation 13 tend to be lower for flow durations 10% and 90%, with the greatest disparity for the smaller drainage area. Widths calculated from the varying coefficient formulation also tend to be lower than predicted by the constant coefficient equation. The velocity calculations have the greatest difference at the extremes of flow duration; however, the simple correlation between velocity and and drainage area computed from the data for each flow duration was less than 0.3 in all cases.

The coefficients a, b, and c for equation 9 were developed for each parameter (W, D, V, and A) using 60 or more station-data values. Seven or fewer station values were available for each flow duration for a given basin. Consequently, the constant coefficients for relationships in the form of equation 9 have less predicted variability than the coefficients A_f and B_f. Given the available data, basin parameter relations in the form of equation 9 are more reliable and were adopted for the flow model for the Sangamon and South Fork Sangamon.

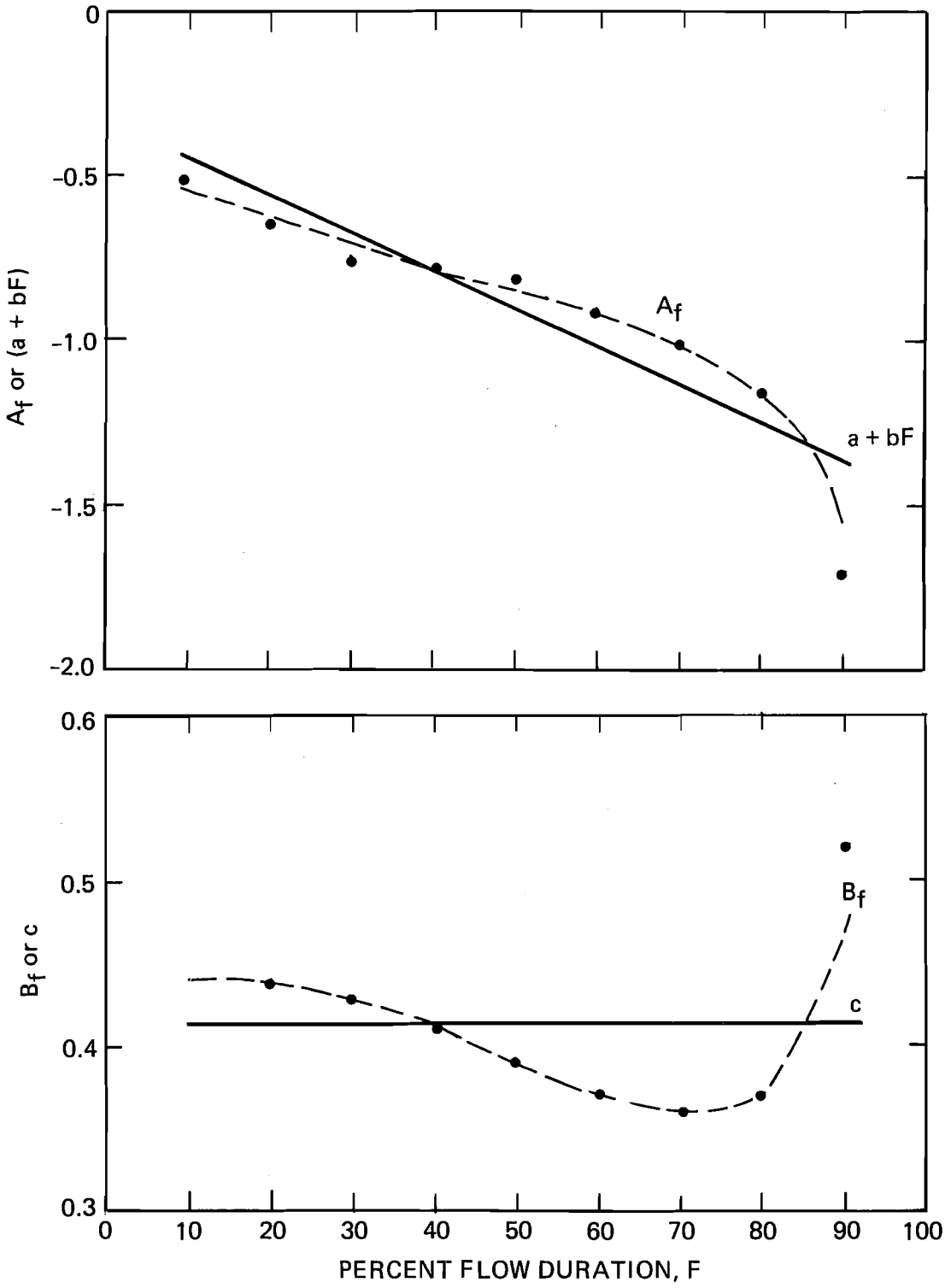

Figure 19. Relationship between depth regression coefficients and flow duration, F, for the Sangamon basin

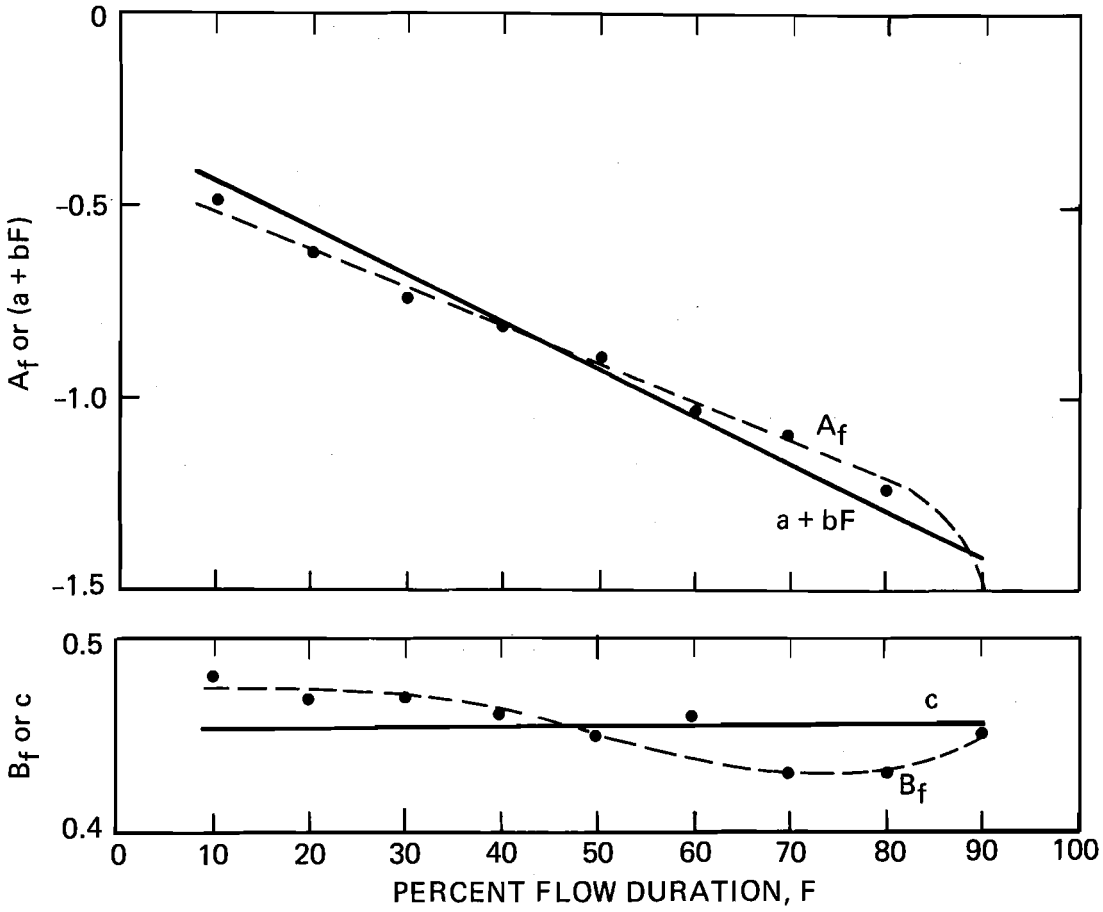

Figure 20. Relationship between Depth Regression Coefficients and Flow Duration, F, for the South Fork Sangamon Basin

TABLE 9

Values of W, D, and V Computed from
Two Regression Equation Formulations

Equation (9) $\log (VAR) = a + bF + c (\log A_d)$

Equation (13) $\log (VAR) = A_f + B_f (\log A_d)$

			Sangamon			South Fork Sangamon		
			A_d			A_d		
Freq.	Var.	Equation	50	200	500	50	200	500
.1	W	9	29.11	65.33	111.45	32.97	70.38	116.18
		13	28.54	63.80	108.50	34.00	64.34	98.07
	D	9	1.78	3.13	4.54	2.18	4.10	6.21
		13	1.58	2.90	4.34	2.02	3.93	6.10
	V	9	1.44	1.71	1.92	1.07	1.18	1.25
		13	1.84	1.88	1.89	1.08	1.22	1.32
.3	W	9	20.38	45.74	78.04	21.47	45.82	75.64
		13	20.96	45.56	76.11	20.72	42.03	67.06
	D	9	1.04	1.82	2.65	1.25	2.34	3.54
		13	1.07	1.95	2.89	1.23	2.35	3.61
	V	9	1.12	1.34	1.50	0.82	0.90	0.96
		13	1.36	1.46	1.53	0.78	0.85	0.89
.5	W	9	14.27	32.03	54.64	13.97	29.83	49.24
		13	15.85	34.56	57.73	13.62	29.21	48.35
	D	9	0.61	1.06	1.54	0.71	1.33	2.02
		13	0.62	1.07	1.52	0.73	1.37	2.06
	V	9	0.88	1.05	1.18	0.63	0.69	0.73
		13	0.94	1.10	1.22	0.64	0.69	0.73
.7	W	9	9.99	22.42	38.26	9.10	19.42	32.06
		13	10.01	22.7	38.80	7.95	19.04	33.91
	D	9	0.35	0.62	0.90	0.40	0.76	1.15
		13	0.40	0.66	0.94	0.43	0.78	1.15
	V	9	0.69	0.82	0.92	0.48	0.52	0.56
		13	0.53	0.73	0.89	0.49	0.54	0.57
.8	W	9	8.36	18.76	32.01	7.34	15.67	25.87
		13	7.47	17.64	31.14	4.27	11.74	22.92
	D	9	0.27	0.47	0.69	0.31	0.57	0.87
		13	0.29	0.48	0.67	0.34	0.62	0.91
	V	9	0.61	0.72	0.81	0.42	0.46	0.49
		13	0.41	0.61	0.81	0.43	0.48	0.52
.9	W	9	7.00	15.70	26.79	5.92	12.64	20.87
		13	4.53	12.13	23.24	3.01	10.49	23.94
	D	9	0.21	0.36	0.53	0.23	0.43	0.66
		13	0.18	0.34	0.52	0.21	0.39	0.58
	V	9	0.54	0.64	0.72	0.37	0.40	0.43
		13	0.29	0.50	0.70	0.33	0.37	0.41

FIELD STUDY

STUDY REACHES

Nine reaches were selected for field measurements. Four reaches are located in the South Fork Sangamon Basin and five are located in the Sangamon River Basin. Drainage areas range from 13.4 to 715 sq mi in the South Fork Basin and from 19.1 to 1439 sq mi in the Sangamon Basin. The reaches selected are representative of the natural channel -- they are located in sections of streams not affected by backwater from dams or modified by bridge crossings. Reaches are straight or slowly meandering. Each study reach was surveyed to locate 3 consecutive riffles and 2 intermediate pools.

Streams in the Sangamon and South Fork Sangamon basins have alluvial channels. Bed materials found in the study reaches ranged from silt to medium size pebbles, with the largest pebbles having an approximate diameter of 1". Bed materials were examined to assist in identifying riffles and pools. Riffles were characterized by sand or by sand and pebbles, and all pools had silt deposits up to several inches thick as observed at the time of the field work.

Field personnel frequently observed the existence of shallow spots between well established riffles. During low flows some relatively shallow sections (having less depth than conditions immediately upstream and downstream) may be easily identified; during medium flows these shallow spots are not evident and only well defined riffles may be readily observed. The so-called shallow sections had bed materials homogeneous with the deeper portions of the pool. Only riffles, well defined by lower depths and coarser bed materials, were used to establish the study reaches. Additional descriptive information for the reaches is listed in Table 10. The reaches in the Sangamon Basin are numbered 1-5 and those in the South Fork Basin are numbered 6-9.

FIELD PROCEDURES

Thirteen transects were measured in each reach. One transect was located at each riffle and five transects were located in each pool.

TABLE 10

Study Reaches

Sta No.	Nearest Town	Township Range Section	Stream Name	A_d (sq mi)	Reach length (ft)
SANGAMON					
1	SAYBROOK	T23N R5E S27	SANGAMON	19.1	329.0
2	GIBSON CITY	T22N R7E S06	SANGAMON	55.8	166.0
3	FISHER	T21N R8E S06	SANGAMON	240.0	860.0
4	ALLERTON PARK	T18N R5E S30	SANGAMON	613.0	1200.0
5	RIVERTON	T16N R4W S25	SANGAMON	1439.0	825.0
SOUTH FORK SANGAMON					
6	NOKOMIS	T11N R2W S36	S.F. SANG.	13.4	550.0
7	FINDLAY	T13N R2E S22	FLAT BRANCH	77.3	165.0
8	MOWEAQUA	T14N R1E S34	FLAT BRANCH	190.5	570.0
9	ROCHESTER	T14N R4W S03	S.F. SANG.	715.0	1183.0

Transects were equally spaced between riffles. Six uniformly-spaced depth and velocity readings were made across each transect. Thus, there were a total of 78 data points for each discharge measured in a reach. The schematic sketches in Figure 21 show the location of transects and the position of measurements across the stream. Additional velocity and depth measurements were made at one or more transects for accurate computation of discharge.

A Price type A current meter was used to measure velocities at depths greater than approximately 0.5 feet and a Price pygmy meter for lesser depths. Velocities were measured at 0.6 the total depth from the water surface.

Measurements were made from a boat for discharges at both the 715- and 109.5-sq-mi drainage-area reaches in the South Fork Basin, and at the 1439- and 613-sq-mi drainage-area reaches in the Sangamon Basin. One discharge measured at the 240-sq-mi reach in the Sangamon required the use of a boat. The remaining measurements were conducted by wading across the stream sections.

Velocities and depths were measured for two different discharges. The flow durations of the discharges have the greatest difference that could be achieved during the 5-month field study. Field work was conducted during relatively dry periods, timed to avoid unsteady flow conditions after rainfall events. Field work was accomplished between April and August of 1985. An unusually wet June, July, and August 1985 prevented flow from receding to relatively low flow (high value of flow duration). Flow durations of measured discharges ranged from 19% to 82% with most of them between 30% and 70%. The flow durations corresponding to the flows observed in the field were computed by interpolating between the computed flows at various flow durations with the regression equations previously presented in Table 1.

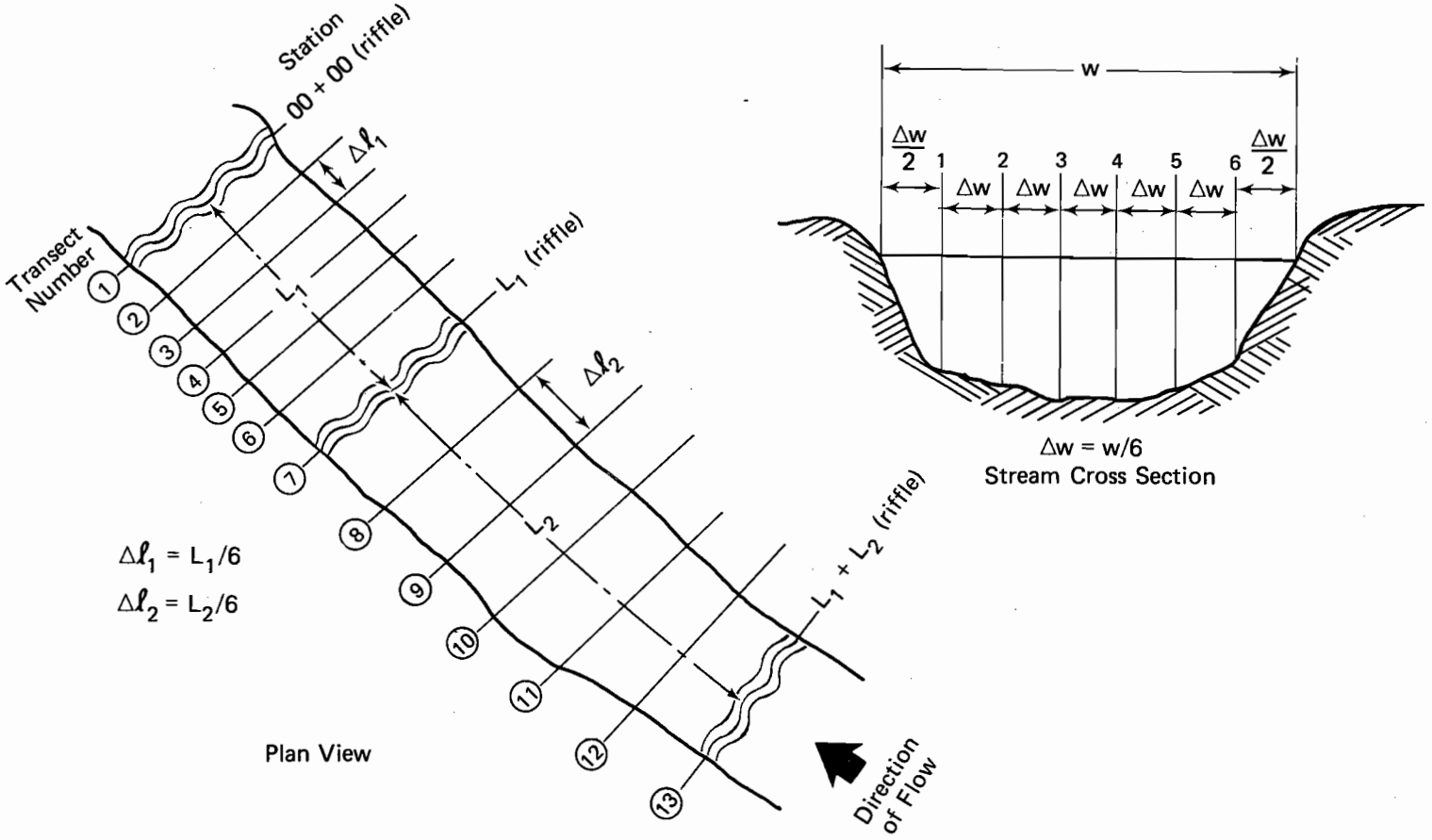

Figure 21. Schematic sketch of transect locations and divisions of channel cross section

ANALYSIS OF FIELD DATA

Field data were entered and stored on the Illinois State Water Survey VAX computer. Recorded information includes the reach drainage area, discharge, flow duration, stationing of transects, cross-sectional area of flow, top water width at each transect, and the 78 velocity and depth measurements. Transect average depths and velocities and flow cross-sectional area were computed.

Each depth and velocity sampled is assumed to represent flow conditions in a portion of the reach designated by a quadrilateral flow surface area. The bounds of the quadrilateral are defined by the mid-point distance between measurements. A weighting factor, proportional to the ratio between this quadrilateral stream surface area and the total surface area of the pool riffle sequence, was computed for each data point. The weights are equal if stream width is constant and the transects are equally spaced. The weights were used in all statistical calculations. The average and standard deviation of all measured depths and velocities were computed for each observed discharge at each of the nine reaches. For purposes of discussion, these values will be referred to as averages and standard deviations for each reach.

Discharge, flow duration, beginning date of field work, and reach average parameter values are listed in Table 11. The two discharges measured at each reach are designated a and b.

RIFFLES AND POOLS

Along the stream length, riffle to riffle spacing typically reported in the literature is 5 to 7 times the channel width (Leopold and Maddock, 1953; Harvey, 1975). Channel width increases with drainage area. Thus the distance between riffles increases as drainage area increases. The spacing between riffles has been shown to correlate closely with average flow widths calculated from hydraulic geometry relations for the 20% flow duration discharge (Harvey, 1975). The relationship between logarithms of riffle spacing and width is linear. A logarithmic plot of riffle-spacing for the study reaches versus width (width, W_{20}, corresponds to 20% flow duration) was developed using the combined data

TABLE 11

Discharge and Average Values of W, D, V, and A Measured at Study Reaches

Sta No.	Q No.	Start date	Q (cfs)	Flow Duration	Average values W	D	V	A
SANGAMON								
1	a	06-05-85	4.7	46	21.4	0.43	0.60	9.0
	b	07-11-85	4.0	48	21.4	0.42	0.57	9.0
2	a	06-03-85	14.8	46	26.4	1.08	0.69	28.7
	b	08-13-85	8.3	56	20.3	0.96	0.50	18.7
3	a	06-10-85	58.0	49	49.7	2.05	0.59	102.2
	b	08-14-85	23.3	64	45.7	1.72	0.32	78.7
4	a(1)	06-18-85	383.0	29	84.8	4.34	1.07	370.0
	a(2)	06-19-85	317.0	33	81.2	3.79	0.96	307.2
	b	07-26-85	137.0	52	72.9	2.49	0.77	181.6
5	a	07-17-85	683.0	36	114.8	4.17	1.44	475.5
	b	08-09-85	398.0	49	106.6	2.54	1.33	267.3
SOUTH FORK SANGAMON								
6	a	07-03-85	10.6	19	17.8	1.04	0.57	18.2
	b	06-20-85	2.8	43	16.9	0.72	0.30	11.9
7	a	07-08-85	8.7	56	15.5	0.75	0.68	11.6
	b	07-23-85	0.9	82	9.7	0.57	0.25	5.9
8	a	07-10-85	16.0	61	28.5	1.59	0.37	44.5
	b	07-19-85	4.3	78	27.2	1.26	0.19	33.7
9	a	06-26-85	182.0	43	63.5	3.42	0.82	217.8
	b	07-18-85	35.1	72	55.3	2.27	0.27	126.5

from both the basins and is shown in Figure 22. Two points are plotted for each reach, representing the spacing between transects located at the three riffles identified by field personnel. The reach number appears adjacent to the plotted point in the figure. A straight line was fit by eye to the data and is shown in the figure. The points for the intermediate drainage-area reaches show a linear trend. The smallest drainage area reaches, 1 and 6, had more erratic riffle spacing, and the plotted points for those reaches do not fall on the line. This may be attributable to dredging activities in these reaches. The apparent riffle pool sequences differ with discharge at reach 5. This may be the result of an unobserved obstruction downstream but the plotting position of riffle spacing, based on transect location, suggests that reach 5 may comprise only one riffle pool sequence. Alternatively, a point representing the full reach length versus W_{20} is also plotted. This point plots near the line indicated by the other data.

The average riffle spacing for the Sangamon and South Fork Sangamon for all the reaches was 7 times the width (calculated for 20% flow duration). Excluding the relatively long spacing found at the smallest drainage area reaches, the average spacing is 4.5 times the width. When the alternate value of riffle spacing for reach 5 is substituted, the average is 5.0. Figure 23 is a histogram depicting riffle spacing in terms of stream width, W_{20}. The spacing between each pair of riffles in a reach was used to construct the histogram (the two riffle spacings for Reach 5 were included).

An attempt was made to develop a means of estimating relative lengths of pools and riffles in a reach without direct field observation. The terms riffle and pool refer to relative differences in flow conditions and bed materials, and are not precisely defined in terms of hydraulics. The transition zone between a riffle and a pool, and vice versa, has by definition intermediate flow conditions. For the purpose of estimating riffle and pool lengths from hydraulic data alone, a working criterion was applied to classify conditions measured at a transect as either pool or riffle. Insofar as only low to medium flows were measured, riffle conditions are assumed if the transect average depth is less than the reach average depth and, simultaneously, the transect average velocity is

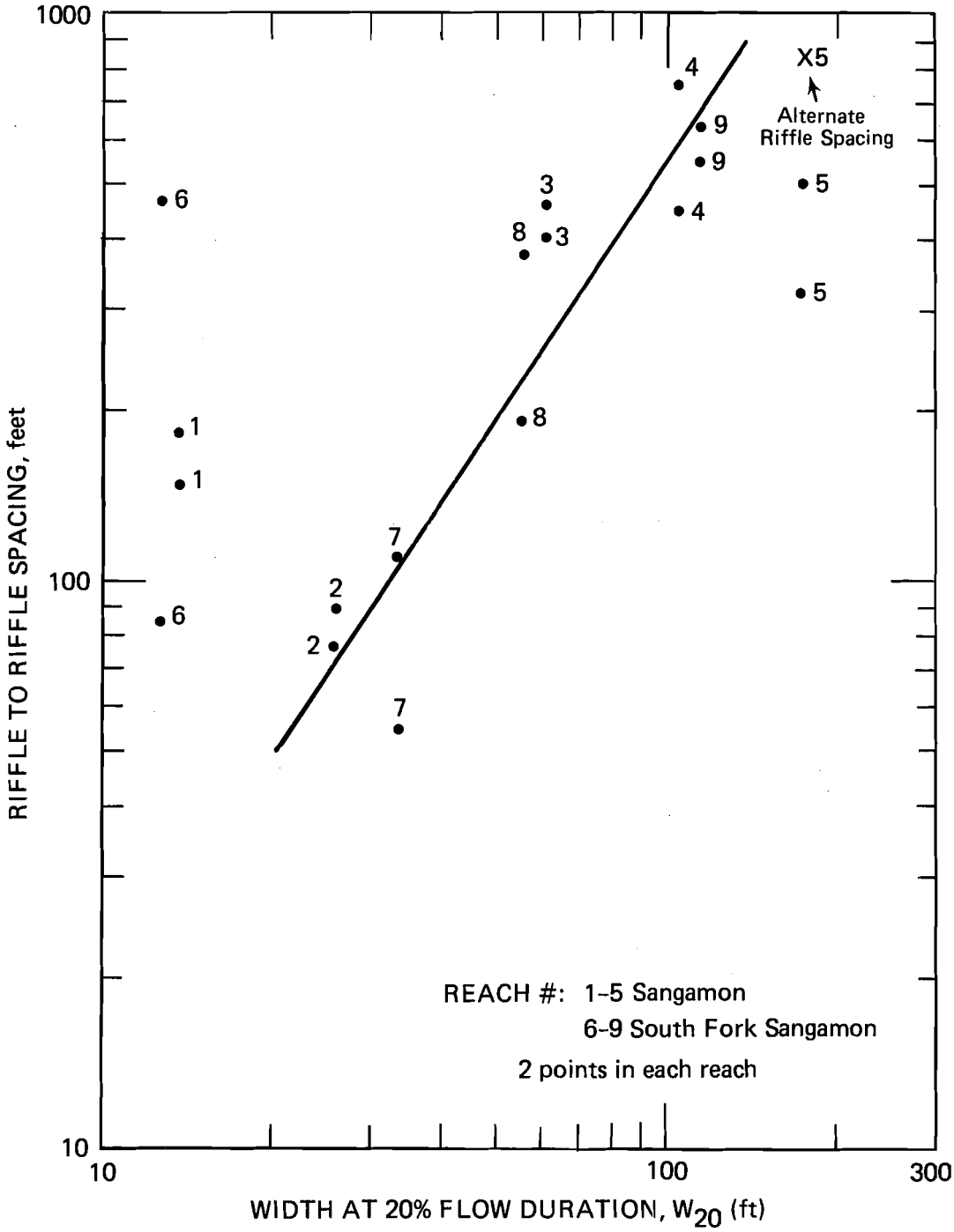

Figure 22. Study-reach riffle spacing versus W_{20}

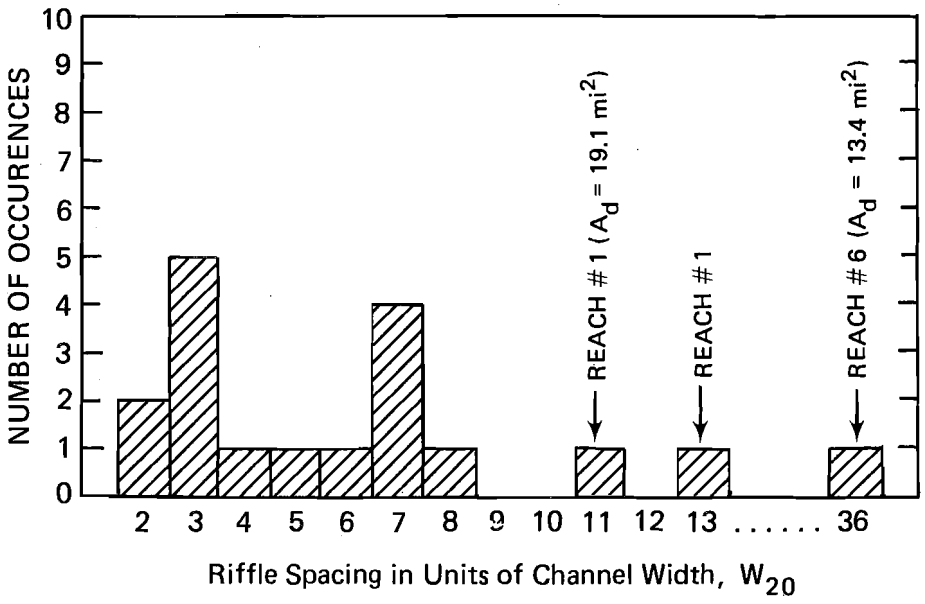

Figure 23. Histogram of study-reach riffle spacing

greater than the reach average velocity. The relative spacing between transects and the parameter values at adjacent transects were taken into consideration when proportioning lengths between transects with riffle conditions and transects with pool conditions. Usually, the transect average values are assumed to be representative of conditions up to a point midway between adjacent transects.

In some reaches the transect locations coincided with the position of silt-laden, intermediate shallow sections of pools (observed by field personnel between well defined riffles). Typically at low discharges these transects had average depth and velocity which satisfied the adopted criterion for riffle flow conditions. Another interpretive problem occurs when one pool has depths considerably greater than the other in a study reach, in which case flow depths in the shallower pool may be less than the reach average. The spacing between riffles was considered when interpreting the data.

The lengths of riffles vary with discharge for a given reach as the transition zone from riffle- to pool-like conditions moves toward the higher points in the streambed with increasing discharges and toward the deeper points as flows decrease. Therefore, the proportion of riffle-like conditions in a reach is expected to increase as flows diminish.

The relationship between flow duration and the relative lengths of riffle and pool conditions in a reach was investigated by computing the ratios of riffle-like conditions to pool-like conditions for each reach at both discharges. Considerable judgement was necessarily involved in determining the lengths of riffles and pools; however, the riffle to pool ratios calculated do tend to increase with increasing flow duration (or decreasing discharge).

The relatively low depths and high velocities found at the silted, shallow sections of pools hampered efforts to define flow conditions unique to riffles and to pools. The apparent dependence of riffle lengths (and pool lengths) on flow duration adds another dimension to the problem of subdividing Sangamon and South Fork Sangamon streams into riffle sections with characteristic flow condition, spacing, and length, and pool sections with unique flow conditions, spacing, and length. The

variation of depth and velocity through the riffle and pool sequence in the study reaches is better described as a continuum of values rather than discrete sections of a reach with characteristic depth and velocity. The continuum conceptual model was adopted in developing the flow model for depth and velocity.

DEPTH DISTRIBUTIONS

The reach average depth, D, computed for each discharge ranged from 0.4 ft to 4.3 ft and 0.6 ft to 3.4 ft in the Sangamon and South Fork Sangamon, respectively. The distribution of depths measured in each reach was investigated by ranking them from low to high and computing the cumulative non-exceedance probability, p. This was computed with the weighting scheme, from the plotting position formula:

$$p = m_i/N+1$$

where N = number of data points

$$m_i = \sum_{k=1}^{i} w_k$$

w_k = weight computed for each data point, k, as a function of flow surface area

$$\text{and} \quad \sum_{i=1}^{N} w_k = N \qquad (17)$$

For each flow, the measured depths and computed probabilities were plotted on normal probability paper. The plotted points fall on an approximately straight line between the 10% and 90% non-exceedance probability levels. The slope of the lines varies with discharge and drainage area. The reach average depth plots at approximately the 50% non-exceedance probability for each case.

The standard deviation of a variable with normal distribution is a measure of the spread of values about the mean. The variation of depth in a channel is predominantly influenced by pool and riffle formation; thus, the standard deviation is a measure of the difference between pool

and riffle depths. The difference between pool and riffle depths increases with an increase in drainage area. The standard deviation of field measured depths, S_d, is typically greater for a larger drainage-area reach than for the smaller drainage-area reach.

Plots of S_d versus drainage area are drawn in Figure 24a and b for each basin. A straight line (shown dashed) was fit by eye to the data. The slope of the line is similar for the two basins. The corresponding flow duration is noted above each data point. A comparison of S_d for the two discharges measured in each reach shows that in most cases S_d is larger at the smaller flow duration. This corresponds to greater variability in depths for low discharges. However, the difference is small. The relationship between S_d and flow duration cannot be defined without conducting field measurement over a broader range of flow durations. The simple linear relation shown in the plots is the best estimate with the available data. The relationship for the South Fork Basin data is fairly well approximated by the straight line. The relatively greater data scatter for the Sangamon Basin reaches may be attributable in part to conditions unique to the reaches measured or to field conditions at the time the measurements were made.

Common practice in central Illinois is to dredge natural channels to improve farmland drainage. Dredging would smooth out channel variations and result in a lower standard deviation of depths than might be found in a natural channel with the same drainage area. Three sites in the Sangamon Basin with drainage areas between 10 sq mi and 25 sq mi were inspected and all appeared to have had some artificial modification of the channel. Reach 1 is located in a channel which has been periodically dredged. Local residents report that the latest dredging occurred in 1983. The apparently low values of computed standard deviation indicate that the stream may not yet have returned to its natural regime.

The configuration of the two pool riffle sequences measured at reach 6 were different. The distance between the upstream riffle and the middle riffle is 85 ft, whereas the next riffle does not appear until another 465 ft downstream. This particular pool riffle sequence may also be in a period of transition.

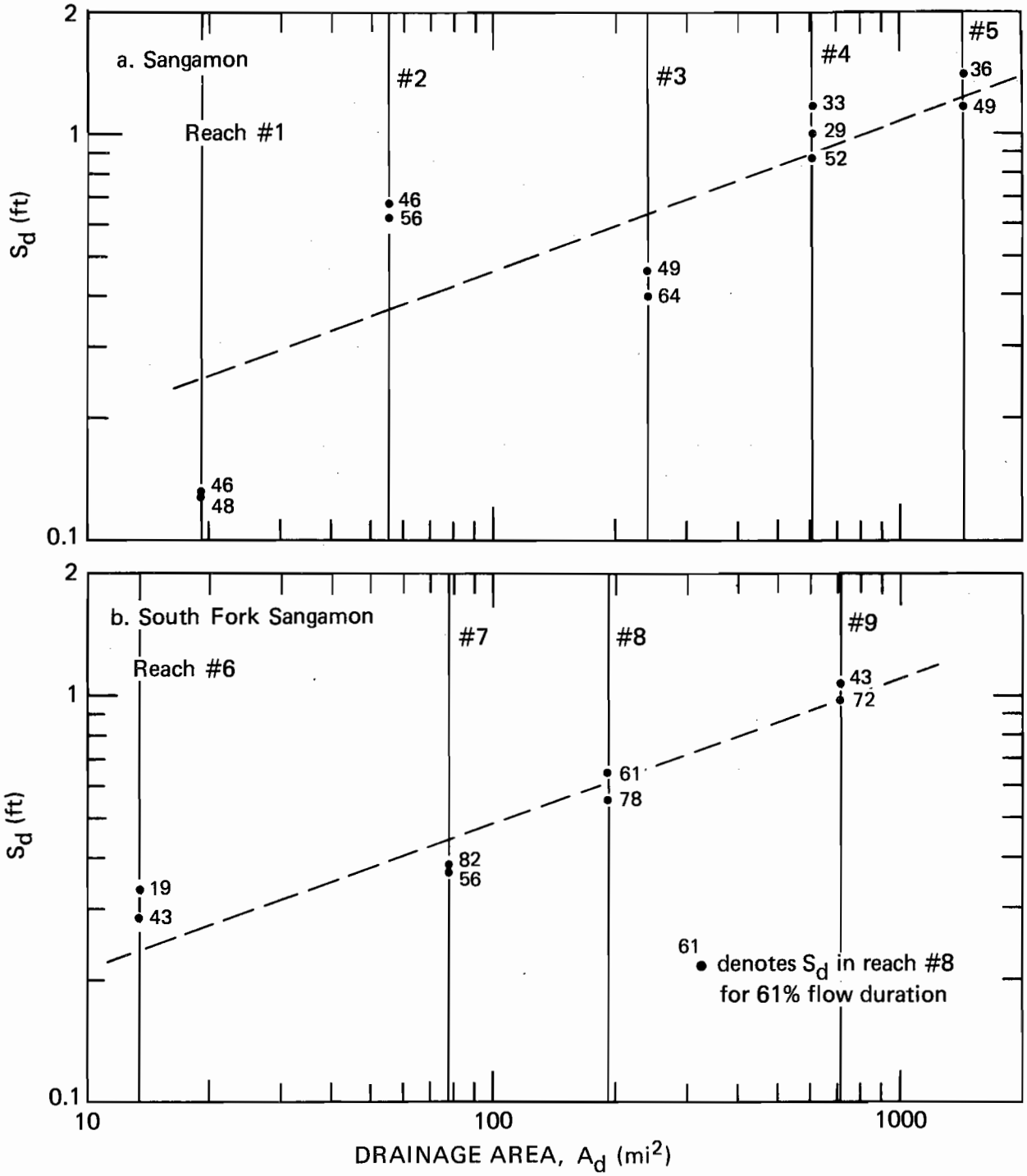

Figure 24. Standard deviation of depth, S_d, versus drainage area, A_d

One measurement at reach 3 was conducted while the discharge was decreasing. Timing and weather did not permit another measurement at the site. The standard deviation of depths may be high due to the unsteady flow. The flow duration was approximately 29% for one riffle pool sequence measured and 33% for the riffle pool sequence measured the following day. These were taken into consideration when fitting the lines shown in Figure 24.

The variety of local depths expected within a reach for a given flow duration can be determined from the combined results of hydraulic geometry relations and relations developed from field data defining the distribution of depth. The average or mean depth, D, is calculated from the basin hydraulic geometry equation for depth. The distribution of normalized depths, Z, in a reach can be obtained from the normal cumulative probability distribution:

$$P(Z) = \frac{1}{\sqrt{2\pi}} \int_{-\infty}^{Z} \exp\left(-z^2/2\right) dz \qquad (18)$$

where P is the non-exceedance probability and $Z = (d - D)/S_d$, and d is the actual depth for which P is calculated.

The value of Z is computed for a level of non-exceedance probability using an approximate numerical solution of the inverse standard normal probability distribution function. The standard deviation of depth is a function of the drainage area of the reach; its value is obtained from the relationship shown in Figure 24a or b. Substituting the appropriate values of D, S_d and Z, the depth d for a given non-exceedance probability level, i, can be evaluated by solving for d_i, as

$$d_i = Z_i(S_d) + D \qquad (19)$$

For example, 30% of the depths measured in a reach will be less than or equal to the depth, d_{30}, calculated from the value of Z at P(Z)=0.30. The frequency of occurrence for each calculated depth is equal to the difference between successive non-exceedance probabilities; e.g., 10% of the depths in a reach will range between d_{20} and d_{30}, and the average depth in that range will be about d_{25}.

Following this methodology, the hydraulic geometry and depth distribution relationships developed for the basin can be used to compute the expected values of local depths in a reach for any drainage area, over a full range of flow durations.

VELOCITY DISTRIBUTIONS

The reach average velocity, V, computed for each measured discharge ranged from 0.32 feet per second (fps) to 1.44 fps for the Sangamon Basin reaches and from 0.19 to 0.81 fps for measurements made in the South Fork Sangamon Basin. Local measured velocities varied over a fairly large range of values in a reach; a measure of the variability of velocity is the standard deviation. The standard deviation of velocity, S_V, for each discharge was computed with the 78 values of measured velocities and ranged between 40% and 95% of the reach average velocity. The standard deviation increased in value as the reach average velocity increased. The simple correlation coefficient r between V and S_V was 0.97% for the Sangamon Basin, 0.97% for the South Fork Sangamon, and 0.98% for all 18 discharge measurements together. The linear regression coefficients relating S_V as a function of V were identical to one significant figure for all three sample groups. The three equations expressing the least squares regression line are:

Basin		n*	r
Sangamon	$S_V = 0.12 + 0.38V$	10	0.97
South Fork	$S_V = 0.091 + 0.43V$	8	0.97
All data	$S_V = 0.10 + 0.40V$	18	0.98

*n = sample size

Figure 25 shows a plot of S_V versus V for the 18 discharge measurements. The number appearing by each point is the reach number. The value of the standard deviation of velocity appears to be predominantly related to the magnitude of velocity and to be independent of drainage area. There is little scatter in the plots of S_V versus V and there does not appear to be any ordering or segregation of data by drainage area (as indicated by the reach numbers).

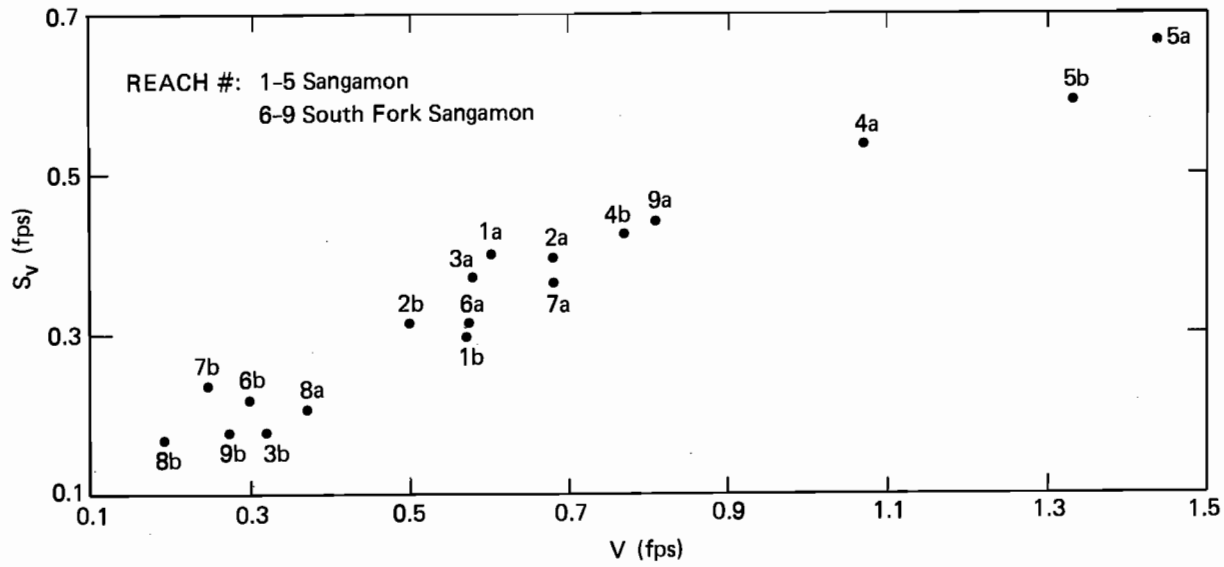

Figure 25. Standard deviation of velocity, S_V, versus reach average velocity, V

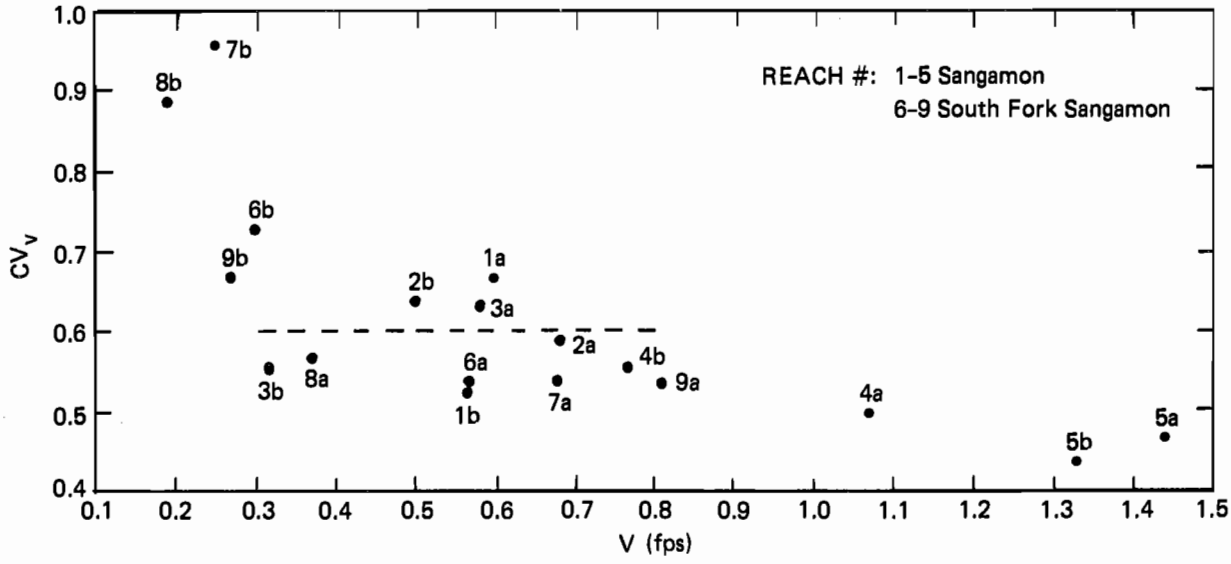

Figure 26. Coefficient of Variation of Velocity, CV_V, versus Reach Average Velocity

The coefficient of variation for the velocities, $CV_V = S_V/V$, was plotted with respect to V, as shown in Figure 26. There is an apparent trend of decreasing CV_V with increasing V; i.e., the standard deviation becomes a larger percent of the average velocity as the average velocity decreases. The trend flattens for V between about 0.3 fps and 0.8 fps, and the approximate average value of CV_V is about 0.6 in this range. In a single reach CV_V will increase with flow duration as velocity decreases. This generality can be observed in the hydraulic geometry station plots where there is greater scatter in the data at low discharges than at high discharges. The exact nature of the relationship cannot be determined from limited flow measurements.

JOINT DISTRIBUTION OF DEPTH AND VELOCITY

The joint distribution of depths and velocities was investigated by grouping velocities according to the cumulative probability of the simultaneously measured depth. Ten divisions of cumulative probability of depth between 0 and 1.0 were delineated, each corresponding to a probability interval of 0.1. The velocities measured concurrently with a depth having a non-exceedance probability between 0 and 0.1 form a group, velocities associated with depths having a non-exceedance probability between 0.1 and 0.2 form a group, and so on. For each flow measured in a reach there are between 7 and 9 velocity and depth measurements within each incremental range of depth cumulative probability. Plots of velocity versus coincident depth non-exceedance probability were developed for each discharge. The variation of measured velocities within each depth probability group was then considered.

For comparison purposes, velocity ratios were computed by dividing each measured velocity by the reach average velocity for the discharge. Velocities in each depth probability interval typically varied between 0.2 and 2.0 times V for groups with small to greater than average depths and with cumulative probability under 0.8, and between 0.2 and 1.8 times V for groups with greater depths and with cumulative probability above 0.8. The ratio computed for the minimum velocity in each probability group did not vary substantially between groups or from discharge to

discharge. There were some extreme velocities such as 4 to 6 times V; however, they were only isolated values.

The velocities associated with lesser depths, those depths having non-exceedance probability less than about 0.2, were, on the average, less than the reach average velocity. The combination of relatively low velocity and depth reflects conditions which are sometimes encountered near stream banks where depth is less and velocity is reduced by side friction. The velocities measured with these lesser depths lower the overall average velocity for the depth probability group. The majority of depths in this probability range were measured at the first position from the bank in the transect, i.e., closest to the bank. However, not all measurements made at the ends of a transect fall within this depth probability range.

Velocities measured with depths having non-exceedance probability between about 0.4 and 0.7 on the average are greater than the reach average velocity. Velocities with depths having higher non-exceedance probabilities averaged near the reach average velocity.

Though the joint distribution of depths and velocities suggests these general observations, local non-uniformities in flow conditions frequently result in a fairly wide range of velocities which may occur over any limited range of depth values in any given reach.

The velocity ratios in each group (associated with each range of depth probability) have a fairly large range of values about the mean. Frequently the maximum and minimum velocity in each group is significantly different from the mean. For example, if the average velocity ratio for a group is 1.0, most velocities associated with depths in that range will be between 0.5 and 1.5 times V. There may also be a velocity measured with a depth in that range which is 2.0 times V, and a velocity which is only 0.2 times V.

A velocity distribution was constructed from the general observations drawn from an examination of individual plots of velocity versus coincident depth probability and the relationship between reach average velocity and its standard deviation. The velocities range between a minimum of 0.2 times V to a maximum of 2.0 times V. The velocity

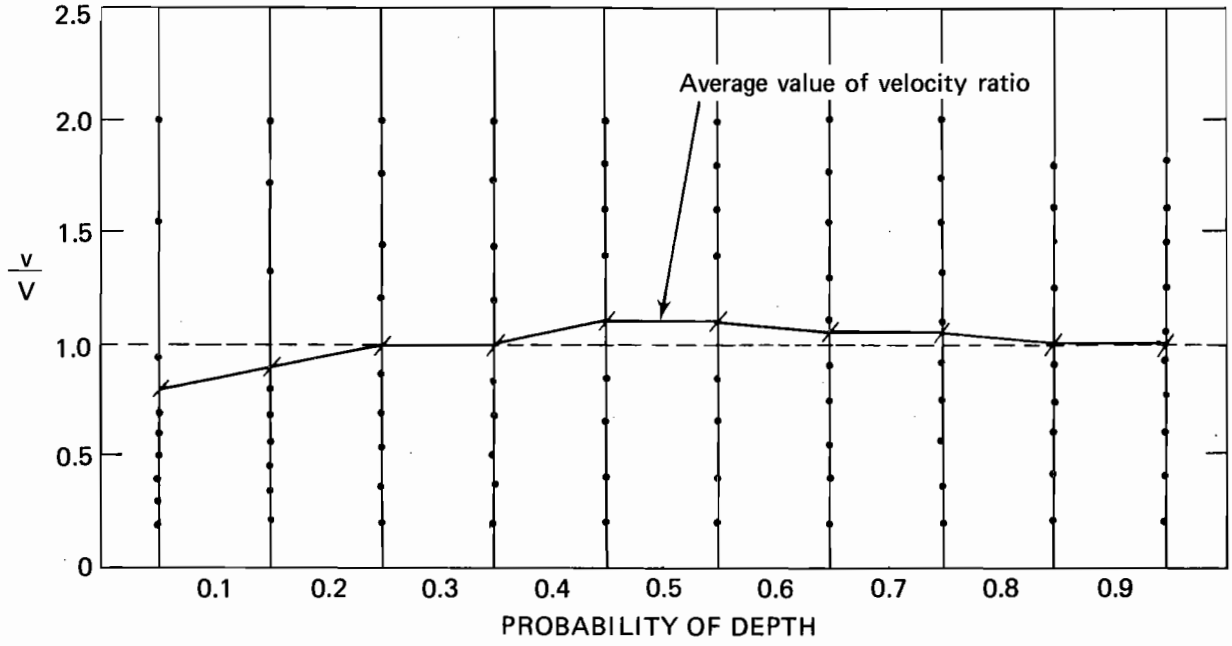

Figure 27. Velocity ratio distribution for Sangamon and South Fork Sangamon basins

distribution is shown in Figure 27. The solid line drawn in the figure represents the approximate average velocity ratio for each probability level. Ten velocity ratios are plotted for each probability level, and the points are distributed so that their average equals the average shown by the solid line for that probability range. The average of all the velocity ratios is 1.

If the variates are defined by the ratios to the mean, the coefficient of variation equals the standard deviation because the mean is unity. Thus, the standard deviation of the velocity ratios defining the distribution in Figure 26 is equivalent to the coefficient of velocity variation for the reach. The distribution of velocity ratios illustrated has a standard deviation of 0.6, compatible with the average coefficient of variation for velocities between 0.3 and 0.8 fps.

The distribution may be used for velocities in the range of 0.3 to 0.8 with relatively small error; the error becomes greater as V deviates significantly from this range. This can be seen in Figure 26 where the departure of the data values from the straight line (constant coefficient of variation representing the proposed velocity distribution) becomes greater the farther V is from this range. The velocity distribution may not predict the full range of velocities throughout a reach if the average velocity is very small. Local velocity values may cluster more about the mean for high average velocity. The joint distribution illustrated is approximate and is a composite of the observed variation of velocities with depths as measured in the field. The complex interaction of velocity magnitude, channel area, and local variations in channel shape creates a multitude of velocity patterns which may be observed simultaneously with depths having a limited range of values. On the assumption that the field measured velocities represent typical flow conditions for the Sangamon and South Fork Sangamon, the distribution developed will approximate the average distribution of velocities found over a sufficiently long reach in either basin.

The range of 10 expected velocities for any depth probability can be determined from the distribution. The reach average velocity is computed from hydraulic geometry equations. Each of the 10 velocity ratios

identified for the depth probability is multiplied by the reach average velocity. Selecting 10 depths having probabilities of 5, 15, 25...95%, ten velocities can be computed for each depth, generating 100 depth and velocity pairs defining the expected variation of depth and velocity in a reach.

COMPARISON OF FIELD DATA AND RESULTS OF HYDRAULIC GEOMETRY EQUATIONS

The basin hydraulic geometry equations predict flow and average values of depth, velocity, and width for a stream as a function of drainage area and flow duration. Width, depth, and velocity were calculated using the appropriate basin equations for the study reach drainage areas and flow durations corresponding to the measured discharges. There are considerable differences between calculated values and those from field measurements. These differences are not random, but have a systematic pattern. Depths and widths predicted by the basin equations were in nearly all cases lower than the average of measured values for each of the reaches in both basins. Velocities computed from the equations were higher than the reach average velocities computed from the field data. For the Sangamon Basin, the calculated widths were on the average 60% of field measured widths, the calculated depths were 70% of reach average depths, and the calculated velocities were 150% of the reach average velocities for the five reaches. Similarly, for the South Fork Sangamon, the calculated widths were on the average 70% of the average reach widths, the depths were 70% of reach average depths, and the velocities were 150% of the reach average velocities.

In order to compose a frame of reference for evaluating these differences, the average width, velocity, and depth measured at the riffles located in the study reaches (i.e., transects 1, 7, 13) were computed and compared to the reach average values for each discharge. The flow width measured at riffles did not vary significantly from the reach average, ranging within ±15% of the average reach width. The average riffle depth in the Sangamon reaches was 81% of the reach average and in the South Fork Sangamon reaches the riffle depths averaged 68% of the reach average depth. The composite average was 75%. The average velocity at the riffles was 120% of the reach average velocity for the Sangamon Basin reaches and 170% of the reach average velocity for the South Fork Sangamon Basin reaches. The composite average was 145%. A comparison of riffle depths and velocities with those from the hydraulic geometry equations suggests that the hydraulic geometry equations better estimate riffle than reach average conditions. The implication is that the USGS flow measurement data used to develop the station equations and

ultimately the basin equations were obtained near riffles and relatively shallow portions of the pools.

The average depths and velocities computed from the field data represent a sampling from a range of flow conditions throughout riffles and pools. The object of the flow measurements made by the USGS personnel is to accurately determine the discharge. Wading measurements are made at sections where depths do not exceed 3 ft, flows are least turbulent, and velocities are sufficiently high to produce an adequate number of current-meter revolutions in a reasonable time. Although not an established practice, it would be expected that in the interest of expediency narrow flow sections would be preferred for routine measurements. In general, these criteria systematically exclude the deeper portion of pools with low velocities and shallow riffles with more turbulent flow conditions. The data used to develop hydraulic geometry relations have a strong potential for bias. The predicted flow parameter values need to be adjusted as indicated by field measurements.

Through a determination of correction coefficients, parameter values predicted by the hydraulic geometry equations may be adjusted to better reflect reach average values measured in the field. The difference between the field measurements and hydraulic geometry predictions increases as flow duration increases or flow decreases. However, the drainage area seems to be a significant factor in defining the actual relationship. There was little difference between field values of W, D, and V and the calculated values from the hydraulic geometry equations, for the discharges having flow duration 36% and 49% measured at the 715-sq-mi drainage-area reach and the 43% flow duration discharges measured at the 1439-sq-mi drainage-area reach. While the discharges having flow durations between 40% and 60% measured at the other, smaller drainage area reaches had, with only one exception, depths 1.5 to 1.7 times greater in the field than predicted by the equations, field measured velocities were between 0.5 and 0.7 times the values calculated from the equations. The average parameter values for the lowest flow measured (flow durations 64% to 82%) were substantially different from the calculated ones, regardless of drainage area.

There are insufficient data to conclusively define a functional relationship for a correction factor. Flow measurements over a broader range of discharges in a number of reaches are needed to develop the relationship between the correction factor and flow duration and drainage area. The best approximation which can be estimated from the available data is a simple constant coefficient. The suggested coefficient, C, for a variable is the average ratio of field parameter values to values calculated by hydraulic geometry as:

$$Cvar = Var(field)/\ Var(hydraulic\ geometry) \qquad (20)$$

The correction coefficients for both basins are the same and are:

$C_w = 1.2$

$C_d = 1.4$

$C_v = 0.6$

in which subscripts w, d, and v refer to width, depth, and velocity. The coefficients can be used to adjust the values calculated from hydraulic geometry equations for flow durations exceeding 60% for all streams regardless of drainage area, and for flow durations between 40% and 60% in reaches with drainage areas less than about 700 sq mi. The results of hydraulic geometry equations for larger drainage area streams at low flow durations or higher discharges may not be significantly different from actual values.

DEVELOPMENT OF THE FLOW MODEL FOR BASINWIDE ASSESSMENT OF WEIGHTED USABLE AREA

The objective of the flow model is to simulate the needed hydraulic information to evaluate the WUA (Weighted Usable Area) for streams throughout a basin. The model must predict the local variation of depth and coincident velocities throughout a stream reach as well as the proportion of the reach characterized by each depth and velocity pair.

Using the IFG method for calculating the WUA, a stream reach is conceptually segmented into cells having a measured surface area and hydraulically represented by measured or interpolated depth and velocity. The probabilistic approach to flow modeling does not provide depth and velocity information for a specific cell in a known reach. Rather, pursuing the statistical approach, depth and velocity are estimated for a given frequency of occurrence.

The depth distribution developed defines the cumulative non-exceedance probability of a given depth. The velocity distribution provides information on the various velocities expected to occur for each of a number of depth intervals related to the cumulative depth probability function. Depths and velocities calculated at successive cumulative probabilities have a frequency of occurrence equal to the difference between the current and the previous cumulative probability. Evaluating depth and velocity at uniformly incremented cumulative probability levels yields an equal frequency of occurrence for each depth-velocity pair.

The data collection and analysis conducted in this study were structured such that the probability of occurrence for the depth-velocity pair is related to a percentage of a riffle pool sequence surface area. For illustration purposes, consider 10 depths evaluated at the 5%, 15%, 25% and so on up to 95% cumulative probability level for a given drainage area and flow duration. Each calculated depth has an equal frequency of occurrence from riffle center to riffle center (i.e., one riffle pool sequence). Ten percent of the stream (as measured by flow surface area) will be represented by the 5% cumulative probability depth, d_{05}; 10% by the 15% cumulative probability level depth, d_{15}; and so on. Ten velocities associated with each depth may be calculated from the

applicable velocity distribution. Each depth-velocity pair, therefore, represents 1/100 of the stream flow surface area. The reach may be any length provided the drainage area remains approximately the same and extends through at least one riffle-pool sequence, beginning and ending at the same location relative to the riffle pool sequence (e.g., riffle to riffle). The total surface area of the reach is the product of the reach length and the average flow width.

The calculation of the WUA of a stream using the basinwide flow model is illustrated by the following example.

System Input

Basin: South Fork Sangamon

Stream Drainage Area: 200 mi^2

Approximate Reach Length: 2000 ft

Flow Duration: 60%

Target Fish Species and Life Stage: Bluegill, juvenile

I. Flow Model Calculations

A. Calculate average W, D, and V from basin hydraulic geometry relations.

$\log W = 0.68 - 0.93\ (0.60) + 0.55\ (\log 200);\ W = 24.4$

$\log D = -0.31 - 1.22\ (0.60) + 0.45\ (\log 200);\ D = 0.99$

$\log V = -0.03 - 0.59\ (0.60) + 0.07\ (\log 200);\ V = 0.60$

B. Adjust results of hydraulic geometry equations.

Drainage area is less than 700 mi^2, so use correction factors:

$C_w = 1.2$

$C_d = 1.4$

$C_v = 0.6$

The adjusted values, W', D', and V' are calculated:

$W' = C_w \times W = 29.3$

$D' = C_d \times D = 1.39$

$V' = C_v \times V = 0.36$

C. Determine the distribution of depths in the reach by computing 10 depths with equal frequency of occurrence.

1. Obtain the estimate of standard deviation of depth for a 200-sq-mi drainage area reach from Figure 24b; $S_d = 0.62$.
2. Compute the normalized variable Z, representing 10 equal intervals of cumulative probability between 0 and 1.0. The 10 cumulative probabilities and values of Z are listed in Table 12.
3. Substituting the adjusted reach average depth D' and the standard deviation of depth, solve for depth at each selected cumulative probability as:

   $d_i = (Z_i)(S_d) + D'$, $i = 5, 15, 25 \ldots, 95$

   The difference between successive probabilities is 10%; thus each computed depth has a 10% frequency of occurrence, e.g., represents 10% of the riffle pool sequence area.

   The computed depths are:

   $d_{05} = 0.35$ $d_{15} = 0.73$ $d_{25} = 0.96$ $d_{35} = 1.14$ $d_{45} = 1.30$

   $d_{55} = 1.46$ $d_{65} = 1.62$ $d_{75} = 1.80$ $d_{85} = 2.03$ $d_{95} = 2.41$

D. Compute 10 velocities associated with each depth. Figure 27 provides the ratios or local velocity to reach average velocity, $(\frac{v}{V})_{i,j}$ for each depth (i=5, 15, ..., 95, corresponding to the percent cumulative probability of the depth, j=1,10). Computed velocities, $v_{i,j}$ are similarly double-subscripted. The first subscript i identifies the depth cumulative probability; the second j, ranges from 1 to 10 for each of 10 velocity ratios obtained from the distribution. The velocities are computed as:

$$v_{i,j} = (\frac{v}{V})_{i,j} \times V'$$

The following tabular joint frequency distribution of depths and velocities is developed. Each depth velocity pair (d_i, $v_{i,j}$) represents 1/100 of the surface area of the stream reach.

TABLE 12

Selected Values of the Inverse Normal (0,1) Probability Distribution Function from the International Math and Science Library Routine MDNRIS

Cumulative probability $P_i(x)$	Z_i $(d-D')/S_d$
0.05	-1.645
0.15	-1.036
0.25	-0.674
0.35	-0.385
0.45	-0.126
0.55	0.126
0.65	0.385
0.75	0.674
0.85	1.036
0.95	1.645

i	d_i (ft)	Values of $v_{i,j}$, fps, for j equal to 1	2	3	4	5	6	7	8	9	10
05	.35	.07	.11	.14	.18	.22	.25	.29	.34	.56	.72
15	.73	.07	.12	.16	.20	.24	.29	.33	.48	.62	.72
25	.96	.07	.13	.19	.24	.30	.36	.43	.52	.63	.72
35	1.14	.07	.13	.19	.24	.30	.36	.43	.52	.63	.72
45	1.30	.07	.14	.23	.31	.36	.40	.50	.57	.65	.72
55	1.46	.07	.14	.23	.31	.36	.40	.50	.57	.65	.72
65	1.62	.07	.13	.20	.27	.33	.40	.47	.55	.63	.72
75	1.80	.07	.13	.20	.27	.33	.40	.47	.55	.63	.72
85	2.03	.07	.14	.22	.27	.32	.38	.45	.52	.57	.65
95	2.41	.07	.14	.22	.27	.32	.38	.45	.52	.57	.65

E. Compute the flow surface area of the reach. The total flow surface area of the reach (A_R) is the product of the reach length and the average flow width, $A_R = W \times 2000 = (29.3)(2000) = 58{,}600\ ft^2$. W_{20} can be computed and Figure 22 checked to verify that 2000' is greater than one riffle pool sequence.

Each cell represented by (d_i, $v_{i,j}$) has a flow surface area, $a_{i,j} = 1/100 \times A_R$. It follows:

$$A_R = \sum_{i=1}^{10} \sum_{j=1}^{10} a_{i,j}$$

II. WUA Calculations

The WUA is computed from a modified form of equation 1.

$$WUA = \sum_{i=1}^{10} \sum_{j=1}^{10} S(d_i) \times S(v_{i,j}) \times a_{i,j}$$

where S(d) and S(v) are the fish suitability indexes defined earlier. Taking $a_{i,j}$ out of the summation the resulting equation is

$$WUA = \frac{A_R}{100} \sum_{i=1}^{10} \sum_{j=1}^{10} S(d_i) \times S(v_{i,j}) \qquad (21)$$

A tabular index of fish suitability function or fish suitability is used to determine the values of S(d) and S(v) for the desired fish species and life stage (Singh and Ramamurthy, 1981). The value of S(d) and S(v) for each depth and velocity in the joint distribution is thus

determined. The 100 products of the depth and velocity suitability indexes are summed, and for the juvenile bluegill:

$$\sum_{i=1}^{10} \sum_{j=1}^{10} S(di) \times S(v_{i,j}) = 13.48$$

Substituting this sum and the value of A_R into equation 21, the WUA for the juvenile bluegill for the example drainage area and flow duration is:

$$WUA = \frac{58{,}600 \text{ ft}^2}{100} \times 13.48 = 7899 \text{ ft}^2$$

This procedure is repeated for any flow duration, and for any drainage area.

The relationship between discharge and WUA may be determined by computing the discharge for the corresponding flow duration from equation 5 and Table 1. The discharge and WUA computed for the example reach at three different flow durations are tabulated below.

Flow duration	Q(cfs)	WUA ft^2
40	54.3	9599
60	18.0	7899
80	3.8	5069

CONCLUSIONS AND RECOMMENDATIONS FOR FURTHER RESEARCH

The following conclusions are based on an examination of historical data, field data collected as part of this study, and relationships developed from the data for the Sangamon and South Fork Sangamon River Basins. The conclusions pertain to those basins but in some cases they may have broader application.

1. Hydraulic geometry relations are an effective tool for predicting average flow parameter values for unmeasured streams. Relationships developed from data obtained at a single stream cross section represent average flow conditions at that section. Relationships developed from data gathered at multiple stream cross sections represent an average of a variety of flow conditions which may be quite diverse. Unless flow is uniform, the predicted average parameter values may or may not actually occur at any given sections of the stream. Additional information defining the distribution of parameter values is needed to describe local flow conditions.

2. The data scatter in station plots of W, D, A, and V versus Q, measured by wading, is largely attributable to the practice of not performing discharge measurements at the same stream transect each time. The variation in values of W, D, and V for the same discharge in the plots is an indication of the variability of flow conditions throughout a reach.

3. The routine discharge measurements made by USGS personnel for gage calibration tend to be made at stream sections which typically have riffle-like flow conditions. Hydraulic geometry relations developed from these data more closely model average riffle conditions as opposed to reach average flow conditions. The results of these equations can be adjusted to reflect reach average values.

4. The utility of discharge data collected by the USGS would be greatly expanded if measurements were made systematically throughout the riffle pool sequence, and if records were kept of the location of the measurement relative to the riffle pool sequence.

5. The relationships between flow parameters (W, D, A, V, and Q) at natural stream cross sections differ from the corresponding relationships for these parameters at stream cross sections modified by bridge piers and abutments. Only data collected at natural stream sections should be used to calibrate hydraulic geometry equations.

6. The standard deviation of depths, S_d, in a reach increases with increasing stream drainage area, A_d. The variation of depths in a reach is a reflection of semi-regular bed undulations identified as riffles and pools. The relationship between S_d and A_d is consistent with recognized, systematic patterns of channel formation in the stream network. Flow duration may influence the magnitude of S_d found in a single reach.

7. The variation of velocity throughout a reach is principally related to the magnitude of the bulk velocity of the flow. The greater the bulk velocity, the less variation there is in velocity values in a reach.

8. The probabilistic flow model provides the necessary hydraulic information to evaluate a stream aquatic habitat using the IFG Weighted Usable Area (WUA) model. In this capacity the probabilistic flow model has two distinct advantages over conventional hydraulic functional models. First, hydraulic geometry relations combined with relationships defining the distribution of depth and velocity in a reach provide a valuable link relating flow conditions throughout a basin. Models based on equations such as Manning's must be calibrated by direct field measurements for each reach. Secondly, for low discharges flow models based on Manning's equation or other uniform flow equations are subject to gross inaccuracies due to the non-uniformity of the flow. The calibration of such models for low flows is dependent on designation of physically unrealistic values for the friction factor. The probabilistic flow model is not based on the assumption of uniform flow, but on a general relationship derived directly from field data. The variability of local depths and velocities is directly addressed in the probabilistic model by determination of the standard deviation of those parameters.

9. The basinwide probabilistic flow model, interphased with the IFG methodology, may be used to evaluate the stream network aquatic habitat for any discharge scenario. This flexibility enhances the utility of applying the IFG methodology to quantify instream flow needs for water allocation planning.

Further research is recommended in the following areas:

1. Additional discharge measurements in the study reaches over a broader range of flow durations necessary to:
   a) define the relationship between flow duration and the correction factor for values predicted from hydraulic geometry relations in the Sangamon and South Fork Sangamon, b) determine if the flow duration (discharge magnitude) has a significant effect on the standard deviation of depth in a reach and if so evaluate the relationship, and c) define the joint distribution of depths and velocities by developing additional distributions for varying flow durations (i.e., velocity magnitudes).
2. The relationship defining the depth and velocity distributions needs to be verified by comparison to independent field measurements not included in the model development.

BIBLIOGRAPHY

Bovee, K. D., and R. T. Milhous, 1978. Hydraulic Simulation in Instream Flow Studies: Theory and Techniques. Cooperative Instream Flow Services Group, Instream Flow Information Paper No. 5 FWS/OBS-78/33, 130 p.

Buchanan T.J. and W.P. Somers, 1976. Discharge Measurements at Gaging Stations. USGS Techniques of Water Resources Investigations, Book 3, Chapter A8.

Chow, Ven Te (Ed.), 1964. Handbook of Applied Hydrology. McGraw-Hill, New York.

Chow,Ven Te, 1959. Open Channel Hydraulics. McGraw-Hill, New York.

Dunne, T., and L. Leopold, 1978. Water in Environmental Planning. W. H. Freeman and Co., San Francisco, CA.

Edwards, C. J., B. L. Griswold, R. A. Tubb, E. C. Weber, and L. C. Woods, 1984. Mitigating Effects of Artificial Riffles and Pools on the Fauna of a Channelized Warmwater Stream. North American Journal of Fisheries Management 4: 194-203.

Griswold, B. L., C. Edwards, L. Woods, and E. Weber, 1978. Some Effects of Stream Channelization on Fish Populations, Macroinvertebrates, and Fishing in Ohio and Indiana. Fish and Wildlife Service, U.S. Department of the Interior, FSW/OBS-77/46, 64 p.

Harvey, A. M., 1975. Some Aspects of the Relations Between Channel Characteristics and Riffle Spacing in Meandering Streams. American Journal of Science, Vol. 275, April, pp. 470-478.

Herricks, E. E., et al., 1980. Instream Flow Needs Analysis of the Little Wabash River Basin. University of Illinois Environmental Engineering Series 61, 151 p.

Illinois State Water Plan Task Force, 1984. Illinois State Water Plan. Springfield, Illinois, 75 p.

Leopold, L. B., and M. G. Wolman, 1957. River Patterns: Braided, Meandering, and Straight. U.S. Geological Survey Professional Paper 282-B.

Leopold, L. B., and T. Maddock, 1953. The Hydraulic Geometry of Stream Channels and Some Physiographic Implications. U.S. Geological Survey Professional Paper 252.

Loar, J. M., and M. J. Sale, 1981. Analysis of Environmental Issues Related to Small-Scale Hydroelectric Development, V. Instream Flow Needs for Fishery Resources. Oak Ridge National Laboratory Publication 1829, 123 p.

Milhous, R. T., and K. D. Bovee, 1978. The Stochastic Variation of Instream Values in Rivers. ASCE Journal of the Hydraulic Division, HY8, pp. 630-637.

Milhous, R. T., and W. J. Grenney, 1981. The Quantification and Reservation of Instream Flows. Water and Science Technology, Vol. 13, No. 3, pp. 129-154.

Miller, B. A., and H. G. Wenzel, 1984. The Low Flow Hydraulics in Alluvial Channels. University of Illinois Water Resources Center, Research Report 192, 50 p.

Nunnally, N. R., and E. Keller, 1979. Use of Fluvial Processes to Minimize Adverse Effects of Stream Channelization. Water Resources Research Institute of the University of North Carolina, Research Report 144, 115 p.

Rzhanitsyn, N. A., 1960. Morphology and Hydraulic Regularities of the Structure of the River Net, translated by D. B. Krimgold, for Soil and Water Conservation Research Division and USGS Water Resources Division, originally published by Gidrometeoizdat, Leningrad, U.S.S.R.

Schmal, R. N., and D. F. Sanders, 1978. Effects of Stream Channelization on Aquatic Macroinvertebrates, Buena Vista Marsh, Portage County, Wisconsin. Fish and Wildlife Service, U.S. Department of the Interior, FWS/OBS-78/92, 80 p.

Singh, K. P., 1981. Evaluation of Hydraulic Geometry Parameters for Various Low Flow Releases Downstream of Dams on Illinois Streams. Illinois State Water Survey Contract Report 251, 42 p.

Singh, K.P., and G. S. Ramamurthy, 1981. Desirable Low Flow Releases from Impounding Reservoirs: Fish Habitats and Reservoir Cost, Volume 1, Illinois State Water Survey Contract Report 273, 155 p.

Stall, J. B., and Y. S. Fok, 1968. Hydraulic Geometry of Illinois Streams. University of Illinois Water Resources Center, Research Report 15, 47 p.

Stall, J. B., and C. T. Yang, 1970. Hydraulic Geometry of 12 Selected Stream Systems of the United States. University of Illinois Water Resources Center, Research Report 32, 73 p.

Stall, J. B., and C. T. Yang, 1972. Hydraulic Geometry and Low Streamflow Regimen. University of Illinois Water Resources Center, Research Report 54, 31 p.

Stalnaker, C. B., 1979. The Use of Habitat Structure Preferenda for Establishing Flow Regulation Necessary for Maintenance of Fish Habitat, In "Ecology of Regulated Streams," by J. V. Ward and J. A. Stanford (editors), Plenum Press, New York, pp. 321-337.

Tsai, C., and M. L. Wiley, 1983. Instream Flow Requirements for Fish and Fisheries in Maryland. Maryland Water Resources Research Center, Technical Report 69, 90 p.

Williams, R. D., and R. N. Winget, 1979. Macroinvertebrate Response to Flow Manipulation in the Strawberry River, Utah. In "Ecology of Regulated Streams," by J. V. Ward and J. A. Stanford (editors), Plenum Press, New York.